

10-1995

# The Evolution and Testing of an Aerovalve Pulsejet Engine

Gregory V. Meholic

*Embry-Riddle Aeronautical University - Daytona Beach*

Follow this and additional works at: <https://commons.erau.edu/db-theses>



Part of the [Aerospace Engineering Commons](#)

---

## Scholarly Commons Citation

Meholic, Gregory V., "The Evolution and Testing of an Aerovalve Pulsejet Engine" (1995). *Theses - Daytona Beach*. 142.  
<https://commons.erau.edu/db-theses/142>

This thesis is brought to you for free and open access by Embry-Riddle Aeronautical University – Daytona Beach at ERAU Scholarly Commons. It has been accepted for inclusion in the Theses - Daytona Beach collection by an authorized administrator of ERAU Scholarly Commons. For more information, please contact [commons@erau.edu](mailto:commons@erau.edu).

**THE EVOLUTION AND TESTING OF AN AEROVALVE  
PULSEJET ENGINE**

by

Gregory Vincent Meholic

A Thesis Submitted to the  
Aerospace Engineering Department  
in Partial Fulfillment of the Requirements for the Degree of  
Master of Science in Aerospace Engineering

Embry-Riddle Aeronautical University

Daytona Beach, Florida

October 1995

UMI Number: EP31943

### INFORMATION TO USERS

The quality of this reproduction is dependent upon the quality of the copy submitted. Broken or indistinct print, colored or poor quality illustrations and photographs, print bleed-through, substandard margins, and improper alignment can adversely affect reproduction.

In the unlikely event that the author did not send a complete manuscript and there are missing pages, these will be noted. Also, if unauthorized copyright material had to be removed, a note will indicate the deletion.

**UMI<sup>®</sup>**

---

UMI Microform EP31943  
Copyright 2011 by ProQuest LLC  
All rights reserved. This microform edition is protected against  
unauthorized copying under Title 17, United States Code.

---

ProQuest LLC  
789 East Eisenhower Parkway  
P.O. Box 1346  
Ann Arbor, MI 48106-1346

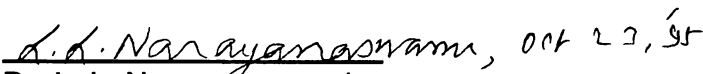
# THE EVOLUTION AND TESTING OF AN AEROVALVE PULSEJET ENGINE

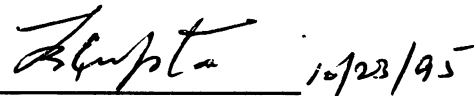
by

Gregory Vincent Meholic

This thesis was prepared under the direction of the candidate's thesis committee chairman, Dr. L. L. Narayanaswami, Department of Aerospace Engineering, and has been approved by the members of his thesis committee. It was submitted to the Department of Aerospace Engineering and was accepted in partial fulfillment of the requirements for the degree of Master of Science in Aerospace Engineering.


## THESIS COMMITTEE:

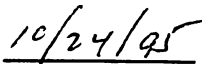
  
Dr. L. L. Narayanaswami  
Chairman

  
Dr. Tej R. Gupta  
Member

  
Dr. R. Luther Reisbig  
Member

  
Dr. David T. Kim  
Chair, MSAE Program

  
Dr. Allen I. Ormsbee  
Department Chair, Aerospace Engineering

  
Date



## ACKNOWLEDGMENTS

I would like to express my sincerest love and gratitude to my parents Monica and Ken and my step parents Paul and Gayle for their wonderful support and assurance through my education and for this project.

My great appreciation and sincerest thanks go to my thesis advisor Dr. L. L. Narayanaswami for sharing his knowledge, recommendations, and enthusiastic support of my work. His encouragement strengthened my focus and helped to keep me within reasonable bounds of my thesis research. I am very proud to have been a student of his and to have worked closely with him in many endeavors. Equal gratitude goes to my thesis committee mentors Dr. Tej R. Gupta and Dr. R. Luther Reisbig to whom I am indebted for their assistance and guidance through my education and in the production of this project.

Mr. Donald Bouvier deserves my highest appreciation and gratitude for his assistance in the construction of the pulsejet. He has become a valued friend and has graciously shared his machining expertise and experience. Special thanks go to Professor John Novy and Dr. Ernest Jones for their cooperation in providing technical assistance and research material.

I would also like to give special recognition to Mr. Roy Lumb, the turbine engine test facility instructor, for his insight and supervision while running the pulsejet. High regards go to Mr. Andrew Roberts who patiently assisted me on many occasions during testing. Funding for this project was granted from

Professor David Hazen, chairman of the Aerospace Engineering department, to which I extend my grandest appreciation.

My deepest love and thanks also go to Ms. Ivana Hrbud whose unbounded inspiration lead me through impatient times. She has become a very important part of my life and means more to me and this project than she will ever know.

In conclusion, the following businesses have been an instrumental part of the research and deserve many thanks for their help and generosity:

A&W Muffler, Atlas Welding, Baker Brothers Refrigeration, Daytona Bolt and Nut, Daytona Gas, Discount Auto Parts, Ferran Engineering, Jenks Metals, Pameco R&R Supply, Radio Shack, Ridgewood Shell, Sid Harvey Industries, Southside Auto Parts, Wal-Mart, and W. W. Grainger, Inc.

# ABSTRACT

Author: Gregory V. Meholic  
Title: The Evolution and Testing of an Aerovalve Pulsejet Engine  
Institution: Embry-Riddle Aeronautical University  
Degree: Master of Science in Aerospace Engineering  
Year: 1995

The goal of this project was to develop and test a self-aspirating aerovalve pulsejet and measure its operating characteristics. An investigation of pulsejets developed by previous experimenters revealed design trends associated with the engine geometry. These trends were followed in the development of an aerovalve pulsejet engine entitled the *Astra*. The engine employed variable fuel injection methods, ignition location and exhaust pipe length to show that certain combinations of geometry relations and fuel injection methods were more conducive to pulse combustion. Even though the engine pulsed with forced inlet air, the *Astra* did not self-aspirate as did the engines on which its design was based due to insufficient mixing of fuel and air. Data regarding combustion chamber pressures and temperatures were collected to verify pulsating behavior. The project also included extensive documentation of engine design changes and experimentation to serve as a guideline for future aerovalve pulsejet developers.

# TABLE OF CONTENTS

<b>ACKNOWLEDGMENTS</b> .....	iii
<b>ABSTRACT</b> .....	v
<b>LIST OF TABLES</b> .....	ix
<b>LIST OF FIGURES</b> .....	x
<b>CHAPTER 1 INTRODUCTION</b> .....	1
<b>1.1 Research Goals</b> .....	1
<b>1.2 Overview of Pulse Combustion Research</b> .....	1
<b>1.3 Thesis Summary</b> .....	3
<b>CHAPTER 2 PULSE COMBUSTION PRINCIPLES AND DEVICES</b> .....	4
<b>2.1 General Observations About Pulse Combustion</b> .....	4
2.1.1 The Basics of Pulse Combustion .....	4
2.1.2 Pulse Combustor Model and Function .....	5
2.1.3 Thermodynamic Analysis .....	8
2.1.4 Pressure Magnitudes and Frequency .....	11
<b>2.2 Pulse Combustors and Pulsejets</b> .....	13
<b>2.3 Pulsejet Components and Operating Cycle</b> .....	14
2.3.1 Components .....	14
2.3.2 Operating Cycle .....	15
<b>2.4 Types of Pulsejets</b> .....	18
2.4.1 Mechanically-Valved Pulsejets.....	19
2.4.2 Aerodynamically-Valved Pulsejets .....	21
<b>2.5 Comparison of Pulsejets to Other Propulsion Systems</b> .....	24
<b>2.6 Applications of Pulsejets</b> .....	26
<b>2.7 Variables Affecting Pulsejet Performance</b> .....	27
2.7.1 Inlet Lip Shape .....	27
2.7.2 Inlet Pipe Length .....	28
2.7.3 Inlet Pipe Cross-Sectional Area .....	29
2.7.4 Combustion Chamber Geometry .....	29
2.7.4.1 <i>Inlet Bulkhead</i> .....	30
2.7.4.2 <i>Combustor</i> .....	31
2.7.4.3 <i>Exhaust Nozzle</i> .....	32
2.7.5 Exhaust Pipe Geometry.....	33
2.7.6 Fuel/Air Mixing Characteristics.....	34

<b>2.8 Trends in Pulsejet Design</b> .....	37
2.8.1 Variable Definition .....	37
2.8.2 Inlet Relationships .....	39
2.8.3 Exhaust Relationships .....	40
2.8.4 General Observations .....	42
<b>CHAPTER 3 DEVELOPMENT OF EXPERIMENTAL PULSEJET</b> .....	45
<b>3.1 Pulsejet Research Objective History</b> .....	45
<b>3.2 Engine Development and Configuration</b> .....	49
3.2.1 Baseline Lockwood Engine .....	49
3.2.2 Using the Trends in Pulsejet Design .....	51
<b>3.3 Astra General Design Considerations</b> .....	52
3.3.1 Material Selection Concerns .....	52
3.3.1.1 <i>Heat Exposure</i> .....	52
3.3.1.2 <i>Machining Ability</i> .....	53
3.3.1.3 <i>Material Cost and Availability</i> .....	54
3.3.2 Off-the-Shelf Parts and Part Modification .....	54
3.3.3 Engine Vibration and Hardware .....	55
<b>3.4 Final Astra Layout and Components</b> .....	55
3.4.1 Part 1: Inlet Lip .....	57
3.4.2 Part 2: Inlet Pipe .....	58
3.4.3 Part 3: Inlet Bulkhead .....	58
3.4.4 Part 4: Combustor .....	59
3.4.5 Part 5: Exhaust Nozzle .....	59
3.4.6 Parts 6 and 7: Inner and Outer Exhaust Pipes .....	60
3.4.7 Parts 8, 9 and 10: Assembly/Mounting Rings and Gaskets .....	61
3.4.8 Parts 11 and 12: Fuel Injector and Spark Plug Mounting Plates .....	62
3.4.9 Parts 13 and 14: Fuel Injector Housing and Fuel Injectors .....	63
3.4.9.1 Part 14A: <i>Axial Fuel Injection Assembly</i> .....	64
3.4.10 Part 15: Fuel Injector Mounting Plate Plugs .....	65
<b>CHAPTER 4 SUPPORT SYSTEMS, SAFETY AND TESTING FACILITY</b> .....	66
<b>4.1 Support Systems</b> .....	66
4.1.1 The Fuel System .....	66
4.1.1.1 <i>Choosing the Right Fuel</i> .....	67
4.1.1.2 <i>Propane Tank and Throttle Valves</i> .....	68
4.1.1.3 <i>High-Pressure Hose</i> .....	69
4.1.1.4 <i>Check Valve and Pressure Gauge</i> .....	70
4.1.1.5 <i>Fuel Injector Housings and Fuel Injectors</i> .....	70
4.1.2 The Ignition System .....	71
4.1.2.1 <i>The Power Box</i> .....	71

4.1.3 The Air System.....	72
<b>4.2 Safety Concerns.....</b>	<b>73</b>
<b>4.3 Testing Facility.....</b>	<b>75</b>
<b>CHAPTER 5 ENGINE TESTING AND RESULTS.....</b>	<b>76</b>
<b>5.1 Original Engine Configuration.....</b>	<b>76</b>
<b>5.2 Test History of the Astra.....</b>	<b>78</b>
<b>5.3 Data Acquisition Equipment Setup.....</b>	<b>104</b>
5.3.1 General Layout.....	104
5.3.2 Fuel and Air Inlet Pressures.....	105
5.3.3 Pressure Across the Engine.....	105
5.3.4 Combustion Pressure Variation.....	106
5.3.5 Temperature Measurements.....	107
<b>5.4 Data Acquisition Procedure.....</b>	<b>107</b>
<b>5.5 Testing Results.....</b>	<b>110</b>
5.5.1 Fuel and Air Inlet Pressure.....	110
5.5.2 Total Pressure Measurement at Inlet ( $h_{T IN}$ ) and Exhaust ( $h_{T EX}$ ).....	112
5.5.3 Combustion Temperatures.....	113
5.5.4 Combustion Pressure Traces.....	117
5.5.4.1 <i>Oscilloscope Plot Description</i> .....	117
5.5.4.2 <i>Pressure Signal Trace</i> .....	117
5.5.5 Pulse Combustion Verification.....	121
5.5.6 Engine Frequency.....	122
5.5.7 Operating Pressures (Max. Peak-to-Peak and Avg. Voltages).....	123
<b>CHAPTER 6 CONCLUSIONS AND RECOMMENDATIONS.....</b>	<b>124</b>
<b>6.1 Conclusions.....</b>	<b>124</b>
6.1.1 Engine Geometry.....	124
6.1.2 Combustion Conditions.....	126
<b>6.2 Recommendations.....</b>	<b>127</b>
<b>REFERENCES.....</b>	<b>128</b>
<b>APPENDIX A ASTRA CONSTRUCTION DRAWINGS.....</b>	<b>130</b>
<b>APPENDIX B PROPERTIES OF LIQUEFIED PETROLEUM GAS.....</b>	<b>140</b>
<b>APPENDIX C RAW DATA FROM THREE-PHASE TESTING.....</b>	<b>142</b>
<b>APPENDIX D THERMOCOUPLE &amp; PRESSURE GAUGE CALIBRATION.....</b>	<b>150</b>

## LIST OF TABLES

Table 2-1. Pulsejet Inlet Relationships .....	40
Table 2-2. Pulsejet Exhaust Relationships .....	41
Table 2-3. General Pulsejet Relationships .....	43
Table 3-1. Geometric Comparison of Lockwood and <i>Astra</i> Engines .....	51
Table 5-1. <i>Astra</i> Data at Various Operating Conditions .....	111

## LIST OF FIGURES

Figure 2-1. Pulse Combustor Model.....	6
Figure 2-2. Pulse Combustor Cycle .....	7
Figure 2-3. Otto Cycle Diagrams.....	8
Figure 2-4. Pulse Combustion Cycle Diagrams.....	9
Figure 2-5. Pulse Combustion Pressure Signature .....	12
Figure 2-6. Simple Pulsejet .....	15
Figure 2-7. Pulsejet Cycle .....	16
Figure 2-8. Argus 109 Mechanically-Valved Pulsejet.....	19
Figure 2-9. Argus Engine Cycle .....	20
Figure 2-10. Marconnet Aerovalve Pulsejet .....	22
Figure 2-11. SNECMA Escopette.....	23
Figure 2-12. SNECMA Ecrevisse .....	23
Figure 2-13. Lockwood U-Tube and Thrust Augmentors .....	24
Figure 2-14. Aerovalve Inlet Shapes.....	28
Figure 2-15. Combustion Chamber Components.....	30
Figure 2-16. Pulsejet Geometry Variables .....	38
Figure 3-1. Ported-Rotor Valve Cycle .....	46
Figure 3-2. Lockwood Model HH(5.25")-5 Aerovalve Engine .....	50
Figure 3-3. <i>Astra</i> Experimental Engine .....	51
Figure 3-4. <i>Astra</i> Component Assembly .....	56
Figure 3-5. Inlet Lip Cross-Section.....	58
Figure 3-6. Pressure Ring Assmebly.....	61
Figure 4-1. Fuel System Schematic .....	67
Figure 4-2. Ignition System Schematic.....	71
Figure 5-1. <i>Astra</i> Component Assembly with Ported-Rotor Valve System .....	77
Figure 5-2. Interchangeable Inlet Pipe Concept.....	83
Figure 5-3. Inlet Pipe and 45-Degree Inlet Bulkhead.....	95
Figure 5-4. Crimped-End Fan-Pattern Fuel Injectors .....	96
Figure 5-5. Opposing Fan-Pattern Fuel Injectors.....	100
Figure 5-6. Axially-Injecting Central Fuel Nozzles .....	101
Figure 5-7. Data Acquisition Equipment Setup .....	105
Figure 5-8. Combustion Temperature Versus Combustor Length .....	115
Figure 5-9. Oscilloscope Traces of Combustor Pressure Variation .....	118



# **CHAPTER 1**

## **INTRODUCTION**

### **1.1 Research Goals**

The goal of this project is to develop and test a self-aspirating aerovalve pulsejet and measure its operating characteristics. An investigation will also be conducted into pulsejet design trends established by previous experimenters to demonstrate that experimental conclusions regarding pulsejets may sometimes differ from those of the governing theory. In addition, the project includes extensive documentation of design changes made during the experimental stage of the work to provide an evolutionary history of the engine configuration. The purpose of this task is to provide a developmental record of an aerovalve pulsejet to serve as a guideline for future pulsejet developers.

### **1.2 Overview of Pulse Combustion Research**

Pulse combustion is similar to the well-observed and widely-known phenomenon of combustion-driven oscillation (first noted around 1800), but has only been researched since the turn of the century. The most significant difference is that pulse combustion can be used to produce work where

combustion-driven oscillations cannot (Ref. 1). This observation leads to the development of pulse combustion devices such as pulsejet engines for propulsion and pulse combustors for heat generation.

Although many companies and individuals experimented with pulse combustion in the 1940's and 1950's, some of the work later found to be significant in pulse combustor development was insufficiently documented. The companies or individuals associated with the "new" science of pulse combustion eventually redirected their focuses due to lack of funding, interest and profitable applications. In addition, the unfavorable reputation of pulsejets established by the German V-1 "buzz bombs" made pulse combustion an unpopular and little-understood science. As a result of these issues, only a limited number of studies have been conducted on pulse combustors and pulsejets, and the available information is sometimes vague or incomplete.

Most of the literature researched for this project employed pulsejets to observe various pulse combustion characteristics. These reports described the design of the device, the experimental goals and procedure, and the results. The pulsejets used in the experiments were independently developed by various researchers and none of the documentation described how the engines were developed or if any problems were encountered during testing.

### **1.3 Thesis Summary**

The theory and operation of pulse combustion devices will be discussed in Chapter 2. Also in this chapter will be a review of aerovalve engine design trends found in literature. Chapter 3 will describe the experimental engine built for this project and all of its associated components. Chapter 4 will focus on the facility where the engine experimentation was conducted and the safety issues concerned with such tests. This chapter will also describe the support systems necessary for the engine function (fuel, ignition and air systems). The history of the engine design will then be given in Chapter 5 along with the experimental results of the engine's operating characteristics. Chapter 6 will discuss the conclusions made from the project and evaluate future recommendations for its continuation.

## **CHAPTER 2**

# **PULSE COMBUSTION PRINCIPLES AND DEVICES**

This chapter will describe the theories governing pulse combustor and pulsejet operation as well as the differences between the two. The discussion will then focus on types of pulsejets, their advantages over other types of propulsion, applications, and the variables that control their function.

### **2.1 General Observations About Pulse Combustion**

#### **2.1.1 The Basics of Pulse Combustion**

One of the simplest ways to understand pulse combustion is to observe a camping lantern or any device utilizing a retractable, flammable wick. When a burning wick is sufficiently raised above its housing, the flame is steady and exhibits stability even during modest disturbances. The surrounding air is being consumed with the fuel such that the flame draws as much air as it requires to maintain itself. The fuel/air mixture ratio is constant and the flame burns robust. As the wick is lowered into the housing, the area of the flame exposed to the air is reduced and the flame burns less intense as the mixture becomes fuel rich. Eventually, the flame stability will reach a lower limit and will enter a pulsation

mode, which the author has frequently observed with residential space heaters and wick-burning lamps. This usually occurs when the flame is just about to enter the housing. Fully retracting the wick would cause the mixture to become too rich for combustion and the flame would extinguish. At the pulsation point, the flame tries to draw the surrounding air to burn with the rich zone around the wick. When sufficient air arrives, the flame burns more robust while consuming the fresh supply. The air is expended, the air pressure surrounding the flame falls, and the flame again draws in a new supply of air. This cycle repeats several times a second.

A steady flame causes little variation in stagnation pressure. Inside a gas turbine engine combustor, for example, where the pressures can be 15 times greater than ambient, the steady flame causes little variation. During the combustion phase of the pulse cycle, however, the pressure rises sharply due to the constant-volume nature of the process discussed later in Section 2.1.3. This rise in stagnation pressure can be observed as a measurable, usable force.

### 2.1.2 Pulse Combustor Model and Function

Pulse combustion can also be observed in wickless burners, the simplest being the “jam pot” combustor developed by Reynst and shown in Ref. 1. A small portion of gasoline is poured into a glass container onto which a lid with a hole at the center is placed. When a match is held near the hole the fuel vapors ignite and the flame pulses, following the same principle as the lantern. An

extension of the concept is to contain the flame inside a chamber with an air source, fuel nozzle, ignition source, and exhaust path. The containment of the flame and the subsequent pressure variation form the basis for a typical pulse combustor (Figure 2-1).

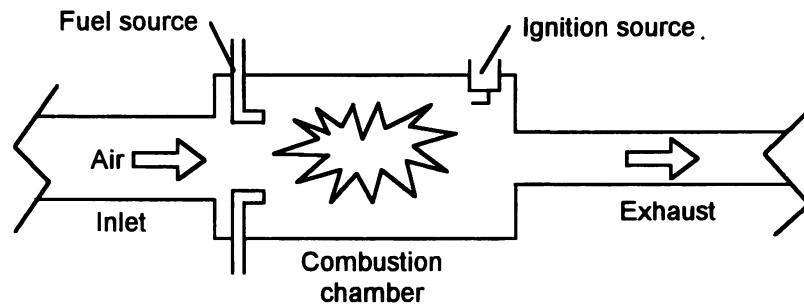


Figure 2-1. Pulse Combustor Model

Figure 2-2 demonstrates the cycle of a pulse combustor. As the combustor is functioning, air is drawn from the inlet into the combustion chamber on the low-pressure valley of the cycle (2-2a). The inertia of the incoming air slightly compresses the residual gases in the chamber left over from the previous cycle. At the same time mixing with a new fuel charge also occurs. The low pressure also pulls hot gases from the exhaust pipe back into the chamber, helping the compression process even further (2-2b). When the hot exhaust gases arrive inside the chamber, the mixture ignites and causes an even greater pressure rise in the combustion chamber (2-2c). This high-pressure forces the combustion products out through the inlet and exhaust pipes (2-2d). The combustion pressure drops and the cycle repeats. Pulse

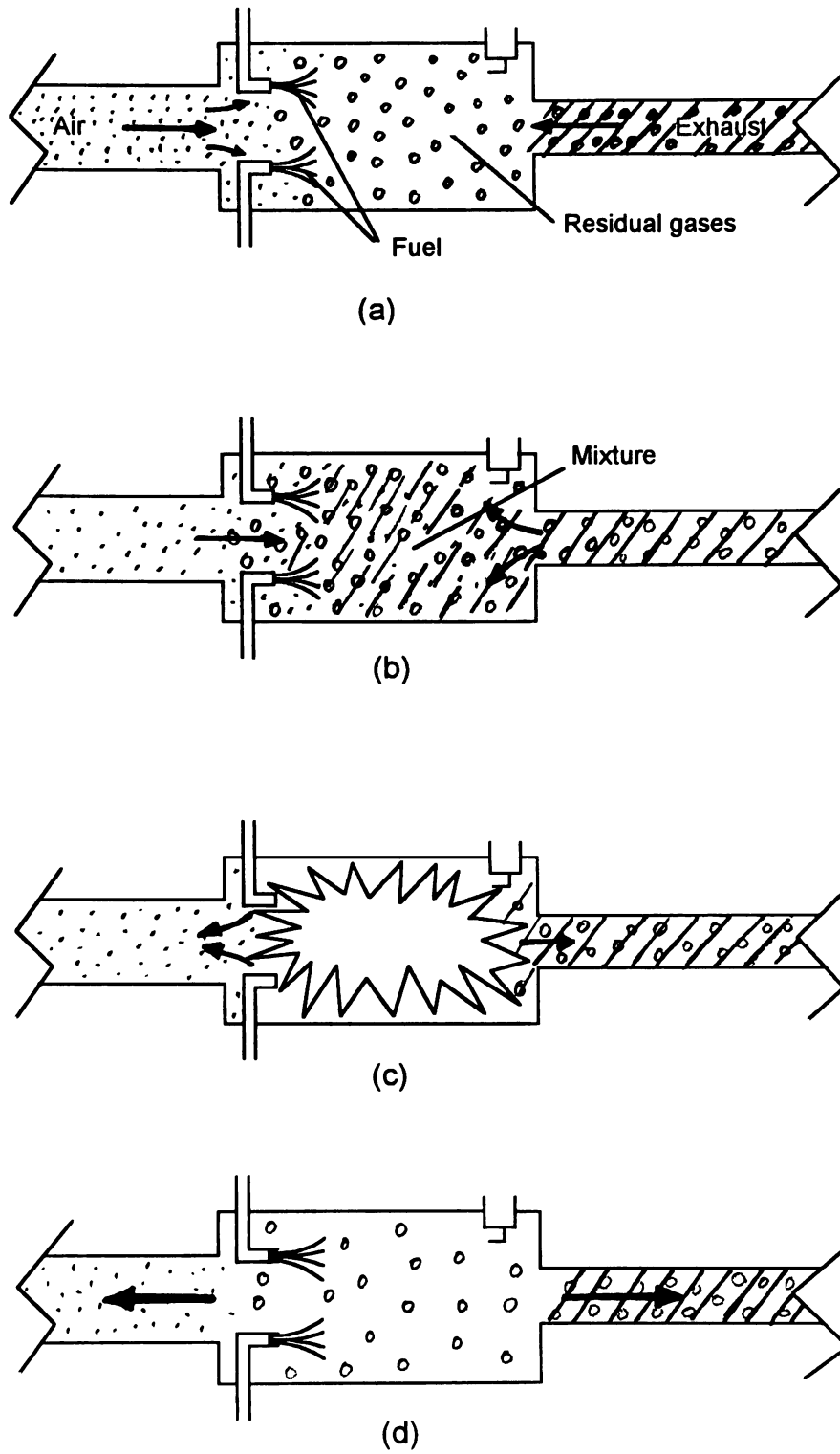


Figure 2-2. Pulse Combustor Cycle

combustors can function with or without moving parts and are usually self-aspirating. Further details on pulse combustors are given in Section 2.2.

### 2.1.3 Thermodynamic Analysis

Reciprocating engines obey either air-standard Otto or Diesel cycles and gas generators operate under the Brayton cycle. These three cycles take in air, compress it, mix and combust the air with fuel, and exhaust the products while producing work. Figure 2-3a represents the pressure-volume (P-v) diagram and 2-3b the temperature-entropy (T-s) diagram for the Otto cycle (gasoline engines) as shown in Ref. 12. Although variations of these cycles cause the diagrams to shift in some direction, they all have the same four steps. Step 4-1 represents air intake, 1-2 compression, 2-3 combustion, and 3-4 expansion.

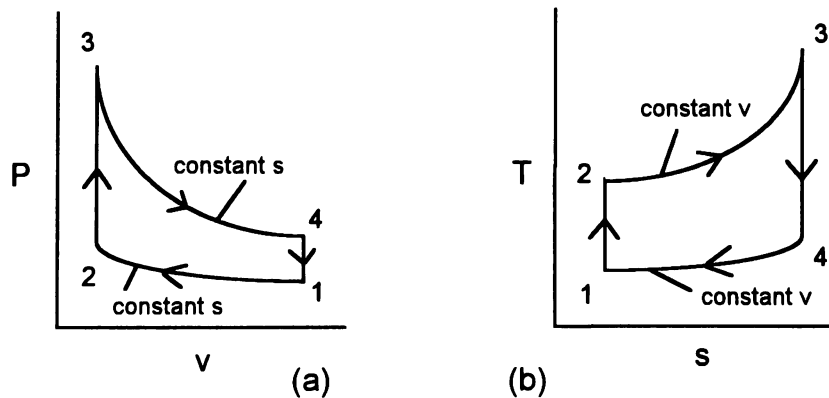


Figure 2-3. Otto Cycle Diagrams



The operational cycle of a pulse combustor combines the processes of the Otto and Diesel cycles. As in the Otto cycle, constant entropy occurs in the expansion and exhaust phases of pulse combustion. The property of the Diesel cycle associated with pulse combustors is the ignition of the combustion mixture by a rise in pressure and temperature of the residual gases, and not by an external source. Figure 2-4a and 2-4b illustrate the P-v and T-s diagrams of a pulse combustor cycle.

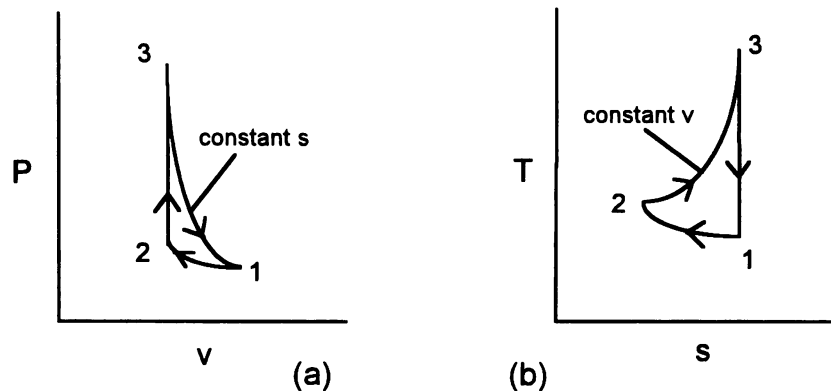


Figure 2-4. Pulse Combustion Cycle Diagrams

The figure above illustrates only a three-step process when there are indeed four. The intake and compression processes are combined since they occur at the same time, thus point 2 on the diagrams is actually points 1 and 2 and point 1 on the diagrams is actually point 4 if comparison to a four-step cycle is made. During the intake/compression process represented by 1-2, the inlet air column and a portion of the exhaust products both draw into the combustion chamber and slightly compress the residual gases from the previous cycle (and

also a new fuel charge), as mentioned earlier. This causes a pressure rise and a slight volumetric decrease of the trapped mixture. The hot gases then ignite the new fuel/air combination at the moment proper mixing has made it suitable for combustion, and the cycle undergoes an isochoric process. Pressure, temperature, and entropy rise sharply as shown in step 2-3. The last process of gas expansion and exhaust, step 3-1, occurs as the combustion products isentropically expand through the inlet and exhaust pipes. Combustor pressure drops and the cycle begins again with a new charge of fresh air and fuel.

An explanation must be given about assuming that the combustion process is isochoric. Putnam *et al.* (1), has observed that the pressure begins to rise in the combustor as the combustion reaction flame rapidly expands during the first half of the combustion cycle. Maximum pressure is reached when the flame has completely filled the chamber. The pressure then begins to fall as the combustion reaction flame wanes during the second half of the process and the gases exit through the inlet and exhaust pipes. The isochoric assumption is based on the observation that very little of the reaction products exit from the combustor during the pressure-rise portion of the cycle.

A thermodynamic description of the pulse combustion cycle is given by Winiarski (2). His paper investigated the thermal efficiency of an ideal pulse cycle (with precompression effects) and compared its efficiency to other air-standard cycles. Winiarski and others (Severyanin, Doyle and Faulkner, Gill and Bhaduri, all given in Putnam [1]) also attempted to describe the pulse

combustion cycle as being driven by acoustics. This theory assumed that the pressure variations and mixture ignition resulted from standing pressure waves inside the combustion chamber. This was thought to be true in the early days of pulse combustion analysis until functioning pulse combustors were developed whose geometry prohibited standing waves from forming. As knowledge of the combustion gas dynamics grew, it had been accepted that although acoustic processes may assist the pulse cycle for combustors designed to support standing waves, all pulse combustors operated on an air-standard cycle that could be thermodynamically modeled.

#### 2.1.4 Pressure Magnitudes and Frequency

Another way to look at pulse combustion is what has been called the “jet pump” effect. The pulse cycle “pumps” air by using the combustion process to vary the pressure inside the combustion chamber. Figure 2-5 shows that the pressure variation during operation. Although acoustic resonance waves (mostly generated from the exhaust pipe) and combustion unsteadiness slightly distort the signal during the pressure peaks and valleys, Putnam *et al.* (1), has shown that there is a general uniformity in the pressure signals from many types and designs of pulse combustors with the only significant differences being in firing rates and pressure magnitudes.

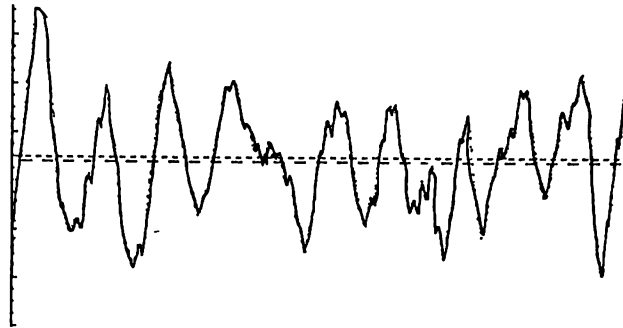


Figure 2-5. Pulse Combustion Pressure Signature

At the peak of this particular pressure cycle (immediately following combustion), the pressure increases to around two atmospheres. After most of the products have left the chamber, the pressure falls to about one-half an atmosphere. This yields a mean pressure of one and a quarter atmospheres. One of the research goals in pulse combustion has been to increase the mean pressure by raising the peak pressure, thus creating a stronger jet pump effect for a given fuel/air ratio. Since the intake and compression processes occur simultaneously, however, compression of the new mixture prior to combustion through aerodynamic or mechanical means without affecting the other steps in the cycle has been most challenging.

Empirically determining the operating frequency of the pulse cycle has often proved unsuccessful. Putnam *et al.* (1), has shown that several mathematical models have attempted to approximate the frequency based on various operating conditions and engine geometries, but their results do not often compare well with experimental findings. Although some models have done so successfully for a specific combustor design, the data deviate

unacceptably when any conditions are changed. Since the pulse cycle lacks adiabatic conditions due to the rapid heat transfer between combustion gases in all cycle phases, fundamental acoustic frequency and harmonic equations based on combustor and exhaust pipe (or resonance tube) geometry could not be used because they require the speed of sound. The constant-volume combustion process and unsteadiness of the pulse cycle, however, dictate that the correct temperature in determining the speed of sound must be higher than the adiabatic flame temperature. An historical trend also shown by Putnam *et al.* (1), indicates that most pulse combustors and pulsejets operate between frequencies of 80 Hz and 150 Hz, with geometry and fuel type being the most significant factors in combustor operating frequency.

## **2.2 Pulse Combustors and Pulsejets**

Although pulse combustors and pulsejets operate on the same cycle, there are differences in their design and application. Pulse combustors need not be self-aspirating and can vary greatly in configuration. They are usually designed to produce heat or for use in combustion research while often not extracting work from the combustion reaction and the exhaust products. Pulse combustor performance is somewhat dependent on combustion chamber geometry and their exhaust pipes can be of any length, as shown by Putnam *et al.* (1) (inlet pipe length is discussed in section 2.7.2). Employing pulse combustion for heat production has been shown to be more efficient than steady

combustion due to greater flame temperatures, increased heat transfer rates, and reduced nitrogen oxide (NO<sub>x</sub>) emissions (Putnam *et al.* [1]). Lennox Industries of Allen, Texas has developed a pulse combustion home furnace that uses only about half the fuel as a conventional gas furnace. The Lennox furnace also extracts 96% of the heat from the combustion process to heat the home, as stated by Merva (3).

Pulsejets are designed to use the stagnation pressure rise following combustion as a propulsive force. They are always self-aspirating and generate static thrust. Self-aspiration and thrust production occur via the jet pump effect making pulsejet performance dependent on geometry with respect to mixing dynamics and airflow (explained further in Section 2.7). The intake and exhaust pipes of pulsejets have specific lengths such that they are “tuned” to the engine frequency to optimize cycle efficiency, as in two-cycle gasoline engine and Helmholtz resonator-type exhaust systems.

## **2.3 Pulsejet Components and Operating Cycle**

### **2.3.1 Components**

Most pulsejets without moving parts have three primary components: the inlet pipe, the combustion chamber or combustor, and the exhaust pipe. Inside the combustion chamber there are fuel nozzles and an ignition source only used to start the engine. In keeping with the fact that the inlet and exhaust pipes must

have specific lengths based on combustion chamber size, a simple pulsejet is shown in Figure 2-6 (not to scale).

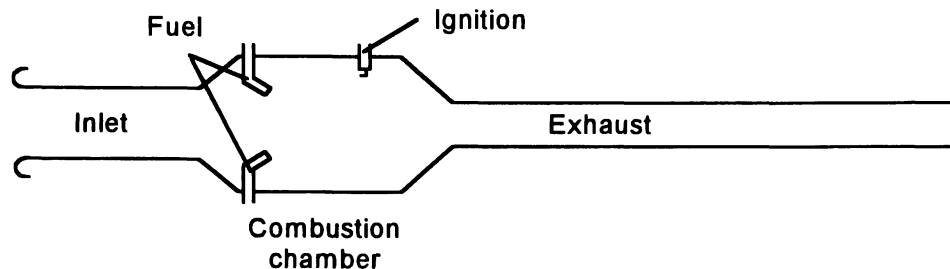


Figure 2-6. Simple Pulsejet

The three primary components have circular cross-sections and are free of any internal protrusions large enough to disrupt the airflow through the engine. For reasons that will be explained in the following section, the inlet pipe has a larger area than the exhaust pipe but is much shorter in length. The fuel nozzles vary in size, shape, spray pattern, and location inside the chamber and will be discussed further in Section 2.7.6. The ignition source is generally located at the center or the aft end of the combustor.

### 2.3.2 Operating Cycle

The most significant difference between a pulse combustor cycle (Figure 2-2) and that of a pulsejet is the exhaust dynamics prior to the intake/compression stage of the cycle. This effect is a direct result of engine geometry and is how the pulsejet generates its thrust. A simplified pulsejet cycle is shown in Figure 2-7.

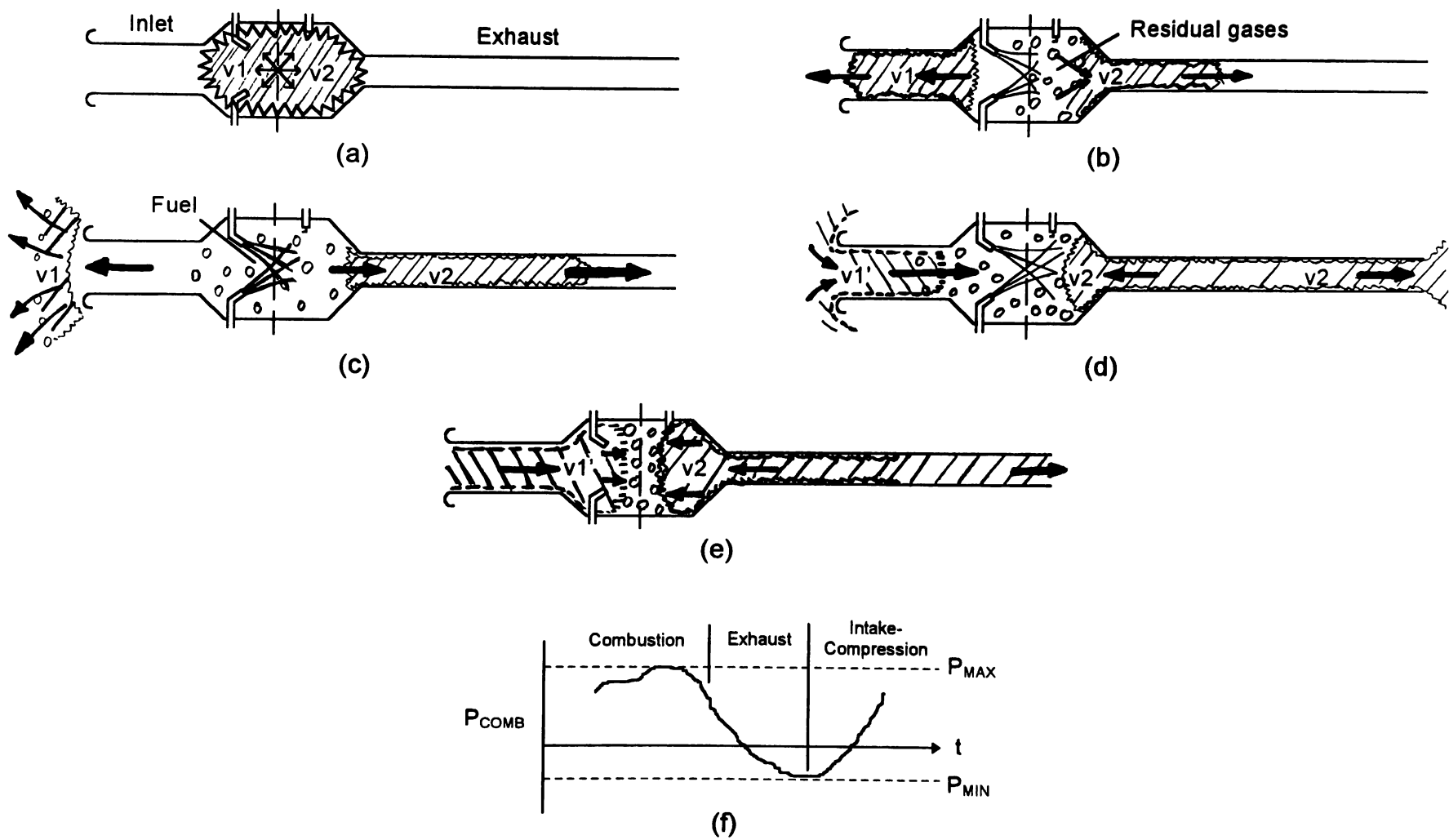


Figure 2-7. Pulsejet Cycle



Figure 2-7a shows that the cycle begins with the isochoric, complete combustion reaction of a well-stirred fuel/air mixture. This stage illustrates that the combustion reactions occur so quickly that they instantaneously fill the combustor. The pressure in the combustor also reaches its maximum value here as shown in Figure 2-7f. Since the pressure rise tends to force the uniformly-distributed exhaust products out of the combustor at both ends, two volumes of exhaust gas,  $v_1$  and  $v_2$ , will leave each opening. These volumes are not necessarily equal as shown by Ponizy and Wojcicki (4) and Narayanaswami and Richards (5), but will be assumed so for simplicity.

Figure 2-7b illustrates part of the exhaust process. Because the inlet area is larger than the exhaust area, less resistance is encountered by  $v_1$  as it leaves the combustor, while at the same time  $v_2$  will take a slightly longer time to exit the combustor completely under the same pressure. This causes residual gases to remain inside the combustion chamber as the intake cycle commences. The pressure now begins to fall within the combustor due to the expansion.

Figure 2-7c is the remainder of the exhaust phase but shows the significance of inlet and exhaust pipe length. Due to the length of the inlet pipe,  $v_1$  does not need to travel far before it is blown out into the atmosphere. On the exhaust side, however, most of  $v_2$  is contained within the much longer pipe and only a small portion is released into the atmosphere. Now that the combustion gases have nearly evacuated the chamber, the pressure inside the combustor

reaches its lowest value of about one half an atmosphere. The fresh fuel that is fed at a constant rate throughout the cycle now creates a rich zone inside the combustion chamber.

Figure 2-7d illustrates only the intake portion of the intake/compression phase. The pressure drop in the combustor pulls gases from both the inlet and exhaust back into the chamber in an attempt to equalize the pressure. Since  $v_1$  has completely left the inlet pipe, a quantity of fresh air,  $v_1'$ , is pulled in with little resistance. Similarly, a small portion of  $v_2$  is also drawn back into the combustor. The pressure begins to rise as the gases return to the combustor volume.

Figure 2-7e completes the cycle by mixing, compressing, and igniting the new mixture. The momentum and flow dynamics of  $v_1'$  mix the fresh air with the fuel and residual gases. At the same time, both  $v_1'$  and the returning exhaust gases compress the mixture to slightly below one atmosphere and raise the mixture to ignition temperature through convection. The pressure sharply rises and the cycle repeats.

## **2.4 Types of Pulsejets**

Although there are several geometry variations and layouts for pulsejets summarized by Putnam *et al.* (1) and Winiarski (2), this section will describe only those influencing the work in this paper. Included will be the significant qualities that each type offers and a description of the performance of each.

### 2.4.1 Mechanically-Valved Pulsejets

Valved pulsejets differs from non-valved engines in that they have a mechanical system that prohibits the backflow of combustion products through the inlet pipe following combustion. The system acts like a check valve allowing only flow from the inlet into the combustion chamber and not vice versa. The valve system is driven by the combustion process itself and not by artificial or external means. Perhaps the most famous valved pulsejet is the Argus 109 engine used to propel the German V-1 “buzz bomb” of World War II (Figure 2-8).

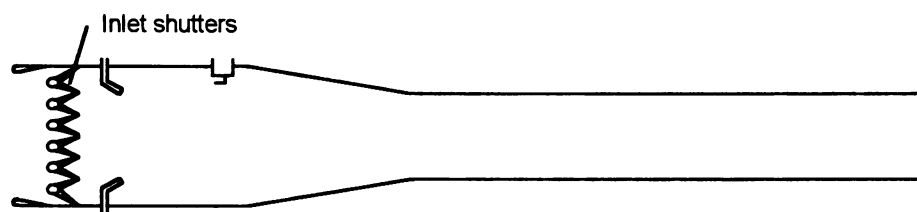


Figure 2-8. Argus 109 Mechanically-Valved Pulsejet

This engine is a derivative of the Schmidt tube device explained in Putnam *et al.* (1) and Kay (6). In the Argus engine, the intake pipe has been replaced with a set of reed-type shutters that close when the combustor pressure rises and open when the pressure falls (Figure 2-8). The cycle of a valved engine does not differ from that shown in Figure 2-6, but requires additional explanation to demonstrate valve operation and purpose.

Figure 2-9a illustrates the combustion process and the inlet valves forced closed under the reaction pressure. Since the exhaust gases can not leave

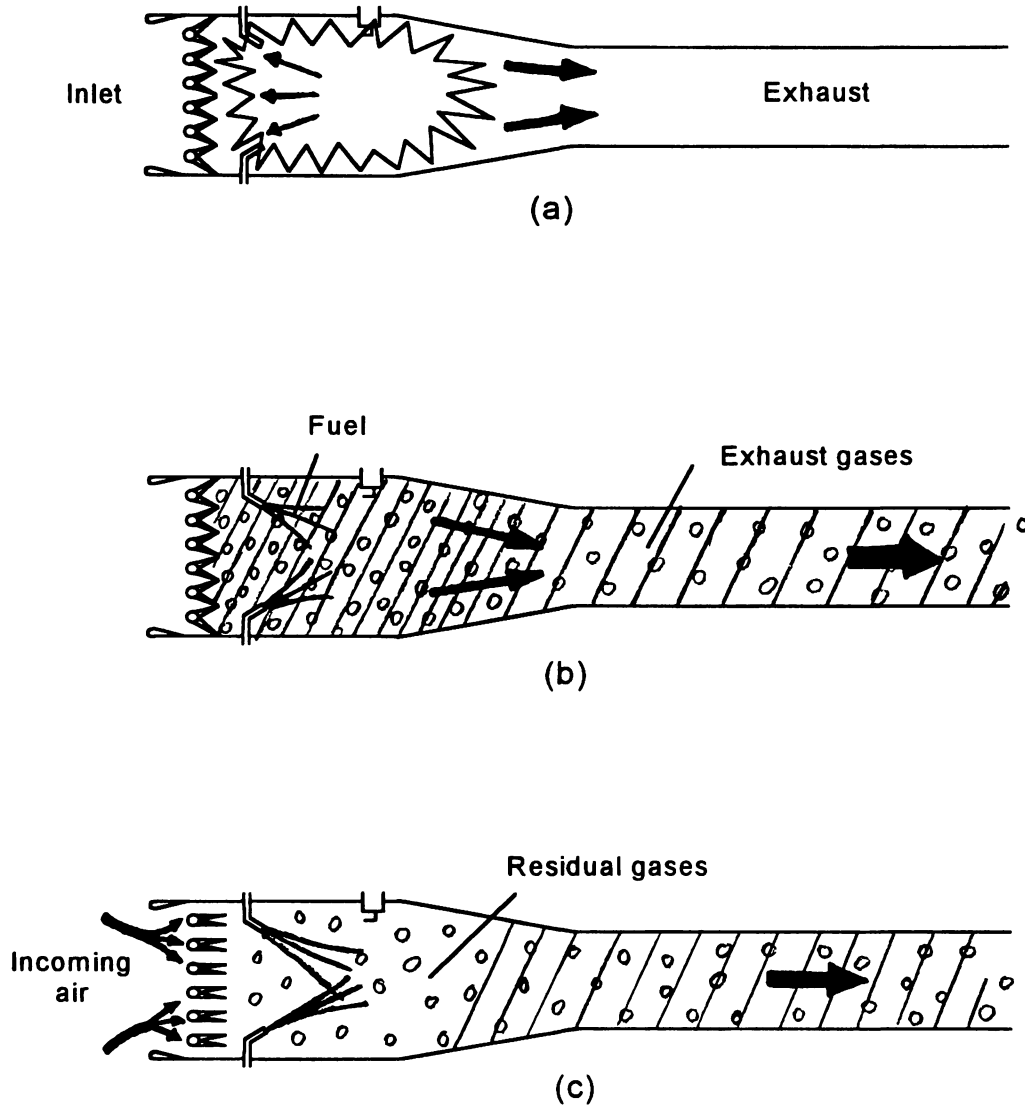


Figure 2-9. Argus Engine Cycle

through the inlet as in a non-valved system, they must exit through the exhaust pipe (Figure 2-9b). The pressure falls below ambient in the combustor, allowing the valves to open and admit a new charge of air (Figure 2-9c). The compression, mixing, and ignition processes of the new charge are identical to those in non-valved systems, and the cycle repeats.

Many variations have been developed on valve systems to control the inlet flow to the combustor, the most significant concern with all of them being valve durability. Exposure to extreme temperatures and rapid heat transfer between cool, incoming air on one side and hot, combustion products on the other, coupled with the high oscillation frequency, have led to the failure of many proposed systems. In addition, designing the valve to admit the proper amount of air in the short time between cycles has also proved to be a difficult task. Once these problems have been surmounted, however, the result will be a shorter engine (lack of an inlet pipe) that produces more static thrust than a non-valved pulsejet of the same dimensions. On the other hand, the noise generated from the valve oscillations can be excessive (reported in some cases to be 130 dBA by Putnam *et al.* [1]) and the engines are prone to mechanical failure.

#### 2.4.2 Aerodynamically-Valved Pulsejets

Pulsejets without any moving or mechanical parts are termed “aerovolve” or aerodynamically-valved engines. These engines and their cycle were

exemplified in Section 2.3. Although the primary advantage of these engines over valved pulsejets is their simplicity, there are many design factors that must be considered before an aerovalve pulsejet can function. Putnam *et al.* (1) has verified that aerovalves are very sensitive to combustor, inlet, and exhaust pipe geometry. Once a basic engine has been built, the associated areas and volumes must be tailored to accommodate the cycle frequency and fuel requirements. They are supposedly quieter than valved engines, but are not as efficient in thrust production since a portion of the fuel injected during the combustion process gets blown out of the inlet with the exhaust gases during the expansion phase. In addition, no net thrust is produced by engines of axisymmetric configuration since the same mass flows leave in opposite directions through the inlet and exhaust pipes.

The first aerovalve pulsejet (Figure 2-10) was developed in 1909 by a French engineer, Marconnet. His pulsejet was designed for propulsion and was later converted to a valved engine for which he was awarded a patent. This engine has the axisymmetric arrangement mentioned earlier.

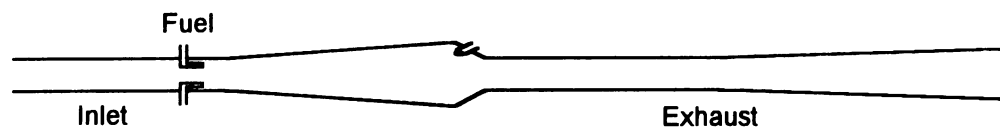


Figure 2-10. Marconnet Aerovalve Pulsejet

Perhaps the most significant contributor to aerovalve development was from a French engine company, SNECMA, who in 1950 produced the Escopette engine in Figure 2-11.

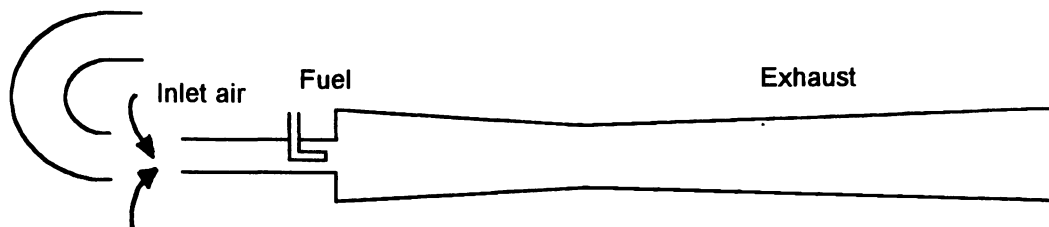


Figure 2-11. SNECMA Escopette

This design redirects the exhaust products ejected from the inlet through a rearward-facing duct. Thrust is produced now that all exhaust flows from the engine in the same direction. The gap between the U-tube and the inlet pipe permits inlet airflow for the next cycle.

SNECMA simplified the Escopette concept in 1953 to the Ecrevisse design (Figure 2-12). The Ecrevisse has both the inlet and exhaust pipe facing rearward and is essentially a Marconnet engine with a bent exhaust pipe.

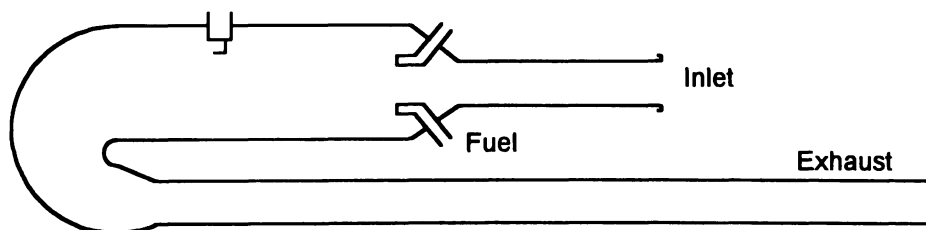


Figure 2-12. SNECMA Ecrevisse

Around 1955, R. M. Lockwood began to investigate thrust augmentation of aerovalve engines and became a research consultant for Hiller Aircraft Company (California) involved with developing efficient pulse combustion engines for propulsion. Together, they conducted extensive research into aerovalve pulsejet design and produced most of the foundations of the subject (Ref. 7). After the research was published around 1962, Lockwood developed a version of an Ecrevisse engine with thrust augmentors and optimum design parameters stated in his research. The Lockwood U-tube (Ref. 8) has unique thrust augmentors (also developed by Lockwood) which utilize the static pressure drop of the jet efflux to draw surrounding air into the jet stream adding more mass to the flow and producing more thrust. Figure 2-13 illustrates the Lockwood engine and augmentor operation.

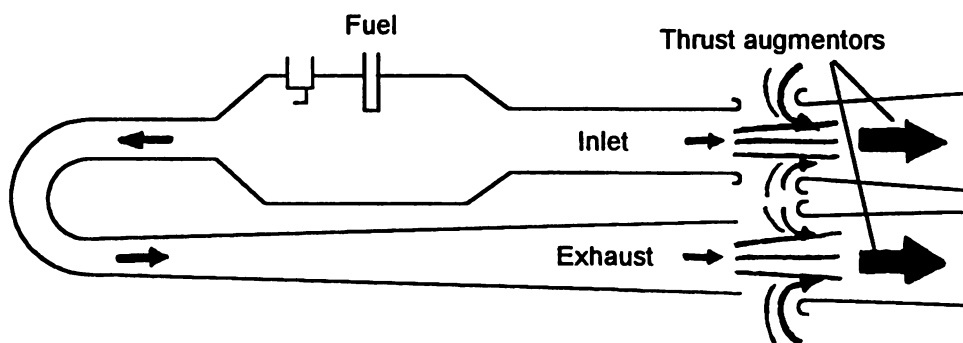


Figure 2-13. Lockwood U-Tube and Thrust Augmentors

## 2.5 Comparison of Pulsejets to Other Propulsion Systems

Since pulsejets use a jet-pump effect and exhaust stream to produce thrust, the comparison to reciprocating or rotary-type engines is not significant.



The closest family of steady-combustion engines to pulsejets with respect to operating cycle and thrust production are ramjets, followed by gas turbine engines.

Ramjets, like aerovalve engines, have no moving parts but their geometry is much different. Ramjets use a centerbody (or inlet duct design) to generate shock waves for compression of the incoming air, inject fuel, burn the mixture under steady conditions, and exhaust the products. Thrust production is primarily from stagnation pressure rise across the engine and from the increased entropy of the exhaust stream due to the heat addition (Rayleigh flow). Unlike aerovalve engines, ramjets cannot produce static thrust and must attain sufficient velocity (through external means) to begin functioning. They also depend on aerodynamic design such that the flow progresses in a steady manner through the engine with minimal losses. Since pulsejets, in effect, function through a series of contained explosions, aerodynamic design is not as significant.

Although the differences between pulsejets and gas turbine engines are extensive, the most notable differences are complexity and efficiency. Gas turbine engines have the disadvantage of moving parts and hundreds of components, leading to increased failure rate and design complexity. They are, however, more fuel efficient than pulsejets and produce more thrust for a given size as consequences of the gas turbine operating cycle. On the other hand, gas turbine engines are costly, heavy, and are extremely sensitive to foreign

object ingestion. Aerovalved pulsejets, however, can ingest a variety of substances (dirt, hay, sand, etc.) with no damage or interruption in cycle, as proven by Lockwood (7).

## **2.6 Applications of Pulsejets**

With respect to the usefulness of pulsejets and pulse combustion devices, early researchers saw a variety of applications ranging from flight propulsion to food product drying. Propulsion, however, saw the largest level of development and has produced most of the design optimization concepts used in engines intended for other applications. The most famous (or infamous) application of pulsejets was powering the German V-1 “buzzbomb” during World War II. Since then Lockwood and Hiller have explored, and in some cases tested, many additional aircraft uses ranging from helicopter rotor tip jets to VTOL aircraft. Currently, pulsejets are being investigated for propulsion of military target drones, remotely piloted vehicles, and some homebuilt aircraft (Taylor [9]).

Established uses for pulse combustors are residential and commercial heating (Lennox pulse furnace), fog/insecticide pumping, hydronic water heating, snow and ice melting, and food product drying (all mentioned in Putnam *et al.* [1]).

## **2.7 Variables Affecting Pulsejet Performance**

Because pulsing operation occurs in the narrow region between steady combustion and flame out states, the dimensions of a pulsejet must allow the proper thermodynamic conditions to occur so that the engine can start and maintain its cycle. Thus, the geometry is critical to how a pulsejet will function, based on thermodynamic cycle and, to some extent, acoustic behavior. Lockwood (7) conducted extensive experimental research into pulsejet component designs and has correlated many geometry relations with engine thrust and thrust specific fuel consumption (TSFC).

This section will discuss the design significance of each component in an aerovalve pulsejet engine and its effect on performance. When possible, each section will include a component comparison of all of the functioning pulse engine designs found during the research of this paper. No information was found concerning valved pulsejets or valve system design. All of the references used in this paper deal with engines at static conditions, and give no discussion on how (or if) engine geometry needs to be changed to maintain performance at altitude or flight speed.

### **2.7.1 Inlet Lip Shape**

The inlet pipe lip of a pulsejet acts similar to a bell-mouth inlet used in gas turbine engine static testing. The wide bell-mouth shape used on gas turbines provides maximum air mass flow with little disturbance into the engine during

operation. Although this is also desirable for pulsejets, Lockwood (7) has shown that the pressure drop over the inlet lip during the intake phase of the cycle acts as a negative thrust on the unit. His results recommend an inlet lip of lemniscate shape that enables a compromise between maximizing the inlet mass flow while keeping the pressure drop to a minimum (Figure 2-14).

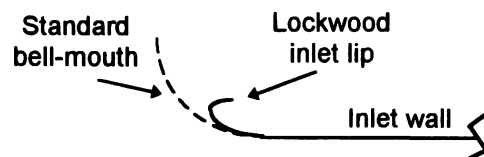


Figure 2-14. Aerovalve Inlet Shapes

### 2.7.2 Inlet Pipe Length

The importance of inlet pipe length was summarized in describing pulsejet operation in section 2.3.2. Each aerovalve pulse combustor has an inlet length required for optimum cycle efficiency. If the inlet length falls short, the combustion products leaving through the inlet pipe will be expelled to the atmosphere before the pressure reaches a minimum inside the combustion chamber. This causes premature ingestion of air, a resulting drop in the cycle peak pressure, and could interfere with the air/fuel mixing process. Conversely, if the inlet is overly long, the engine may not receive enough air for the next cycle since exhaust gases would still be in the tube during the onset of the intake phase. Putnam *et al.* (1) has demonstrated both of these conditions and concludes that there is a definite limit to the maximum length of the inlet pipe for

aerovalue pulsejets. Varying the inlet length will gradually decrease engine performance if lengthened or shortened from optimum. Since valved engines do not encounter backflow through the inlet pipe, their inlet lengths have no length restriction.

### 2.7.3 Inlet Pipe Cross-Sectional Area

Inlet area has a similar effect to inlet length, only this parameter has a direct effect on mass flow. If too large, too much exhaust product will escape during backflow before the cycle reaches a minimum pressure, and if too small, not enough will escape to allow ingestion of fresh air. Putnam *et al.* (1) states that research has shown the optimum inlet cross-sectional area is often substantially smaller than the cross-sectional area of the combustion chamber, but no research has indicated by how much.

### 2.7.4 Combustion Chamber Geometry

The three, distinct parts of a pulsejet combustion chamber (Figure 2-15) must be shaped correctly to accommodate sufficient mixing of air and fuel while allowing uninterrupted passage of inlet and exhaust gases through the chamber. First, the inlet bulkhead is the section immediately downstream of the inlet pipe where the incoming air expands into the second part, the combustor. The combustor portion comprises most of the length of the total combustion chamber

and is usually of constant cross-section. The third part is the aft bulkhead or exhaust nozzle where the reaction products pass into the exhaust pipe.

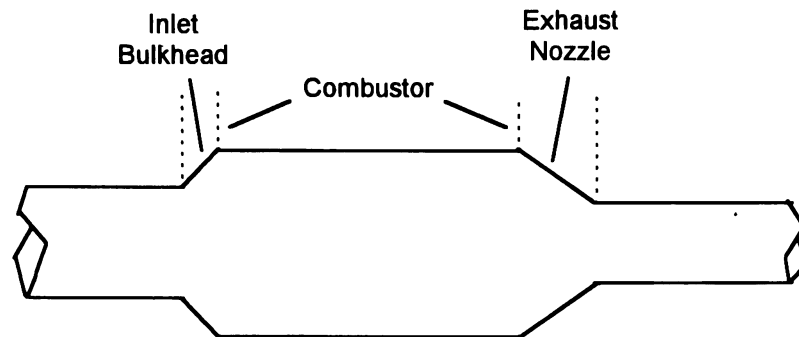


Figure 2-15. Combustion Chamber Components

#### 2.7.4.1 *Inlet Bulkhead*

The inlet bulkhead is typically designed as an expansion from the inlet area. The angle of divergence can range from 90 degrees (flat plate) to no less than 45 degrees (conical). Research of engine designs has shown that either 90 or 45 degree bulkheads are preferred and seem to deliver adequate engine performance. Aerodynamically, the sudden area expansion from the inlet creates the slight pressure rise and velocity decrease of the incoming air. Fuel/air mixing is influenced by the vortices and residual wakes formed as the inlet air passes from the inlet through the bulkhead. Lockwood (7) has demonstrated through extensive engine testing that the best inlet bulkhead design for pulsejets is the 45-degree conical configuration. He also claims that the 90-degree bulkhead, a flat plate at the combustor face, poses structural

difficulty. This conclusion was not explained and seemed to be unfounded since many pulsejet and pulse combustor designs using the 90-degree bulkhead reported no problems with structural integrity (Ponizy and Wojcicki [4], Keel and Shin [10], and Richards and Gemmen [11]).

#### 2.7.4.2 Combustor

Combustor size determines the proportions of a pulsejet's inlet and exhaust pipes. Combustor diameter is the most significant in this respect and has been shown to greatly influence fuel requirements, operating frequency, and overall engine performance (thrust being the most significant). Combustors have always been circular and, with the exception of the Marconnet engine, are of constant cross-sectional area.

Research has been conducted by Lockwood (7) and Putnam *et al.* (1) investigating combustor length and diameter effects on thrust. Lockwood states that as combustor size decreases, the engine thrust-to-volume ratio increases. He also concludes from experimentation that, since the space and time for the fuel and air to mix are reduced, the combustion frequency increases. Eventually, a combustor will be so small (approximately 4-inches in diameter) that the performance of the engine will be compromised, in part due to fuel system miniaturization problems. The last of the conclusions does not seem to be accurate since Putnam *et al.* and the author have noted many researchers who developed and tested engines of smaller diameters with satisfactory

performance and no significant component problems. Lockwood also indicates, but does not explain, that as combustor diameter is decreased the length should increase to maintain optimum performance. This may be a result of the Helmholtz acoustic equations' dependency on combustor volume.

In other terms, Putnam *et al.* (1) finds that the thrust specific fuel consumption increases and the thrust-per-unit exit area decreases if the combustor diameter is reduced. Rehman in Putnam *et al.* compares and substantiates Lockwood's data to other engines to illustrate a trend of rising maximum specific thrust over increasing combustor diameter.

#### 2.7 4.3 Exhaust Nozzle

An exhaust nozzle is present on all pulsejet designs and directs the combustion products into the exhaust pipe during the expansion phase of the cycle. It is designed similar to the inlet bulkhead but converges from the combustor area down to the exhaust pipe area. The converging shape of the nozzle directs the proper amount of exhaust gases into the pipe while still retaining enough for ignition in the combustion chamber. The angle of convergence varies with engine designs, but Lockwood (7) found the best angle for nozzle performance to be between 30 and 45 degrees. Early pulsejets had shallower angles for their nozzles and the valved Schmidt tube (shown in Putnam *et al.* [1]) had no exhaust nozzle at all. Lockwood has illustrated that the 45-degree nozzle drastically reduces the exhaust pipe length required to



maintain the thrust gained by combustor elongation. This allows for a shorter combustor and exhaust pipe and raises the thrust-to-volume ratio. However, no explanation is given, thermodynamic or otherwise, as to the nature of these results. One possibility may be a greater pressure rise and velocity drop of the returning exhaust gases during the intake phase. The effect would be similar to that seen by the incoming air through the 45-degree inlet bulkhead.

#### 2.7.5 Exhaust Pipe Geometry

A substantial portion of the research on pulsejets calls the exhaust pipe a resonance tube because of its role in pulsejet operation. As mentioned earlier, pulsejets must be “tuned” to their operating frequency much like two-cycle reciprocating engines or Helmholtz resonators. The length and area taper of the exhaust pipe control the tuning effect, and play a large part in engine performance and thrust production. In addition to matching acoustic frequency, research has shown that the design objective for the exhaust pipe is to contain sufficient exhaust gases within it such that enough is drawn into the combustion chamber for ignition during the subsequent intake/compression phase while preventing the ingestion of fresh air into the pipe. Owing to this requirement, the inlet pipe and combustion chamber configurations drive the design requirements of the exhaust pipe. Lockwood (7) has exemplified this by having shown that an inlet pipe divergence of around 2 degrees drastically reduced the exhaust pipe length necessary to produce the same thrust as with a straight inlet pipe.

Extensive experimentation concludes that the exhaust pipe length can be used to find the optimum thrust-to-volume ratio. Lockwood also states that the exhaust nozzle angle plays a role in exhaust pipe length, as mentioned in the previous section.

Both Lockwood (7) and Corliss (stated in Putnam *et al.* [1]) have experimented with tapered and constant-area exhaust pipes. Lockwood varied the taper angle and length of several pipes on a baseline SNECMA aerovalve engine and measured the performance, but never attempted a constant-area version. His findings indicated that certain fineness ratios (length-to-diameter) developed either better thrust-to-volume or improved TSFC. Corliss, however, found his tapered pipe results to be contrary to those of Lockwood, and experienced better overall performance from constant-area exhaust pipes. One reason for the differences as explained by Putnam *et al.* is that the Corliss pulsejets did not have as high of a pressure-gain as the SNECMA/Lockwood engines due to the fuel (gasoline) and combustor geometry. Research for this paper has shown that most aerovalve units use a tapered exhaust pipe to take advantage of the pressure rise as the emerging exhaust gases pass from the smaller area at the exhaust nozzle to the larger area of the exhaust pipe end.

#### 2.7.6 Fuel/Air Mixing Characteristics

The mixing dynamics of the fresh air, new fuel charge, and residual exhaust products between each pulse is essential for a pulsejet to function. The

mixture must be sufficiently stirred for combustion at the moment the exhaust gases return to the combustion chamber and ignite it. Since the inlet air column flow is determined by the inlet and inlet bulkhead, optimum efficiency will be achieved only if the fuel nozzle location in the combustor, the fuel nozzle spray pattern, and the mixing time are appropriate.

In addition to fuel nozzle location, Lockwood (7) experimented with nozzle configurations and spray patterns leading to several novel injector designs. His tests focused on nozzle location along the combustion chamber and concluded that the fuel nozzles should be positioned at or near the area in the combustor most likely to experience the highest mean pressure during the cycle. His experiments with nozzle design show that the fuel sometimes gets blown back far enough into the fuel line during the pressure-rise portion that it is not injected into the chamber in time for the next cycle. The addition of restrictors (similar to check valves) in the nozzles prevented this. Although no description was given as to the type of fuel used in the Lockwood engines, it is believed to be gaseous since the above phenomenon would be less likely to occur in a pressurized liquid-fueled system due to the higher density and inertia. Tests were also conducted with the fuel being injected along the engine axis via a fuel line that traversed the inlet pipe and ended at the predicted point of highest mean pressure. Engine performance was the same with only the TSFC suffering due to unburned fuel being blown out of the chamber during the blowback of combustion gases through the inlet. Keel and Shin (10) experimented with axial

injection to some extent on a Helmholtz combustor model with favorable results. Because of the blowback, however, Lockwood's research favored fuel injection perpendicular to the engine axis.

The gas dynamics and flow fields associated with pulse combustion are far from the steady, adiabatic conditions usually exhibited by other cycles. Understanding the methods by which the fuel and air mix and combust would certainly permit pulsejet designers to take advantage of the many phenomena that are observed in experiment but ambiguous in theory. Several experimental procedures have successfully mapped the combustion process with respect to time. Some of the methods include measuring ion currents in the exhaust stream (Keel and Shin [10]), seeding the inlet flow with NaOH and measuring the CH and Na radicals in the exhaust (Ponizy and Wojcicki [4]), and incorporating quartz glass windows on the combustion chamber to photograph the flame dynamics (also Ref. 4).

Using the experimental data, mathematical models of the pulse combustion cycle could be modified to better predict the combustion characteristics. A multitude of variables and high degree of uncertainty associated with the combustion process make mathematical modeling difficult even with today's computer technology and analytical techniques. Putnam *et al.* (1) and Winiarski (2) conclude that, although less expensive, the time it would take to solve the complex equations associated with such models would be just as long (or longer) as the time to build and test a functioning device. In addition,

the models attempt to predict the effects of pulse combustion and are not currently used as a design criteria for pulse combustion devices. Designs that have been shown to function based on mathematical predictions may not work in experiment (Putnam *et al.* [1]), yet others operate very close to the model results (Narayanaswami and Richards [5]).

## **2.8 Trends in Pulsejet Design**

### **2.8.1 Variable Definition**

The information found in the research collected by the author has provided dimensions and/or drawings of eight aerovalve pulsejet designs and of the aerovalve pulse combustor found in Richards and Gemmen (11). The pulse combustor is arranged similar to an aerovalve pulsejet and is, therefore, included in this discussion. All of these devices functioned and were used for experimentation. Comparison of the engines' layout and geometry relations clearly indicate trends on how aerovalve pulsejets have been designed over the years. The geometry variables for an aerovalve engine used in comparison are described in Figure 2-16.

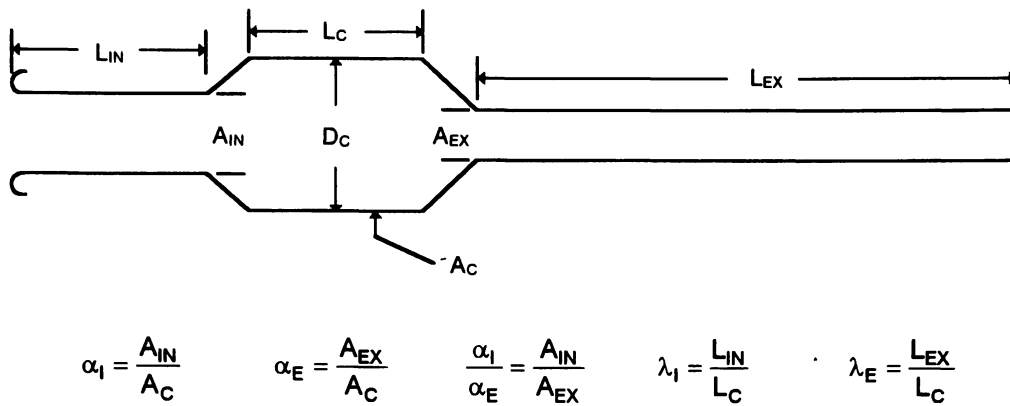


Figure 2-16. Pulsejet Geometry Variables

The areas  $A_{IN}$  and  $A_{EX}$  are measured at the entrance and exit to the combustion chamber and are not necessarily the inlet and exhaust pipe areas. The length of the combustor,  $L_C$ , does not include the length of the inlet bulkhead or exhaust nozzle, and is measured parallel to the engine axis. By defining the areas and lengths as such, all aerovalve pulse combustor and pulsejet designs can be generalized, including those incorporating variable-area components. All five parameters shown in the figure can be used for pulsejets, but only those concerning area dimensions can be applied to pulse combustors.

There are three types of relationships evident from the research: those involving inlet dimensions, those with exhaust dimensions, and general engine layout. The engines compared in the tables to follow are identified by their primary experimenter and the combustion chamber diameter.

## 2.8.2 Inlet Relationships

A trend in aerovalve engine design relates the inlet cross-sectional area to that of the combustion chamber, as denoted by  $\alpha_i$  in Table 2-1. The successful engines designed by Lockwood and Kentfield illustrate that the inlet area is roughly one-third of that of the combustor. The engines of Corliss, Ponizy, and Richards, however, do not follow this trend. This is because the Ponizy and Richards engines were designed for the measurement of combustion dynamics and not for thrust development, as were Lockwood's and Kentfield's. The Corliss engine was designed for thrust production but was known to have performed poorly (Putnam *et al.* [1]). No information on how the area relations were determined have been encountered during research.

Examination of Table 2-1 also shows the inlet pipe length to be very close to that of the combustor. Although the author has not come upon any research to explain the similarity, it is evident that even Marconnet was familiar with the issue in the design of his engine (Figure 2-10). The  $\lambda_i$  values are much closer to one another than those of  $\alpha_i$ , especially when comparing Lockwood's and Kentfield's engines.

Their designs illustrate that the inlet pipe length should be the same as the combustor length, whereas the other experimenters show the inlet length to be roughly two-thirds of the combustor. As with  $\alpha_i$ , this difference is also due to engine purpose (combustion research or thrust production).

Table 2-1. Pulsejet Inlet Relationships

Experimenter ( $D_c$ )	$A_c$ (in <sup>2</sup> )	$L_c$ (in)	$A_{IN}$ (in <sup>2</sup> )	$L_{IN}$ (in)	$\alpha_i$	$\lambda_i$
Lockwood (9.1-in)	65.04	20.0	19.64	20.0	0.3	1.0
Lockwood (5.25-in)	21.65	11.5	8.3	11.5	0.38	1.0
Lockwood (5.25-in)	21.65	11.0	7.67	12.0	0.35	1.09
Lockwood (5.25-in)	21.65	13.0	9.08	13.0	0.42	1.0
Lockwood (5.0-in)	19.64	13.0	7.67	12.3	0.39	0.95
Corliss (4-in)	12.56	8.0	0.99	5.0	0.079	0.625
Kentfield (3-in)	7.41	5.32	1.95	5.59	0.26	1.05
Ponizy (2.5-in)	4.83	12.2	0.487	9.45	0.1	0.775
Richards (2.2-in)	3.82	5.98	.0196	3.94	0.051	0.66
<b>Averages of Lockwood &amp; Kentfield</b>					<b>0.35</b>	<b>1.02</b>

In general, the inlet relations do not seem dependent on combustor diameter, as given in the first column of Table 2-1. The Corliss engine is larger than the Kentfield design, yet deviates from the trends supported by the engines of Lockwood and Kentfield. Similarly, the diameter of the Ponizy engine is only one-half inch less than Kentfield's and also does not comply with trend observations

### 2.8.3 Exhaust Relationships

Table 2-2 shows the exhaust relationships among the available engine geometries. Nearly all the engines have exhaust areas just under one-quarter



the area of the combustor. The exceptions in this case are the engines of Kentfield and Richards.

Table 2-2. Pulsejet Exhaust Relationships

Experimenter ( $D_c$ )	$A_c$ (in <sup>2</sup> )	$L_c$ (in)	$A_{EX}$ (in <sup>2</sup> )	$L_{EX}$ (in)	$\alpha_E$	$\lambda_E$
Lockwood (9.1-in)	65.04	20.0	15.9	108.6	0.24	5.43
Lockwood (5.25-in)	21.65	11.5	4.91	61.5	0.23	5.35
Lockwood (5.25-in)	21.65	11.0	4.91	62.5	0.23	5.68
Lockwood (5.25-in)	21.65	13.0	4.91	72.0	0.23	5.53
Lockwood (5.0-in)	19.64	13.0	4.91	68.25	0.25	5.25
Corliss (4-in)	12.56	8.0	3.14	67.0	0.25	8.38
Kentfield (3-in)	7.41	5.32	0.954	36	0.13	6.77
Ponizy (2.5-in)	4.83	12.2	0.954	40.64	0.2	3.33
Richards (2.2-in)	3.82	5.98	0.444	23.62	0.12	3.95
<b>Averages of Lockwood &amp; Kentfield</b>					<b>0.22</b>	<b>5.67</b>

Table 2-2 illustrates that the Kentfield engine has a high  $\lambda_E$  when compared to the Lockwood designs, with the Corliss engine  $\lambda_E$  being well above the others. The much lower and similar  $\lambda_E$  values of Ponizy and Richards are not a result of their small diameter. Independence of  $\lambda_E$  from combustor size can be justified since Kentfield's combustor is only slightly larger than Ponizy's and yet has over twice the  $\lambda_E$  ratio. In addition, the Lockwood 9.1-inch diameter combustor has a  $\lambda_E$  ratio very close to those of the 5.25 and 5-inch combustors.

The relationships between exhaust geometry and combustor design are a

result of the Helmholtz fundamental acoustic frequency equation, as shown by Putnam *et al.* (1) and Keel and Shin (10). The approximate frequency of a Helmholtz resonator is given by:

$$f = (C/2\pi) \cdot (S/LV)^{0.5}$$

where

- C = speed of sound in exhaust pipe
- S = exhaust pipe neck area
- L = exhaust pipe length
- V = combustor volume

Since the literature on the pulsejets evaluated provided only a few of the above variables, verification of engine design based on the Helmholtz equation was not possible.

#### 2.8.4 General Observations

Table 2-3 illustrates other ratios that can be compared between the nine engines. The area ratio,  $(\alpha_I / \alpha_E)$ , relates the inlet to exhaust areas. For most aerovalve pulsejets, the exhaust area is smaller than the inlet area, which also holds true for the Lockwood and Kentfield engines. This observation does not apply to the Corliss, Ponizy, or Richards designs. The  $(\alpha_I / \alpha_E)$  ratios smaller than unity for those engines indicate that the inlet area is less than the exhaust area.

The reason behind the larger exhaust area may be that the Ponizy and Richards engines were designed for observation, and not propulsion, as

mentioned in Section 2.8.2. The area ratio might also be one cause of poor performance in the Corliss engine since it was intended for thrust. Nevertheless, the more promising engines of Lockwood and Kentfield demonstrate that the inlet area should be slightly less than twice the exhaust area.

Table 2-3. General Pulsejet Relationships

Experimenter ( $D_c$ )	$(\alpha_i / \alpha_E)$	$(L/D)_c$
Lockwood (9.1-in)	1.24	2.2
Lockwood (5.25-in)	1.69	2.19
Lockwood (5.25-in)	1.56	2.1
Lockwood (5.25-in)	1.85	2.48
Lockwood (5.0-in)	1.56	2.6
Corliss (4-in)	0.32	2.0
Kentfield (3-in)	2.04	1.77
Ponizy (2.5-in)	0.51	4.9
Richards (2.2-in)	0.44	2.72
<b>Average of Lockwood &amp; Kentfield</b>	<b>1.66</b>	<b>-----</b>
<b>Average of all exc. Ponizy</b>	<b>-----</b>	<b>2.26</b>

The combustor length-to-diameter ratio,  $(L/D)_c$ , also listed in Table 2-3, shows that the combustor length should be around twice the diameter, with the obvious exception being the Ponizy engine. The Ponizy combustor was elongated to accommodate quartz glass windows for flame observation (mentioned in Section 2.7.6). Even though Lockwood states that the combustor length should be increased if the diameter is reduced, this is only necessary to

maintain the optimum thrust-to-volume for a given engine geometry (see Section 2.7.4.2). Neither Lockwood nor any other researchers explain why the L/D ratio for the combustor should be around two.

Through observation of both mechanically-valved and aerovalve pulsejet designs, the author has noted that the geometries of the two types of engines are similar from the combustor aft. This supports the requirement of matching the exhaust (resonance) pipe to the combustor size and pressures (“tuning” the engine).

## **CHAPTER 3**

### **DEVELOPMENT OF EXPERIMENTAL PULSEJET**

#### **3.1 Pulsejet Research Objective History**

The original goal of the research conducted by the author was to develop and test a novel air inlet valve system for a pulsejet engine. In order to evaluate the valve concept, a pulsejet based on one of the Lockwood engines (the HH (5.25")-5 from Ref. 7) that incorporated the valve system was designed and constructed by the author. The engine included variable fuel injection and ignition locations within the combustor so that its performance could be optimized. Performance parameters were to be measured by instrumenting the combustion chamber to obtain pressure readings, temperatures, and mass flows.

The design objective for the valve system was to minimize or eliminate any mechanical oscillation inherent to reed and flapper-type valve systems (as used on the Argus and DynaJet pulsejets) such that fatigue life would be significantly increased. A valve system was then developed that utilized a ported rotor connected to a turbine that was driven during the pressure rise portion of the combustion cycle (Figure 3-1). As the rotor spun, fresh air would enter the combustor twice during one rotation.

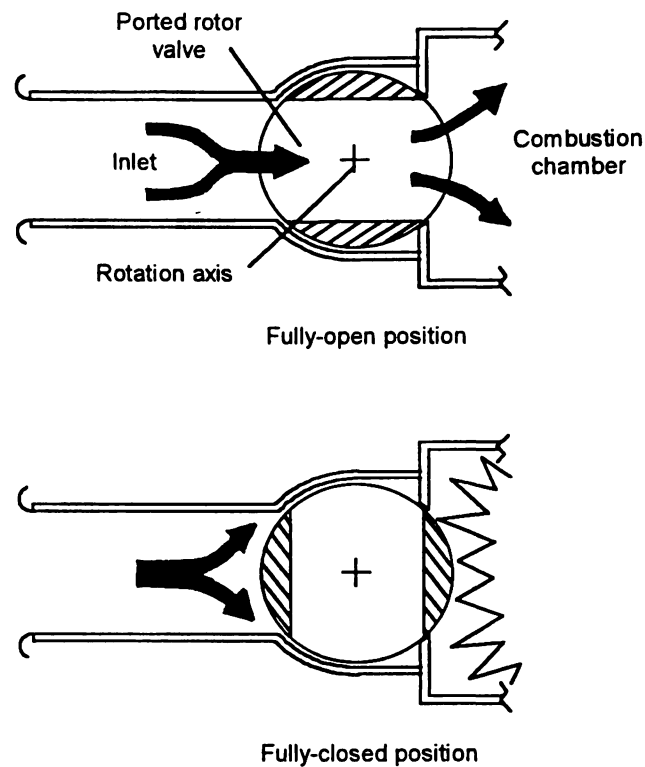


Figure 3-1. Ported Rotor Valve Cycle

Since the valve has only one moving part, which rotates in one direction, fatigue life of the system is greatly extended and the system is much quieter. In addition, each component is easy to manufacture since lower part tolerances are permissible. One significant drawback of the system, however, is that the valve position must be precisely timed with the operating frequency of the engine such that the valve is in the correct position with respect to the combustion cycle (fully-open at minimum pressure and fully-closed at maximum pressure). Another downfall is that the maximum combustion pressure must be sufficient to

drive the turbine/rotor valve system without significantly compromising thrust or cycle efficiency.

The ported rotor inlet valve was tested on the experimental pulsejet engine mentioned earlier and did not function as expected. The reason was not the valve system but the engine geometry. Investigation into the component design according to the research available revealed that the engine was not conducive to pulse combustion behavior. As a result, the components were modified to create an aerovalve engine. The reasoning was that if the engine functioned (pulsed) as an aerovalve, then adaptation of the valve system would be successful since the faulty component geometries would have been corrected. The new aerovalve engine had the same combustor geometry as the valved design (including the variable fuel and ignition locations), but the inlet and exhaust dimensions were slightly different.

Testing of the aerovalve version of the engine also proved unsuccessful. The device would ignite and either burn steady or flame out with no tendency to pulse. After many weeks of part modification and subsequent testing (covered in Chapter 5), the goal of the project then became the production of a self-aspirating aerovalve pulsejet and evaluation of performance through variation of fuel injection and ignition location.

After extensive testing and continual redesign under the new objective, the engine eventually began to pulse, but only when air was directed into the inlet from a compressed air source. If the air pressure was reduced or removed,

the engine would burn overly rich and steady. On the other hand, if the air pressure were increased and the fuel/air ratio was adjusted by adding more fuel, the engine would pulse strongly. Further experimentation revealed the throttleable range of the engine between the too-rich and too-lean flame-out limits of the mixture ratio, with an even narrower range yielding the most robust pulse operation.

It should be noted that all of the testing until this point employed no instrumentation other than fuel and air pressure gauges. The pulsing characteristics of the engine were evaluated based on aural and visual observations made by both the author and testing assistants. Data to support the pulsing and steady operation of the engine will be given in Chapter 5.

Since the engine did not show any tendency to self-aspirate, the goal of the project changed to compare various thrust measurement techniques for pulsejet engines. This issue had never been discussed in detail by any research literature and posed many questions to the author as to the validity of the thrust-measuring methods used to obtain data in the reports. The measurements of the combustor pressure, the total pressure rise across the engine, and the dynamic pressure of the exhaust jets were to be compared using a pressure transducer, a manometer, and a load cell, respectively. Experimenting with each procedure demonstrated that all but the combustion pressure method had numerous sources of error that arose from the non-self-aspiration of the engine,



the engine layout, and the resolution of available instrumentation. These issues will also be discussed later in Chapter 5.

Since a valid comparison between the thrust measuring methods was no longer possible and the deadline for project completion was drawing nearer, the project goal changed back to attaining aerovalve self-aspiration and evaluating performance.

That objective remained until the experimentation was terminated. The following sections of this chapter will describe the design considerations and geometry of each component of the final engine configuration.

## **3.2 Engine Development and Configuration**

There are two primary factors that contributed to the general dimensions of the experimental engine. The first was the baseline engine used by Lockwood from which the overall geometry of the project engine components were scaled, and the second was the historical trends found in pulsejet design as discussed in Section 2.8.

### **3.2.1 Baseline Lockwood Engine**

The Lockwood HH(5.25")-5 engine mentioned in Section 3.1 is shown in Figure 3-2 as illustrated in Ref. 7.

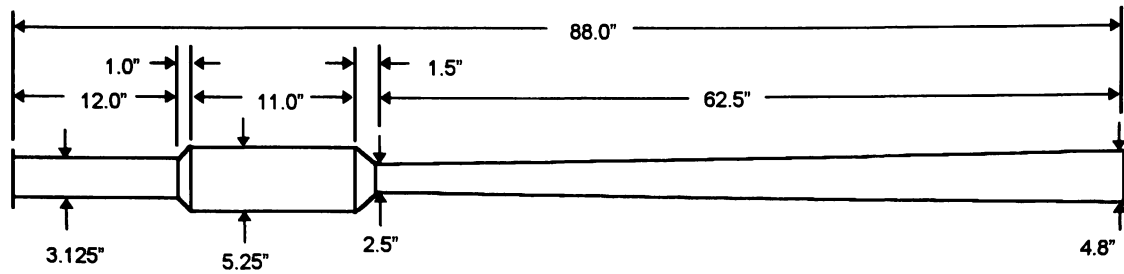


Figure 3-2. Lockwood Model HH(5.25'')-5 Aerovalve Engine

This particular model was selected as a baseline for the experimental engine in this project for its general size and optimized performance as stated in Lockwood (7). Since this engine was larger than desired, however, the engine dimensions were scaled down from a 5.25-inch diameter combustor to a 4-inch diameter for several reasons: First, a smaller engine would yield lower material costs and part manufacturing time; second, the component size of a 4-inch diameter engine could be more easily handled by the machining equipment used in manufacturing; third, smaller components reduce assembly and maintenance time; and fourth, if the diameter were smaller than four inches, sub-system miniaturization problems as expressed in Lockwood (7) may have been encountered, as well as machining and assembly difficulties.

Scaling down of the Lockwood model was justified by the scaling up of the same engine as Lockwood (7) had done on numerous occasions. In addition, Tables 2-1, 2-2, and 2-3 in the last chapter illustrate that the geometry trends are similar regardless of engine size. Thus, the general dimensions of this

project's experimental engine, named *Astra*, in its final configuration are shown in Figure 3-3.

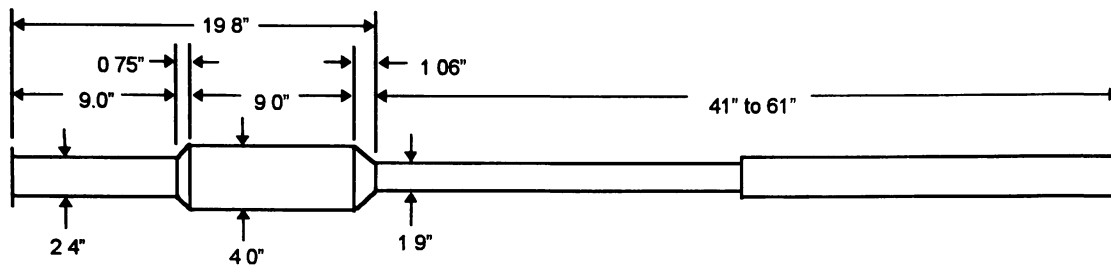


Figure 3-3. *Astra* Experimental Engine

### 3.2.2 Using the Trends in Pulsejet Design

Table 3-1 compares the geometry parameters mentioned in Section 2.8.1 of both the Lockwood HH(5.25")-5 engine and the *Astra* against their average values from Tables 2-1, 2-2, and 2-3.

Table 3-1. Geometric Comparison of Lockwood and *Astra* Engines

	$\alpha_i$	$\alpha_E$	$(\alpha_i/\alpha_E)$	$\lambda_i$	$\lambda_E$	$(L/D)_c$
Lockwood HH(5.25")-5	0.35	0.23	1.56	1.09	5.68	2.10
Averages from Tables	0.35	0.22	1.66	1.02	5.67	2.26
<b>Astra Engine</b>	<b>0.39</b>	<b>0.22</b>	<b>1.78</b>	<b>1.0</b>	<b>5.52</b>	<b>2.25</b>
<b>% Diff. from Averages</b>	<b>11.4</b>	<b>0.0</b>	<b>7.2</b>	<b>2.0</b>	<b>2.7</b>	<b>0.4</b>

As the table illustrates, the *Astra* engine geometry is very close to both the HH(5.25")-5 and to the averages from Tables 2-1, 2-2, and 2-3. Although the percent differences of  $\alpha_i$  and  $(\alpha_i/\alpha_E)$  with respect to the average values are

considerably higher than the rest, they are still acceptable when compared to even higher differences that would be obtained from other engines listed in the Chapter 2 tables. The slight differences between the *Astra* engine and the Lockwood model are primarily from the *Astra* utilizing industry standard, off-the-shelf, and readily available components (i.e. automotive exhaust pipe and brake line fittings, electrical conduit, etc.) that required little modification to adapt into the design.

Even though the geometrical similarities between the Lockwood engine and the *Astra* are very close, the *Astra* does not function as the HH(5.25")-5. This will be discussed further in Chapter 6.

### **3.3 *Astra* General Design Considerations**

There were many issues that had to be considered in the development of the *Astra* pulsejet. Since they were accounted for early in the design phase of the engine, component assembly and engine manufacture proceeded with few setbacks. In addition, no components failed during the entire testing phase of the engine.

#### **3.3.1 Material Selection Concerns**

##### **3.3.1.1 *Heat Exposure***

All of the components of the *Astra* were designed from materials that would not fail when exposed to the combustion process and exhaust gases.

Also important was the materials' resistance to creep and expansion from the heat such that the part would not distort or create excessive thermal stresses on the assembly hardware. The material of choice was 303 stainless steel. Mild steel was often used for other components that were not directly exposed to the combustion reaction. Galvanized materials were avoided whenever possible since corrosion was not a concern. In addition, the galvanization coating burns off under excessive heat and produces harmful vapors.

#### 3.3.1.2 *Machining Ability*

Stainless steel requires roughly three times the machine time and produces three times the tooling wear than other non-stainless steel alloys. In other words, a certain thickness of stainless steel is equivalent to machining a non-stainless variety three times that thickness. The proper thickness for the engine components had to be selected so that the engine would not fail during operation, and still be able to be manufactured without damaging the machines and tooling available. The thickness was chosen to be 22-gauge (0.025") and all custom-made, stainless steel components of the engine were made from the same stock.

The mild steel parts of the *Astra* posed no difficulty in machining or assembly. The actual designation of the steel was not known and was different among the many non-stainless components. The thickness of these parts also varied according to their design specifications.

### 3.3.1.3 *Material Cost and Availability*

Since engine weight was not a concern, the materials used in the construction of the *Astra* were readily available and relatively inexpensive. The large sheet of 303 stainless steel from which most of the primary components were made was shipped from a local sheet metal supplier. All other materials were attained by the author from local businesses at below-cost prices. Had material weight been an important issue, materials that were both light and able to meet the machining and heat requirements could have been obtained, however at a much higher cost.

### 3.3.2 *Off-the-Shelf Parts and Part Modification*

One of the design goals of the engine was to make it inexpensive and from materials or parts that could be changed with little machining. Thus, many of the *Astra* components are slightly-modified parts used in automobiles or other industrial applications. The reason is so that the engine could be built by anyone with a low budget, and the necessary tooling and machining skills. Another reason is that since the funding for the project was from an outside source, expenditures would be kept at a minimum by using off-the-shelf parts. The components that required little modification to adapt into the *Astra* design were obtained from local businesses at or below consumer cost.

Another design goal of the *Astra* was to make all of the components, both custom-made and off-the-shelf, able to be modified to incorporate possible future design requirements. This consideration allowed for part and hardware uniformity and interchangeability to minimize cost and design complexity. In other words, one part can fit on many other parts with the same hardware. This permitted major engine configuration changes either in-the-field or within a very short time.

### 3.3.3 Engine Vibration and Hardware

The vibration of the engine during pulse operation was considered for assembly hardware and fitting selection. In addition to the vibration, the hardware would also experience extreme thermal stresses due to part expansion and heat transfer. The fasteners were thus chosen to be steel with those directly exposed to combustion being stainless steel. The fasteners are common bolts of various sizes and have either lock nuts or are threaded directly into a component. Hardware selection was also done such that a minimum number of tools could be used for engine teardown and assembly. The hardware was obtained through a local supplier for reasonable cost.

## 3.4 Final *Astra* Layout and Components

Figure 3-4 is an assembly drawing of the final *Astra* layout with the general dimensions given in Figure 3-3. The engine is axisymmetric and has

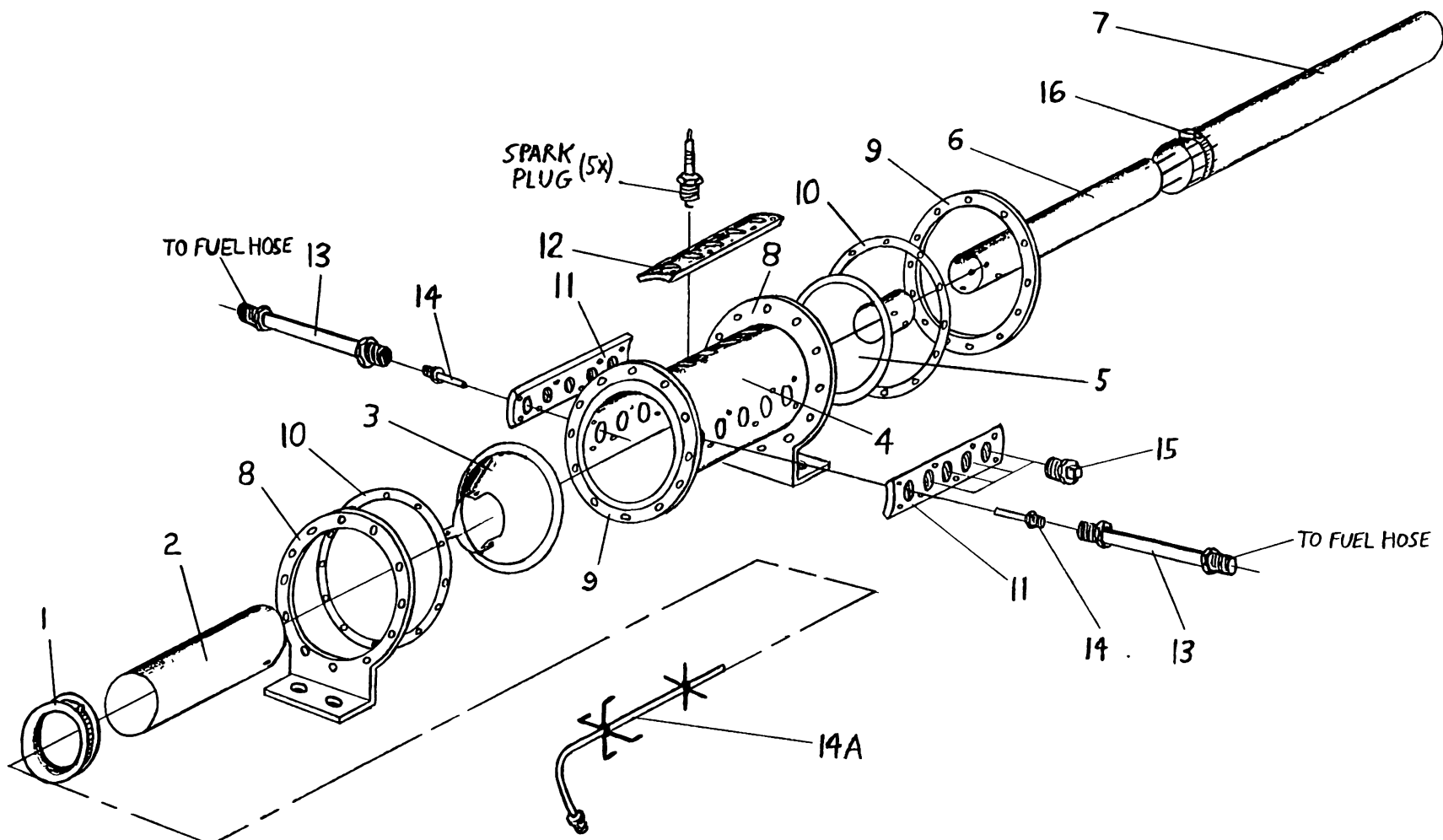


Figure 3-4. Astra Component Assembly



three variable parameters: fuel injection location, ignition location, and exhaust pipe length. Each of the components listed in Figure 3-4 will be briefly described in order of their part number and any special considerations in the design of the part will be mentioned. Detailed dimensions and drawings of the components are provided in Appendix A. Although there were additional components that were used in the experimentation, only those pertaining to the engine function will be mentioned. The specifications for the other parts will be given in Chapter 5.

#### 3.4.1 Part 1: Inlet Lip

The inlet lip of the *Astra* was fashioned in an attempt to conform to the optimum Lockwood design discussed in Section 2.7.1. Since the compound curvature of such a part is difficult to manufacture from sheet metal without a large drop hammer press and a female mold of the lip, an alternate method was employed.

The inlet lip is a prime example of off-the-shelf components requiring little modification. A small length of rubber, heat-resistant, automotive fuel line similar in radius to the lip size stated by Lockwood was cut to the circumference of the inlet pipe. The tubing was sliced down one side and a standard automotive hose clamp was inserted into the slot. The flat surface of the hose clamp widened the tubing and also provided the means to attach the lip to the inlet

pipe. The result, shown in Figure 3-5, is a smooth semi-bell-mouth inlet ring very close to the recommended Lockwood dimensions.

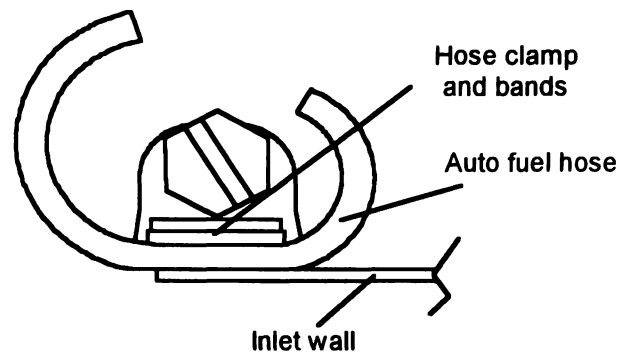


Figure 3-5. Inlet Lip Cross-Section

### 3.4.2 Part 2: Inlet Pipe

The inlet pipe is essentially a length of steel automotive exhaust pipe of necessary diameter to provide the desired  $\alpha_1$  stated in Table 3-1. The pipe is galvanized steel instead of stainless to reduce cost. Although galvanized parts were to be avoided in the design for heat concerns, the temperature associated with the inlet components is much less than around the rest of the engine and is not expected to affect the galvanization coating.

### 3.4.3 Part 3: Inlet Bulkhead

The *Astra's* inlet bulkhead expands the inlet area to the combustor area with a divergence angle of 45-degrees. This is also true for the Lockwood

HH(5.25")-5 engine as shown in Figure 3-2. Lockwood (7) often refers to the 45-degree angle of the inlet bulkhead as a "breakthrough in combustor design" since this design increased the overall performance of the research engines.

The bulkhead is made from 303 stainless steel sheet and is cut from a pattern, rolled into the cone, and welded at the seam. The three tabs on the inlet side are bent parallel to the engine axis and slip inside the inlet pipe. Steel bolts and lock nuts are used to fasten the inlet pipe to the bulkhead. The inlet bulkhead attaches to the combustor using a type of pressure-ring assembly that will be discussed in Section 3.4.7.

#### 3.4.4 Part 4: Combustor

The combustor is also made of 303 stainless steel and is cut, rolled, and welded as was the inlet bulkhead. All holes for bolts, spark plugs, fuel injectors, and mounting screws were made afterwards so that the heat of welding would not cause distortion.

#### 3.4.5 Part 5: Exhaust Nozzle

The exhaust nozzle is made exactly as the inlet bulkhead and the combustor. As in the Lockwood engine, the nozzle reduces the combustor area to the exhaust area through a convergence of 45-degrees. The nozzle attaches to the combustor using the same pressure-ring assembly as the inlet bulkhead. Since the exhaust pipe is much longer and weighs more than the inlet pipe,

using tabs as in the inlet bulkhead to support the cantilever exhaust pipe may not have been successful. To ensure a robust structure, a sleeve is welded onto the exhaust end of the nozzle that fits into the exhaust pipe. Six steel bolts and lock nuts attach the exhaust pipe to the nozzle sleeve.

#### 3.4.6 Parts 6 and 7: Inner and Outer Exhaust Pipes

Since tuning the length of the exhaust pipe to the frequency of the engine is necessary for optimized operation, having a single length of pipe and cutting it down until the correct length was reached was impractical. The solution to the problem is solved by employing a variable-length exhaust pipe.

Similar to the inlet pipe, the inner and outer exhaust pipes of the *Astra* are lengths of steel automotive exhaust pipe. The diameter of the inner pipe (Part 6) allows the desired  $\alpha_E$  listed in Table 3-1 and is directly attached to the exhaust nozzle. The diameter of the outer pipe (Part 7) is larger so that it slides over the inner pipe. Since the two diameters are substantially different, an adapter also made from common automotive stock welded onto the forward end of the outer pipe increases the tolerances between the two pipes and provides a means to set the position of the outer pipe (using a hose clamp [Part 16]). The inner pipe is graduated in half-inch increments so that the forward end of the outer pipe can be aligned to the marks to set a desired length. The total length of the exhaust pipe can range from 41 to 61 inches.

### 3.4.7 Parts 8, 9 and 10: Assembly/Mounting Rings and Gaskets

Parts 8 and 9 are the pressure rings described in Sections 3.4.3 and 3.4.5. These rings are made of mild steel and attach the inlet bulkhead and exhaust nozzle to the combustor. Rings shown in Figure 3-4 as Part 8 also act as engine mounts.

The pressure ring assembly is illustrated in Figure 3-6. The inlet bulkhead, combustor and exhaust nozzle each has a quarter-inch high lip turned perpendicular to the engine axis. When the components are assembled, the lips are flat against each other. The pressure rings on both sides of the lips are bolted to one another with twelve, steel bolts and lock nuts, holding the parts together. Since the pressure rings are larger in diameter than the lips, an aluminum gasket (Part 10) of thickness slightly less than both lips together is placed between the rings. Aluminum was selected for its superior durability and heat resistance compared to the fibrous, high-temperature, automotive gasket material whose performance proved unsuccessful in early engine tests.

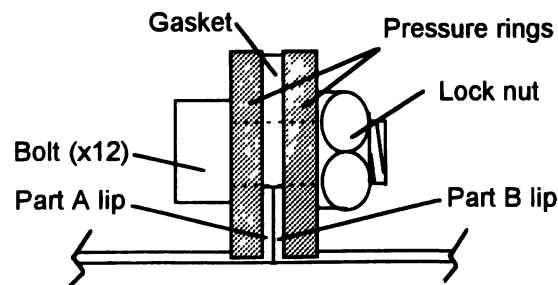


Figure 3-6. Pressure Ring Assembly

The advantages of this part assembly method are that the rings and lips provide a robust structure and an effective seal between the components to retain the pressures inside the combustion chamber. This method also does not require techniques such as welding or excessive material working that can distort the parts. In addition, the only components in the assembly that are most likely to fatigue or fail (mostly from over-tightening or thermal stresses) are the bolts holding the rings together. The primary disadvantage of the assembly is on a part such as the combustor which has lips at both ends to mate with other components. Once the rings are slipped over the combustor and the lips are turned up, the rings can not be removed. Overall, the pressure rings and associated components have performed successfully throughout testing.

#### 3.4.8 Parts 11 and 12: Fuel Injector and Spark Plug Mounting Plates

The *Astra* has two fuel injection assemblies mounted opposite one another and one spark plug assembly on the top of the combustion chamber. The mounting plates for the fuel injectors and spark plugs are made from segments of Schedule 40 industrial steel pipe of 4-inch inside diameter. The plates were made from standard pipe so that their curvature would match that of the 4-inch diameter combustor to provide a good seal. Also, Schedule 40 pipe has sufficient wall thickness to allow tapping for both the spark plugs and fuel injector housings.

Both the fuel injector plates (Part 11) and the spark plug plate (Part 12) have five holes tapped to accommodate the respective component (fuel housing or spark plug). The holes are spaced every 15 percent of the 9-inch combustor length. This allows sufficient material between the holes on both the combustor wall and the plate to reduce distortion under heat while providing a wide range of test points. The plates are each held to the combustor wall by eight stainless steel machine screws that thread into small holes on the mounting plates from inside the combustor.

#### 3.4.9 Parts 13 and 14: Fuel Injector Housing and Fuel Injectors

The injector housing (Part 13) is a small length of 5/16-inch steel plumbing pipe (standard 6-inch nipple) that fits into the fuel injector mounting plate at one end and is attached to the fuel hose at the other via a brass adapter. The housing can readily be moved to any of the five holes on the mounting plate. The metal pipe acts as a heat sink to carry heat away from the fuel hose during engine operation. During some tests, the housing itself acted as the injector by providing a hole in the combustor wall from which the fuel was ejected. The fuel system and hose will be further discussed in Chapter 4.

Threaded into the combustor end of the housing and protruding into the combustion chamber is the fuel injector (Part 14). Since many types of fuel injectors were developed during the research, the injector body was designed to be readily removed from the housing so that a variety of fuel nozzle

configurations can be tested in one session. This is accomplished by manufacturing the injectors from 5/16-inch automotive brake line incorporating a double-flared end and a line nut which threads into the injector housing. This method of attachment also permitted various orientations of the fuel injection pattern with respect to the engine axis. The injector tip designs and patterns tested will be described in Chapter 5.

#### 3.4.9.1 Part 14A: *Axial Fuel Injection Assembly*

The purpose of this assembly is to inject fuel along the engine axis down the center of the inlet pipe. The assembly uses only one of the two fuel injector housings and a long length of automotive brake line attached in the same manner as the perpendicular-injection nozzles (Part 14). The fuel line is suspended at the center of the inlet pipe by two, plus-shaped, strut assemblies welded together from coat hanger wire. Coat hanger wire was selected for its availability, malleability, and because its diameter is large enough to support the fuel line and not obstruct inlet airflow. The most forward strut cross is designed so that the fuel line can slide through its center and remain supported. It also has gripping tines that hold it in place inside the inlet. The second strut cross is fixed axially along the fuel line and keeps the tip of the nozzle located on the engine axis. The strut crosses allow for the fuel injection location (tip of the injector line) to be moved axially from inside the inlet pipe to well inside the combustor while being suspended on the engine axis.



#### 3.4.10 Part 15: Fuel Injector Mounting Plate Plugs

Even though there are ten holes (five on each side of the combustor) from which to inject the fuel into the engine, only two can be used at once since there are only two injector housings connected to two fuel hoses. The other eight holes must be plugged while the engine is operating. For this reason, 9/16-inch, standard pipe plugs are used to fill the unused holes in the injector mounting plates. These plugs have been modified during experimentation to accommodate thermocouples and early fuel injector designs.

## **CHAPTER 4**

### **SUPPORT SYSTEMS, SAFETY AND TESTING FACILITY**

#### **4.1 Support Systems**

Three support systems are utilized during operation of the *Astra*. They are the fuel system, the ignition system, and the air system. Since the *Astra* and the support systems were not kept in storage at the test facility, each system was designed to require minimum set up time and, with exception of the air system, be completely self-sufficient and easily transportable to and from the test cell. On-site repair, cost, material concerns, and operator safety were also driving factors in the design of each system. Each component of the systems will be described as well as any considerations made during system development.

##### **4.1.1 The Fuel System**

The pulsejet is fueled by liquefied petroleum gas (LPG or propane) under pressure in a portable tank. The propane flow rate is controlled by two valves located downstream of the tank and is routed through high-pressure hose to a check valve and pressure gauge. Immediately following the check valve, the

propane is directed to each of the two fuel nozzles in the pulsejet. A schematic of the fuel system is shown in Figure 4-1.

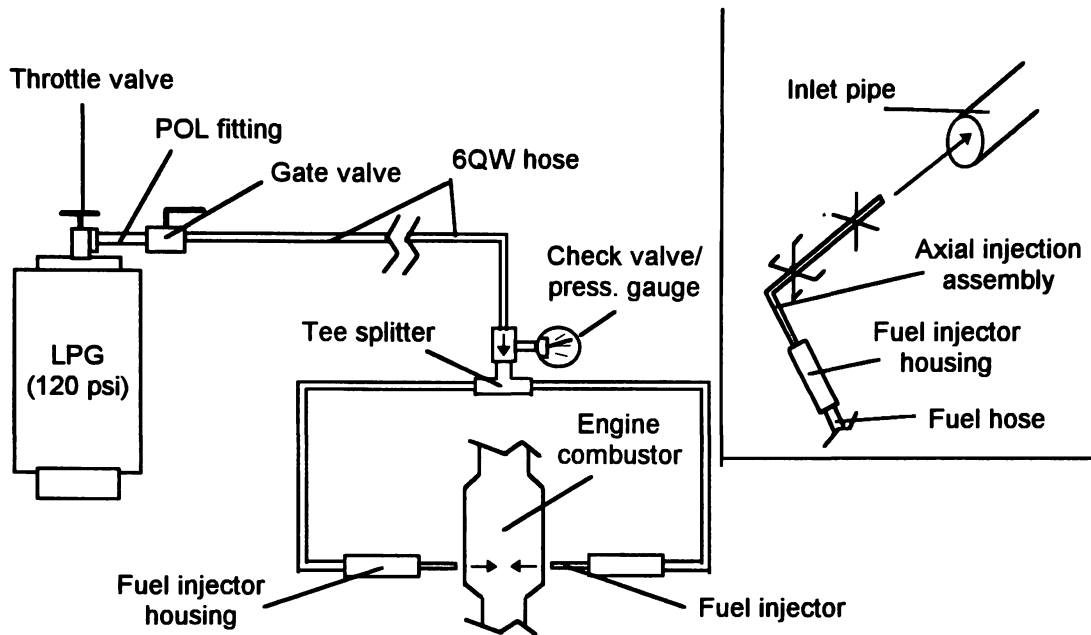


Figure 4-1. Fuel System Schematic

#### 4.1.1.1 *Choosing the Right Fuel*

In general, liquid fuels such as gasoline and kerosene are extremely volatile when mixed with the proper amount of air required for complete combustion. They are also more hazardous in transport since spillage and the resulting ground contamination are more likely. To atomize liquid fuels sufficiently for combustion, a pressurizing system is often required. This leads to additional components that could fail during operation. Special fuel nozzles that deliver proper atomization and spray pattern could eventually become clogged with carbon and fuel contaminants. In addition to component cost, repair, and

the harmful combustion products, running the *Astra* on liquid fuel was not desired.

Gaseous fuels were the next choice. The two fuels that were readily available, safer to handle, and did not require a pressurizing system were propane and butane. Although the two gases are very similar in combustion characteristics, propane was chosen as the fuel due to the higher vapor pressure, cooler flame temperature (for material consideration), and extensive availability. A comparison of commercial propane to commercial butane can be found In Appendix B. Even though propane costs the same per gallon as most liquid fuels, it weighs less and produces less harmful combustion products making it a safer choice with respect to transportability and environmental concerns.

#### 4.1.1.2 *Propane Tank and Throttle Valves*

The fuel tank is twice the size of those found on household gas grills. The tank weighs 40 pounds empty and 69 pounds when full with approximately 9.5 gallons of liquid propane. The tank is equipped with a valve on top that acts as the throttle valve in the fuel system. A special adapter entitled a POL fitting is attached directly to this valve so that fuel lines or additional components such as regulators can be connected to the tank. The POL fitting can be equipped with a shut-off valve that halts the flow of gas if the pressure from the tank is too high.

Since the fuel pressure required for the *Astra* is high enough to activate the POL shut-off valve, a POL fitting without the shut-off option was selected. Tank vapor pressure varied with ambient temperature and averaged about 150 psi.

The second valve is in line with the POL fitting and is a standard propane gate valve. This valve can not control the flow as well as the tank valve but it adds redundancy to the system with respect to fuel shut-off, especially when transporting the tank. During engine operation, the gate valve is opened fully and the primary fuel control is from the tank valve. At engine shutdown, both valves are closed.

#### 4.1.1.3 *High-Pressure Hose*

The type of hose selected is high-pressure, high-temperature propane fuel line similar to that used by propane-powered automobiles and industrial fork trucks. This hose, designated 6QW, is much stiffer than the typical propane fuel line found on gas grills and was chosen for its resistance to rupture by puncture, excessive pressure, and exposure to high-temperatures. The chance of these conditions occurring was minimized during engine testing. The fuel line throughout the system has a 5/16-inch inside diameter and all connections to in-line components are with flared hose fittings. Quick disconnect type couplings were not selected for safety concerns and cost.

#### **4.1.1.4 *Check Valve and Pressure Gauge***

The single fuel line that comes from the gate valve next encounters the check valve/pressure gauge assembly. The check valve only allows fuel flow into the pulsejet and has a port on one side to which an aneroid pressure gauge is attached. The purpose of the check valve is to prevent any backflow into the fuel system during the pressure rise cycle of the pulsejet.

The gauge measures the pressure just before the fuel line splits to go to each of the two fuel injectors nozzles inside the combustion chamber. Ideally, the pressure gauge should be mounted at the fuel nozzle assembly to measure injection pressure directly. To reduce cost and system complexity, however, only one gauge was used at the fuel line junction after the check valve that measures the pressure going into both lines. This is not the true injection pressure due to pressure losses through the remainder of the fuel line (about two feet from the splitter to the nozzle housing), but these losses are considered when computing mass flow rate and fuel/air ratio.

#### **4.1.1.5 *Fuel Injector Housings and Fuel Injectors***

These components were described earlier in Sections 3.4.9 and 3.4.9.1 and will not be discussed here. The insert in Figure 4-1 illustrates how the fuel system is adapted to use the axial fuel injection assembly (Figure 3-4, Part 14A).

### 4.1.2 The Ignition System

The ignition system of the *Astra* generates a high-voltage spark that ignites the mixture inside the combustion chamber. The system consists of a 12-volt DC power box connected to an automobile ignition coil. A typical automotive spark plug cable is run from the coil to a standard, lawnmower spark plug adjusted to allow a 3/8-inch spark across the electrodes. Since the mixture is ignited under atmospheric pressure, no specific gap settings are necessary. Only a discussion of the power box operation will be given. A schematic of the ignition system is given in Figure 4-2.

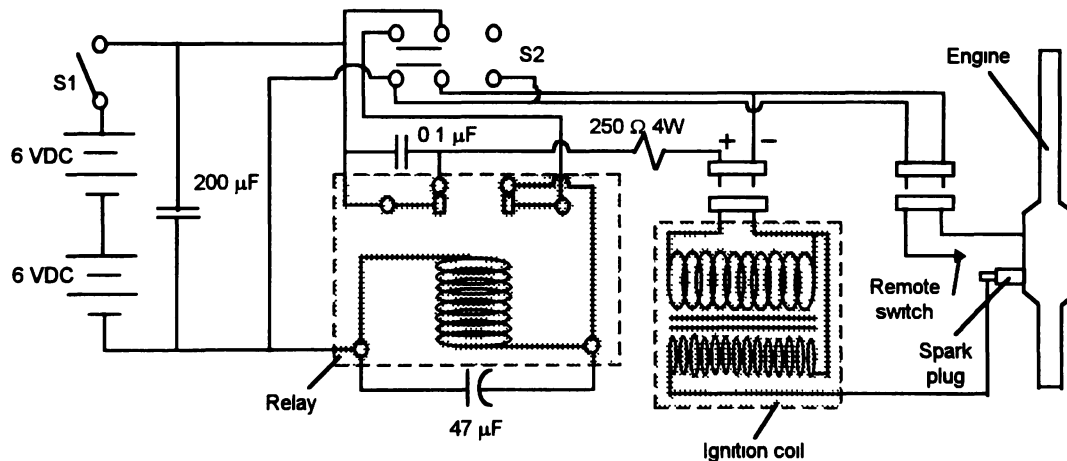


Figure 4-2. Ignition System Schematic

#### 4.1.2.1 The Power Box

This small box designed and built by the author contains two 6-volt lantern batteries that energize a dual throw, dual contact relay switch. As the

relay oscillates, it pulses the voltage to the ignition coil which generates a spark of roughly 30,000 volts every time one set of the relay contacts open. This occurs at such a high frequency that the spark is continuous as seen by an observer. The engine is used as a common ground for the coil and the power box.

The power box is controlled by two switches. The first switch, S1, is the main power switch to activate the box. The second switch, S2, allows for continuous spark operation or for a single spark to be generated when a remote set of contacts is opened. The latter was to be used in conjunction with the valve system employed early in the testing of the *Astra*. The continuous mode was used for ignition in subsequent testing. The capacitors in the system aid in preserving battery life between spark pulses, while the resistors limit the current through the relay points to reduce fouling. The box is designed for quick changing of batteries while at the test facility and all components in the circuitry are readily available at most electronics supply stores.

#### 4.1.3 The Air System

Since the *Astra* requires air to be forced through the inlet to start the combustion process, a compressed air source at the test facility was used. This system consisted of the shop air line coming from the compressor and attached to a regulator/pressure gauge assembly. The regulator permitted



adjustment of the pressure from the air line. The hose from the regulator had no special nozzle attachment and was open to the outside. The air line and the regulator assembly were properties of the test facility.

## **4.2 Safety Concerns**

Many safety issues were considered in the design and testing of the *Astra*. The most important design issue was such that the combustion chamber had sufficient structural integrity to contain the combustion process under sustained operation. This was considered during material selection and assembly methods (Sections 3.3 and 3.4, respectively). The *Astra's* design is supported by encountering no research literature during this project documenting any type of catastrophic component failure or testing accidents. Pulsejets do not explode due to their large inlet and exhaust areas for the combustion forces to exit through. As long as there is a path through which the combustion pressure can be released to the atmosphere during operation, explosive engine failure is not possible. In addition, propane handling procedures and piping methods were investigated to ensure that the fuel would not corrode the materials used in either the fuel system or the engine.

Testing safety issues focused on the operator and equipment within the vicinity of the engine. Both the fuel and ignition system were designed to be operated about twelve feet from the engine. This allowed the operator to be located behind a doorway or wall leading into the testing room. Once the light-

off characteristics and flame limits of the engine had been observed in early testing, locating the operator behind a wall became unnecessary. This was especially true after realizing that the *Astra* would exhibit better light-off performance by directing air into the inlet. All fuel hoses, ignition wires, and surrounding equipment in the test cell were relocated away from the engine to reduce exposure to exhaust flames and heat. Several fire extinguishers and water sources were available and accessible at all times, and testing was never conducted without supervision or assistance.

Additional concern was given to the operator's close proximity to the propane fuel tank. Since the throttle and gate valves are located on the tank, the operator stands directly beside it. Both the POL valve and check valve were installed in the fuel system to prevent any form of flame ingestion by the fuel injectors that may travel back into the tank. Although this was not likely to happen, the precautions were nonetheless taken so that the fuel system used on the *Astra* is just as safe as that on a propane-fueled, barbecue grill.

Also of concern were stray sparks generated by the ignition system that would ignite any gas that may have leaked from the fuel system. Each joint of fuel system was, therefore, tested for leaks and the ignition system was properly shielded.

The current arrangement is that the operator is stationed in front of and to the side of the engine next to the fuel tank with the ignition box and air hose close by. From here, the operator is clear of any flame and heat generated by

the engine and can closely observe the flame characteristics and engine performance. Immediately after the engine has been run and the fuel is shutoff, the ignition system is activated and high-pressure air is flushed into the engine to burn any residual gas left in the device.

### **4.3 Testing Facility**

The *Astra* was tested at the Embry-Riddle Turbine Engine Test Facility located on-campus. The facility instructional specialist, Mr. Roy Lumb, was present for most of the experimentation and provided valuable suggestions for the setup. The facility contains two engine cells and a control room for each. Inside each cell, there are various assemblies used in turbine engine static testing, fire extinguishers, water hoses, a wash sink and a compressed air source. Testing was conducted here under the direction of the Aerospace Engineering department in compliance with insurance and flammable material regulations. The control room contains a large panel for turbine engine operation and monitoring, and was not used during the *Astra* testing.

## **CHAPTER 5**

### **ENGINE TESTING AND RESULTS**

The first half of this chapter will summarize the significant events in the experimentation of the *Astra*. The events follow the evolution of the engine in accordance with the project goals in Chapter 3 and conclude with the final design configuration and last experiment of the engine. This interesting record is the developmental history that is not discussed in any pulse combustion literature (as stated in Chapter 1) and could serve as an example guideline for future pulsejet development. The second half of the chapter will discuss the data taken from various instrumentation that describes the performance and operating conditions of the *Astra*.

#### **5.1 Original Engine Configuration**

The original engine concept employed the ported-rotor inlet valve system described in Chapter 3. Figure 5-1 shows an assembly drawing and component identification of the engine arrangement. The test facility and support systems described in Chapter 4 were used including the compressed air line, even though the engine was designed to start with no artificially-induced airflow. As

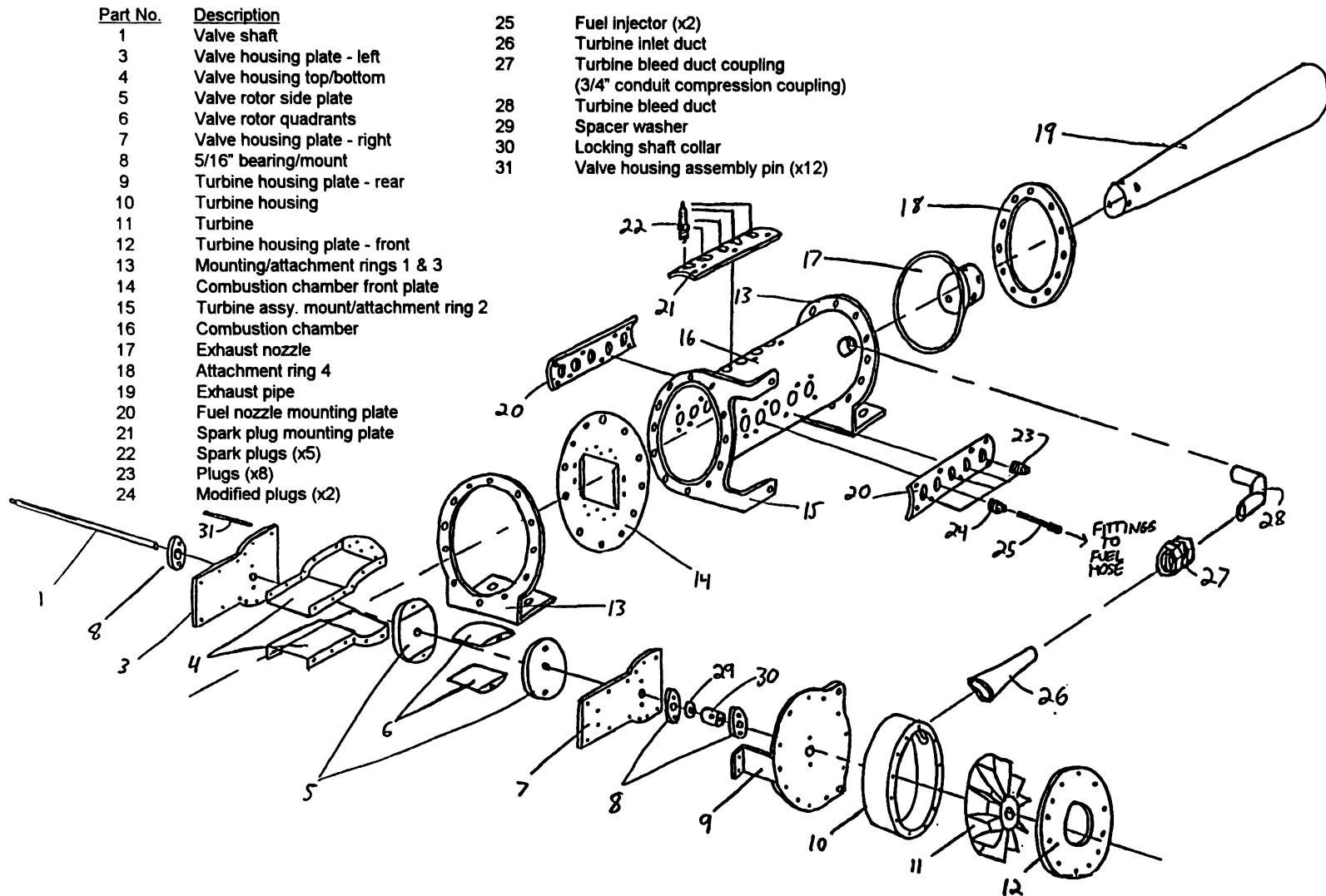


Figure 5-1. Astra Component Assembly with Ported-Rotor Valve System

can be seen from Figure 5-1, the inlet duct and exhaust pipe were smaller in length compared to the final engine design, since the literature available during the design phase did not discuss the importance of the lengths. It was also later found that the areas for both the inlet and exhaust pipes were not correct. The exhaust pipe was slightly tapered following Lockwood (7). The fuel nozzles were 1/8-inch diameter copper tubes inserted into special plugs that fastened to the fuel injector mounting plates. The inlet bulkhead was flat to accommodate the valve system, as was illustrated in Figure 3-1.

The engine was designed with five spark plugs for ignition because dummy plugs with the same thread as a spark plug were not available. Instead, five functioning spark plugs were used with the cable from the coil easily moved between them to vary the ignition location. In other words, only one of the five plugs was active at a time. The spark plugs were located every 15 percent of combustor length, as were the fuel nozzles.

## **5.2 Test History of the *Astra***

### *Run 1:*

The first test of the *Astra* occurred on December 3, 1994. The engine tried to start, producing singular loud bangs and pops, but no pulse tendency or pulse combustion was induced. The valve system was also not responding to the combustion reaction in that the combustion pressure was not sufficient to drive the turbine. Various fuel injection and ignition locations were tested in an

attempt to start the engine but to no avail. The session did show, however, that forcing air through the fully-open valve into the combustion chamber produced a more robust light-off. During the tests, the engine produced a sooty, blue-colored flame from the exhaust pipe characteristic of a rich fuel/air mixture.

*Run 2:*

The inlet and exhaust areas of the engine were then compared to the characteristic length parameters developed by Narayanaswami and Richards (5). These parameters represented the ratio of combustor volume to either the inlet or exhaust pipe area. Narayanaswami and Richards found two combinations of the inlet and exhaust characteristic lengths that worked well in an experimental pulse combustor model evaluated by Richards and Gemmen (11). The *Astra* inlet and exhaust areas were modified to the combination that performed the best (according to Ref. 11) by adding inserts to match the characteristic lengths. The engine was then tested again.

Although the bangs and pops were louder than before, the engine was still burning rich and was thought to be getting too much fuel due to the richness of the exhaust flame. The check valve was modified to reduce the engine fuel inlet pressure and allow more accurate control of fuel tank pressure. This modification produced no change in the light-off characteristics.

*Runs 3 and 4:*

In the next tests, a propane regulator as used on residential barbecue grills was installed in place of the check valve/pressure gauge unit so that a more precise fuel delivery could be possible. The fuel nozzles were crimped closed at the ends and had small holes drilled along their length to enhance the mixing of air and fuel. Also, the turbine bleed tube from the combustor that led to the valve system was closed so that the combustion chamber pressure could be better maintained. Even though these modifications yielded a yellow exhaust flame characteristic of a more balanced fuel/air ratio and created much louder light-offs, the engine still had no tendency to pulse. The exhaust flame was also pulled back into the engine after its ejection from the pipe, indicating that the chamber pressure was dropping in accordance with a pulse combustion cycle.

During these runs, compressed air was being injected into the inlet pipe via the shop air line (Chapter 4). After the initial light-off, the flame would burn steady and strongly proceed through the exhaust pipe. If the air source was removed, the steady flame would remain inside the combustion chamber, burn slowly and become exceedingly rich as observed by soot production and deep blue color. This rich-burning behavior upon the removal of the air supply remained throughout the experimentation of the engine. In addition, no instrumentation other than air and fuel pressure gauges were used in these tests due to their preliminary nature; the goal at this point in the testing phase was to get the engine to function. All tests with the valve system were conducted with



the valve locked in the fully-open position for the reason that if the engine pulsed as an aerovalve, the geometry aft of the inlet bulkhead would be correct to allow pulsing when the valve system was introduced.

*Run 5:*

Additional literature obtained by the author from Lockwood described the latter's studies on exhaust pipe length. The tapering, fixed-length exhaust pipe originally used on the *Astra* was replaced by a constant-area, variable-length design made of common automotive exhaust stock. The length was variable from 22 to 37 inches. High-temperature automotive gasket material was added between the fuel injector/spark plug mounting plates and the combustor wall to further reduce the escape of combustion pressure during operation. Since the fuel regulator did not function as expected (engine still ran too rich), it was removed from the fuel system under the premise that the engine was getting plenty of fuel and not enough air. The engine was tested with forced inlet air (by compressed air line) along with various exhaust lengths and fuel locations, but produced no significant improvement over previous runs.

*Run 6:*

Early in March of 1995, the inlet and exhaust characteristic lengths were re-evaluated and were found to be erroneous. The combustor volume had been calculated incorrectly which lead to improperly-sized inserts for the areas.

Accordingly, new inserts were designed. The fuel nozzles were also moved to the most forward combustor position (15-percent). Although testing yielded the same type of singular bangs and pops that preceded steady combustion, the fuel/air ratio was more balanced due to the enlarged inlet area that allowed more forced air into the engine. As before, no pulse tendency was observed, regardless of exhaust pipe length.

*Run 7:*

The next modification was to the fuel injectors. Although the proper location of the injectors would be near the inlet end of the combustor, this was not achievable since the fuel injector mounting plates did not extend to that location. Instead, the copper tubing nozzles were bent in such a way that they injected fuel parallel to the engine axis at the 15-percent combustor length location. Testing of this configuration yielded better mixing dynamics as visually observed through the inlet pipe during operation, but no pulsing or improvement in performance even with forced inlet air.

*Run 8:*

Since the engine still seemed to be starving for air after the light-off, the valve system was completely removed from the engine and the flat inlet bulkhead remained. A new inlet design, shown in Figure 5-2, was employed that comprised of small lengths of pipe that could be interchanged to fit on the inlet

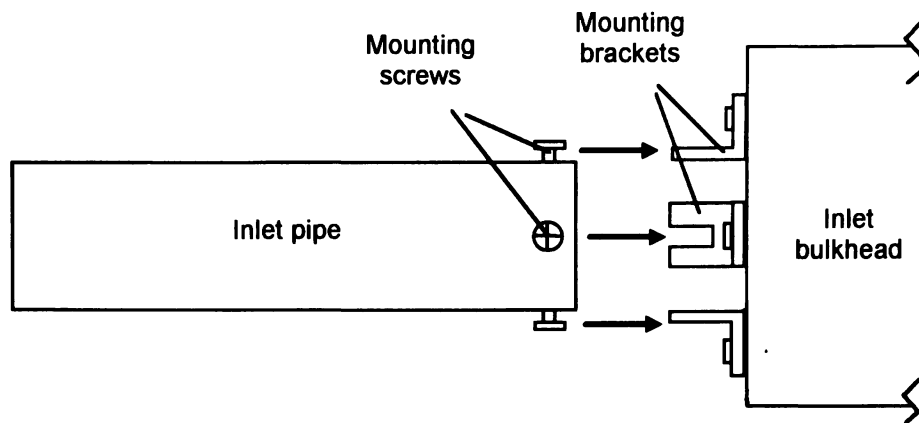


Figure 5-2. Interchangeable Inlet Pipe Concept

bulkhead. The five pipes varied from one to three inches in length every half inch and all had the same area to match the characteristic inlet length. The pipes were attached to the inlet bulkhead by screwing them into small brackets on the bulkhead, providing for easy change-out of the pipes during testing. This arrangement gave some variation of the inlet pipe length.

The absence of pulsing behavior was thought to be due to exhaust gases not escaping into the atmosphere in time to let the new charge of fresh air into the combustor. By making the inlet pipe shorter than the original five-inch long inlet duct used on the valve system, the exhaust gases would escape faster and allow the fresh air inside. The proper length required for this was not known, however, which was why several pipes of different lengths were made and tested.

The *Astra* was tested with the new inlet pipe lengths, the flat inlet bulkhead, axial-injecting fuel nozzles, variable-length exhaust pipe and forced inlet air. To reduce the amount of variables during the test session, the exhaust

length was fixed at 34 inches and the ignition plug used was at 30-percent combustor length. The goal of the test was to observe the effects of different inlet pipe lengths on the combustion cycle.

Although no significant effects were noticed other than the size of the flame that exited the inlet pipe after light-off, delivering excessive fuel pressure during steady-flame burning produced an interesting result. To start the engine in past tests, air would first be blown through the inlet pipe at about 10 psi, then the spark ignition would be activated, then the gate valve would be opened on the fuel system, and finally the tank (throttle valve) would be opened to allow about three psi of propane into the combustion chamber. After ignition, the spark system would be shut off and the engine would burn steady. The interesting event occurred when an excessive amount of fuel pressure (about 10 psi) was delivered after the engine lit and the spark had been terminated. The forced inlet air pressure remained constant, but the high fuel pressure forced the combustion flame out of the exhaust pipe. Once this happened, the air supply was quickly removed and the flame continued to burn at the exit of the exhaust pipe by drawing air and fuel through the engine. As the fuel pressure was slowly reduced, the flame was pulled back inside the exhaust pipe until it had rapidly traveled down the exhaust pipe and ignited the mixture in the combustion chamber. This produced a loud "pop" and ejected flame from both inlet and exhaust pipes after which the engine either extinguished itself or burned very rich.

This behavior was indicative of the first self-aspirating pulse cycle, but would not sustain itself following the second ignition. Before any conclusions could be made as to the mechanisms behind this event, more research had to be done. In the meantime, testing continued to achieve self-aspiration.

*Run 9:*

Research into inlet pipe design showed that most inlet pipes for aerovalve pulsejets were just as long as the combustor. An inlet pipe just short of the nine-inch combustor length was made that attached to the inlet bulkhead in the same manner as the previous pipes. Again, testing revealed no significant results even when attempting to start and run the engine with forced air as described in Run 8.

The characteristic lengths determined by Narayanaswami and Richards (5) were duplicated in the current *Astra* design indicating that the engine was apparently ingesting sufficient air mass through the inlet area. The problem was thus thought to be fuel nozzles not delivering enough fuel in time for the next combustion cycle to begin.

*Run 10:*

The 1/8-inch, copper-tube fuel nozzles used in prior runs were thought to be too small to deliver the required amount of fuel in the time between combustion cycles, causing the engine to flame-out or burn steady after the first

light-off. The two nozzles were replaced by sections of 5/16-inch pipe (standard 6-inch long plumbing nipple) which in later engine configurations acted as the fuel nozzle housings. The new nozzles had no special design at the combustor end and simply provided a large hole through which fuel would flow into the chamber. For safety concerns, the check valve/pressure gauge assembly was reinstalled into the fuel system. The engine was tested with the new fuel nozzles and produced no interesting results even with forced inlet air.

After the test, the process became apparent by which the variables on the engine could be adjusted to find the correct combination for pulsing. The four variables were the inlet length (no inlet, five inlets ranging from 1 to 3 inches, and the 8-3/4-inch length), the fuel injection and ignition location (five locations, one every 15-percent of combustor length), and the exhaust pipe length (ranging from 22 to 37 inches). The three-phase series of tests would narrow down the best operation of the engine based on visual and aural observations of the light-off stability and strength, and the exhaust flame color and robustness. The variable settings that produced the strongest light-off and most robust flame would remain fixed through the next phase. The first phase of tests was to hold the inlet and exhaust length fixed while the fuel and ignition locations were varied. The second phase tests would fix the exhaust length as in the first phase but vary the inlet lengths for the fuel/ignition locations with the strongest light-off or pulse tendency. The third phase would use the best inlet length and fuel/ignition location combinations while varying the exhaust length until the

engine began to pulse. During all three phases, the inlet air and fuel pressure remained constant to establish experimental consistency. Data sheets were made for systematic testing and experimentation began with the first phase. The data collected from all three phases is given in Appendix C.

*Runs 11 and 12:*

The first phase employed the longest inlet length of 8-3/4 inches and fixed the exhaust pipe length at 32 inches. Locating the two fuel nozzles and the spark at different points along the combustor produced a wide variety of light-off characteristics. Each test was rated on a scale from one to six (six having the strongest tendency to pulse or most robust light-off) and important comments were noted. Some yielded weak pops and rich flames while others produced loud bangs and large exhaust plumes. After a minor repair to the ignition power box, the first phase testing continued.

*Run 13:*

The engine began to pulse on April 20, 1995 during one of the final runs of the first phase tests. The pulsing mode would continue as long as air was forced into the inlet. Once the pulsing mode had been established, a throttleable range was found by adjusting the fuel flow to determine the rich and lean limits of the pulse cycle. Another discovery was that more robust pulses were produced if the airflow through the inlet became stronger. If the air source

was removed, however, the cycle would stop and the flame would burn rich and steady. The pulsing characteristics were also found to be independent of ignition location.

Now that the pulsing characteristics of the *Astra* were apparent, second phase testing commenced in an attempt to optimize the cycle performance or achieve self-aspiration.

*Run 14:*

Six of the best fuel/ignition locations were selected from the first phase to be re-evaluated with different inlet pipe lengths during the second phase. The exhaust length remained at 32 inches. During the first test of the second phase, however, the POL valve on the propane tank (described in Chapter 4) was found to shut off the fuel pressure if the tank valve was opened too much. In order to explore pulsing behavior at higher fuel/air ratios, the POL valve was replaced with a similar non-check valve version that would allow the necessary higher fuel pressures. Also during this test, a U-tube manometer and a hand-held pitot tube were used to determine the total pressure rise across the device and, therefore, the thrust. Even though the measurements were successful, the thrust was not computed since doing so would be meaningless at this point in the experimentation.



*Runs 15 and 16:*

This run tested the six best locations from the first phase with different inlet lengths. In some cases, excessive fuel pressure would lead to a rich, steady-burning condition inside the combustor with no flame leaving the exhaust pipe. In other instances, the high fuel pressure would cause the flame to burn about six inches downstream of the exhaust pipe exit. An important observation was that the engine produced more heat and robust pulsing conditions if fuel injection locations were towards the center of the combustor (45 or 60-percent of the length) rather than other forward or aft locations. The inlet lengths that yielded the best pulsing characteristics for the first-phase fuel locations were found to be between 1-1/2 and 2-1/2 inches.

*Runs 17, 18, 19 and 20:*

Seven of the best conditions from the second phase were tested in the third phase with the variable exhaust pipe length. Each test was conducted with the fuel pressure between 3 and 4 psi and the air pressure at around 20 psi held roughly seven inches from the inlet pipe. Testing of the exhaust pipe length began at 22 inches and proceeded every inch to 37 inches. As each test was carefully observed and rated, patterns emerged showing that certain lengths of the exhaust pipe produced more robust pulsing characteristics than others. The groups of lengths that had favorable results (robust pulse tendencies) were re-tested at half-inch intervals to narrow down the optimum length.

Although the groups of favorable exhaust pipe lengths were independent of the inlet length, they were slightly dependent on fuel location within the combustor. Varying the exhaust pipe length did not change the pulse characteristics when the fuel was injected at the center of the combustor, but had a noticeable effect when the injection was moved rearward. Both central and aft locations had patterns of favorable pulsing, but the aft locations yielded a wider range of pulse behavior by varying exhaust length than did the central locations.

Although the three phases of testing adjusted the four engine variables to produce the most robust pulsing, self-aspiration did not occur, possibly due to inadequate fuel/air mixing and engine geometry. At this point in the experimentation, finding an accurate method to measure the thrust of the engine became the goal. Lockwood (7) had measured the thrust of his experimental engines by mounting them vertically (exhaust pipe upwards) on a large floor scale. The validity of this method was questionable because of how the pulsejet would function when arranged as such. When mounted vertically with the exhaust pipe facing upwards, the buoyant force of the hot air from combustion may influence the pulse cycle as the air travels up the exhaust pipe. This would lead to different combustion pressures inside the chamber, and thus different thrust measurements, when compared to a horizontally-mounted engine. The *Astra* was never mounted vertically for this reason and so all data regarding engine performance was taken horizontally.

Three methods were to be investigated and compared to determine the most accurate for estimating the thrust of a pulsejet. The methods consisted of measuring the total pressure across the engine during pulse combustion, obtaining pressure readings from a transducer inside the combustion chamber, and measuring the force developed on a load cell either by using it to measure the forward force of a sliding cart on which the engine was mounted or to register the dynamic pressure of the exhaust gases via a pressure plate device. Although it was possible to collect data on all three methods at once, each was done independently to demonstrate that the available instrumentation could record the necessary measurements.

The ignition location for all following runs in the three-phase testing remained at 45-percent combustor length, since the ignition location was shown to have no influence on the pulsing characteristics of the engine.

*Run 21:*

This run demonstrated that a total pressure change across the engine was being produced from the pulse combustion process and not from the air forced into the inlet. The water-filled manometer and pitot tube described earlier was used to obtain readings. With just the air flowing through the engine, the pressure just aft of the exhaust pipe displaced about three-tenths of an inch of water. While the engine was pulsing, however, the displacement increased to six-tenths of an inch. Readings were not taken at the inlet due to the

interference of the forced air flow. Combustion chamber temperature readings using a Nanmac Corporation Type K shielded thermocouple were also taken so that a temperature map could be constructed showing the hot and cool spots within the chamber.

*Run 22:*

Now that the manometer and thermocouple proved successful in measuring the required data, the pressure transducer and load cell had to be prepared and calibrated. The pressure transducer was a Kistler Instruments Model 206 high-sensitivity piezotron capable of measuring up to 80 psi at 124.7 mv/psi. The transducer was connected to a Kistler Instruments Model 504D charge amplifier that boosted the signal output to a Hewlett-Packard 54601A four-channel, digital oscilloscope. The pressure signal from the transducer was then plotted directly from the oscilloscope to a Hewlett-Packard ColorPro pen plotter. The transducer was mounted in a pipe assembly similar to one of the fuel injector housings such that it was attached to the engine in place of one of the plugs on the fuel injector mounting plate. A modified, plastic, soda bottle filled with ice surrounded the transducer housing and kept it cool during engine operation.

The load cell was an Eaton Corporation Model 3167-25 with a maximum load of 25 pounds in tension or compression. The load cell received its power from a Hewlett-Packard 6114A variable power supply. The output signal was

then input into the HP 54601A oscilloscope. The load cell was first used to measure the forward force on a skateboard on which the *Astra* was mounted. Before the actual test, the engine, skateboard, load cell, and data acquisition equipment were assembled to see if the load cell would register the slight forward forces generated by the engine. The skateboard was set up against the load cell and would detect the slightest tap on the skateboard in the forward direction. A calibration factor for the load cell was then determined by applying known weights and measuring the voltage change. The load cell system was ready for testing.

The *Astra* was set to pulse with forced inlet air and the pressure transducer and load cell/skateboard system were tested. Although the pressure trace on the oscilloscope from the transducer was excellent, the charge amplifier settings were questionable such that no actual pressure data was calculated. The settings were corrected later and will be discussed in Section 5.3.4. The engine was also set to run steady with forced air to demonstrate that the pressure signatures for pulsing and steady operation were significantly different.

As for the load cell, the oscilloscope revealed no output from the system. When the engine was shut off, however, the load cell was as sensitive as before. The observation was made that since the engine is axisymmetric and the exhaust gases leave both the inlet and exhaust pipes at the same time, there would be no net thrust produced that would create a forward force on the load cell. In addition, an unknown 60 Hz signal was being detected by the

oscilloscope that may have distorted the load cell output. Since using the load cell in this manner proved unsuccessful for thrust measurement, it was then employed in a dynamic pressure plate assembly.

*Run 23:*

A stainless steel plate of known area was vertically attached to the load cell. The plate and load cell were to be placed into the exhaust jet of the engine (for a short time due to heat concerns on the load cell) and the dynamic pressure pulses were measured by the oscilloscope.

The dynamic pressure plate system was tested at the same pulsing conditions as the previous run. Again, no signal was detected by the oscilloscope. This was thought to be due to the resolution of the load cell. The forces were much less than the load range for which the cell was designed making the voltage change per pressure pulse too small to register on the oscilloscope. Since using that particular load cell to measure thrust did not work as expected and no other load cells were available, the concept was no longer used.

Measuring thrust through the use of dynamic pressure plates had worked for some researchers, however. Rehman, as described in Putnam *et al.* (1), used impact plates to quantify thrust on his aerovalve pulsejets.

Since the correct charge amplifier settings for the pressure transducer were not known at the time, the only somewhat successful method of measuring

thrust was from the manometer and pitot tube, even though the error in such a system is relatively high. Due to the experimental elimination of other methods to compare with, the quest for the most accurate thrust measuring technique ended. The project goal changed back to achieving engine self-aspiration.

The decision was made to change the geometry of the *Astra* to resemble a scaled-down version of one of the Lockwood engines, the HH(5.25")-5 shown in Chapter 3. The inlet pipe and inlet bulkhead were consequently redesigned such that the inlet pipe was as long as the combustor and had an area according to the trends in aerovalve design (discussed in Chapter 2). The flat inlet bulkhead left over from the valve system was replaced by a 45-degree diverging bulkhead similar to the engine's exhaust nozzle (Figure 5-3) and according to the research conducted by Lockwood (7).

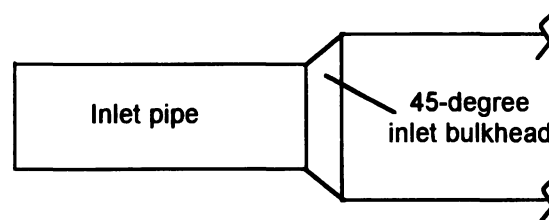


Figure 5-3. Inlet Pipe and 45-Degree Inlet Bulkhead

*Run 24:*

The new engine design was tested with an exhaust length of 34-1/2 inches and showed no tendency to self-aspirate when the forced inlet air was removed. During pulsing operation, however, strong, visually-observable vibrations were noticed throughout the engine indicating that a force was being

produced. Various fuel locations using the same, large, open-hole-type fuel injectors introduced in Run 10 yielded the same pulse strength and combustion characteristics.

*Run 25:*

Now that the inlet geometry had been corrected to represent a working model (Lockwood's engine), the mixing dynamics of the air and fuel were thought to hold the answer to the self-aspiration dilemma. Fuel nozzles were manufactured from automotive brake line that approximated a concept researched by Lockwood (7) and attached to the ends of the fuel injector housings that were currently being used as the injectors. These nozzles (Figure 5-4) were crimped at the ends such that a slit was present to disperse the fuel in a fan pattern.

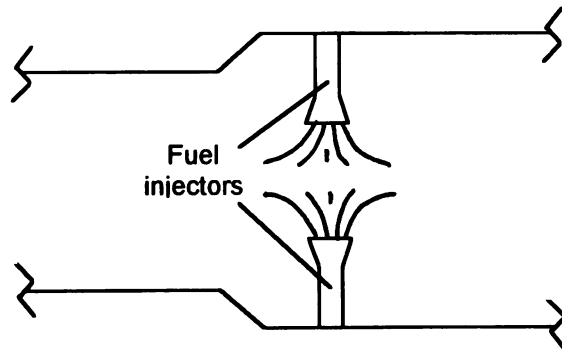


Figure 5-4. Crimped-End Fan-Pattern Fuel Injectors

The two fuel injectors were attached to the injector housings and placed at the 15-percent location on the mounting plates. This location was similar to that used by Lockwood during the investigation of optimum fuel sprayer design



and location. The engine exhibited very little pulse tendency and the overall operation was much worse than before even with the forced inlet air. The injectors were removed on-site and the engine was tested again with exhaust pipe lengths of 37, 34-1/2, 30 and 28 inches. Although there was no significant difference in performance among the tested exhaust lengths, the pulse operation was much improved due to the removal of the injectors.

The effect of the forcing air through the inlet pipe to sustain pulse combustion needed to be investigated in the hope that some clues as to the engine's air requirement might be revealed. To aid in the investigation, a bell-mouth inlet as used by Lockwood and other researchers was constructed from rubber, automotive fuel line and a hose clamp per the specifications described by Lockwood (7) and in Chapter 2.

*Run 26 and 27:*

The *Astra* was run employing the bell-mouth inlet to observe how the engine functioned with the air supply at various positions in front of the inlet. The engine was started and pulsed as before, but the air jet from the hose was moved farther back from the inlet pipe (approximately three to four feet) to reduce the air velocity into the engine. The engine still pulsed well and the fuel pressure had to be adjusted to compensate for the slower air velocity. The bell-mouth made the engine more tolerant of angled air injection and was kept through the remainder of the experimentation.

*Runs 28 and 29:*

Since the geometry of the inlet and combustion chamber was identical to the Lockwood model, the engine should have had no difficulty receiving a sufficient amount of air for combustion. The absence of self-aspiration, therefore, had to have been caused by the combustion dynamics not driving the pressure low enough during the pulse cycle to draw in air. One possible solution was to enhance the fuel/air mixing by employing a stabilizer plate as researched by Keel and Shin (10). This plate was suspended in the center of the combustion chamber close to the inlet bulkhead and was mounted perpendicular to the engine axis. The plate used in the *Astra* was made of mild steel and was suspended in the chamber by two, modified, steel, bicycle spokes. The fuel injectors were located forward of the plate at the junction of the inlet bulkhead and the combustor. The purpose of the plate was to cause the incoming air mass to be deflected towards the sides of the combustor and simultaneously mix with the fuel. The fuel/air mixture would pass by the plate and be ignited by the residual gases of the previous cycle that were trapped in the plate's wake. This method enhanced the mixing dynamics for Keel and Shin, and was thus tried on the *Astra*.

New fuel injectors were also constructed that delivered the fuel in a fan-type pattern parallel to the axis of the engine. The injectors protruded into the combustor about 1-1/4 inches.

The three-inch diameter stabilizer plate was mounted at 22-percent of the combustor length. The location of the plate was fixed throughout the experimentation. The axial-delivery fan-type injectors were employed at the 15-percent location (upstream of the plate). Even with the forced inlet air, the engine did not pulse under the same fuel/air ratio and start-up sequence as prior runs. The engine also did not pulse when the fuel the injectors were moved to 30 percent (downstream of the plate) and the new nozzles were removed.

To further simulate the Keel and Shin experiments, another set of fuel injectors were designed that delivered the fuel in the same fan pattern but protruded further into the combustor (about 1-3/4 inches). These nozzles were also mounted at the 15-percent location and ejected fuel such that it impinged on the plate. There was no noticeable improvement in performance. This indicated that the engine was not receiving enough air for combustion due to airway blockage by the stabilizer plate, even with the forced air supply.

*Runs 30 and 31:*

The plate diameter was reduced to 2-1/2 inches and the engine was run with the same longer fuel nozzles as in Run 29. The pulse tendency with the forced inlet air had returned and occurred at a much higher frequency than before. Although there was a noticeable throttling range, the pulse cycle was not as robust as in previous tests without the stabilizer plate and fuel injectors. Tests were conducted with the fuel injectors oriented parallel and at 45-degrees

to the plate; Again, no pulsing was observed. The fuel injectors were removed and the engine pulsed at a much lower frequency than prior runs even with the same air inlet pressure.

Another set of fuel injectors was developed from automotive, steel, brake line. The injectors were of constant area and protruded into the center of the combustor. The two opposing injectors were close enough such that the fuel streams would impinge on one another and fan out radially, as shown in Figure 5-5. Half of the fuel spray would impact the plate and the other would travel a short distance down the inlet pipe. Testing of these nozzles yielded no pulse tendency by the engine.

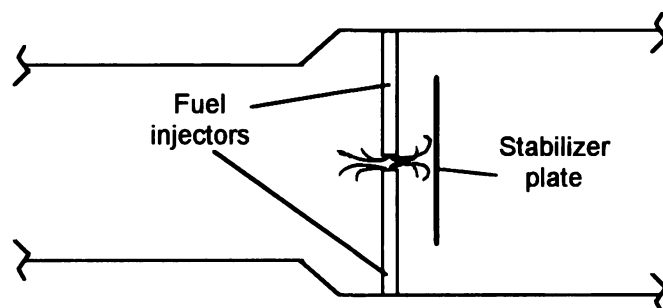


Figure 5-5. Opposing Fan-Pattern Fuel Injectors

*Run 32:*

The plate was further reduced to 2 inches in diameter and another set of fuel injectors was manufactured. These injectors were also long enough to reach the center of the combustor but ejected the fuel axially in two streams along the axis of the engine.

The *Astra* was tested with the new plate size, axially-injecting central fuel nozzles and forced inlet air. In several tests, the injectors were oriented away from and towards the plate both upstream and downstream of the plate (15 and 30-percent combustor length, respectively). A slight improvement in the pulsing characteristics was noticed when the injectors were upstream of the plate and facing down the inlet pipe away from it (Figure 5-6). The injectors were then removed and the engine functioned no differently. The other tests with the different orientations yielded no pulse combustion improvement over Runs 30 and 31.

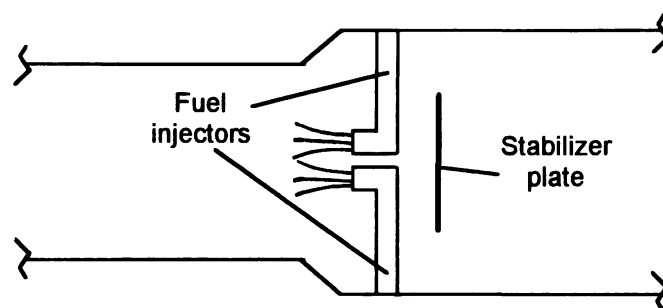


Figure 5-6. Axially-Injecting Central Fuel Nozzles

The stabilizer plate not only impeded the inlet airflow but also the backflow from the engine after the light-off. This created a rich condition since the combustion was not receiving a sufficient amount of air. The plate was thus removed and the engine was tested again with the fuel injectors used in Run 32.

*Run 33:*

Testing without the plate and rearward-facing axial injection at 30-percent combustor length showed a marked improvement in combustion characteristics and pulse behavior with the forced inlet air. The flame color indicated a more balanced fuel/air ratio and the pulsing was nearly as strong and robust as without the fuel nozzles. Additional tests with the injectors at 15-percent and facing them forward (towards the inlet pipe) yielded improved results. With the injectors facing forwards, the single pulse cycle without the ignition or air source as described in earlier runs was achieved, but would burn steady or extinguish immediately afterward. In another test, one injector was turned to face downstream while the other remained facing upstream. This produced no pulsing whatsoever.

The spark location was varied during this run to investigate various light-off conditions with the fuel injectors oriented in different positions. The best ignition location for all cases remained at 45-percent.

Evaluation of additional pulse combustion literature revealed that, in some engines, the fuel was injected through a long, single tube that traveled the length of the inlet pipe and ended where the inlet bulkhead began. A single fuel-injection tube was constructed that was suspended in the inlet pipe on the axis of the engine. This assembly was discussed in Chapter 3. The injector could be moved several inches axially to find an optimum injection position. The fuel system was easily modified to handle the single injector.

*Runs 34 and 35:*

Further research into the Lockwood reports (Ref. 7) and other literature showed that the exhaust pipe length of the *Astra* did not conform to the aerovalve design trends evaluated in Chapter 2. The exhaust pipe of the engine was originally designed according to Lockwood's conclusion that the best exhaust geometry for a compromise between low thrust specific fuel consumption and high thrust-per-volume was a pipe length-to-diameter ratio of 18.5. Contrary to this statement, however, the exhaust geometries of Lockwood's experimental engines had length-to-diameter ratios much greater than 18.5 and followed the trends summarized in Chapter 2. After this discovery, the *Astra*'s exhaust pipe was lengthened to achieve the necessary length ratio ( $\lambda_E$  from Chapter 2). The length of the exhaust pipe was now variable from 47 to 61 inches.

The *Astra* was tested with the single fuel injector such that a stream of fuel was axially ejected into the chamber. The injector was positioned so that its end was at the same point as the exit of the inlet pipe. The exhaust length was varied from beginning to end to isolate the best length for pulsing, which was between 50 and 53 inches. The pulsing characteristics with the forced inlet air were excellent, just as in earlier runs with the two open-hole-type nozzles, but there was still no tendency to self-aspirate. The fuel and air pressures that yielded the most robust pulsing behavior were found (5 psi fuel and 25 psi air) and a throttleable range between rich and flame-out conditions was determined.

The last experiment of the *Astra* was conducted on September 2, 1995, due to time limitations for the project. The tip of the single injector was crimped closed and two slits were cut in the sides to disperse the fuel in a fan pattern that filled the inlet area. The engine was tested and did not pulse as well as with the other method of injection.

Even though the *Astra's* geometry and fuel injection methods were identical to those used by Lockwood and other early experimentors, the engine did not self-aspirate when the starting air supply was removed. Since the experimentation had ended for the project, the only remaining task was to collect data on the pulse characteristics of the engine. The information would show that the engine did pulse by comparing it to data obtained from steady operating conditions.

### **5.3 Data Acquisition Equipment Setup**

#### **5.3.1 General Layout**

The *Astra*, its support systems and the data acquisition equipment were assembled inside one of the turbine test cells at the facility described in Chapter 4. The data to be collected were air and fuel inlet pressures, the pressure difference across the device, oscilloscope traces of the pressure variation inside the combustor during pulsing and steady operation, and the temperatures inside the combustor. Each of these parameters was to be measured for different fuel/air ratios, fuel injection methods and exhaust pipe lengths. The equipment



and settings used to measure each parameter will be described later. The fuel, ignition and air systems (including gauges) were set up as in Chapter 4, so only additional instrumentation is shown in Figure 5-7.

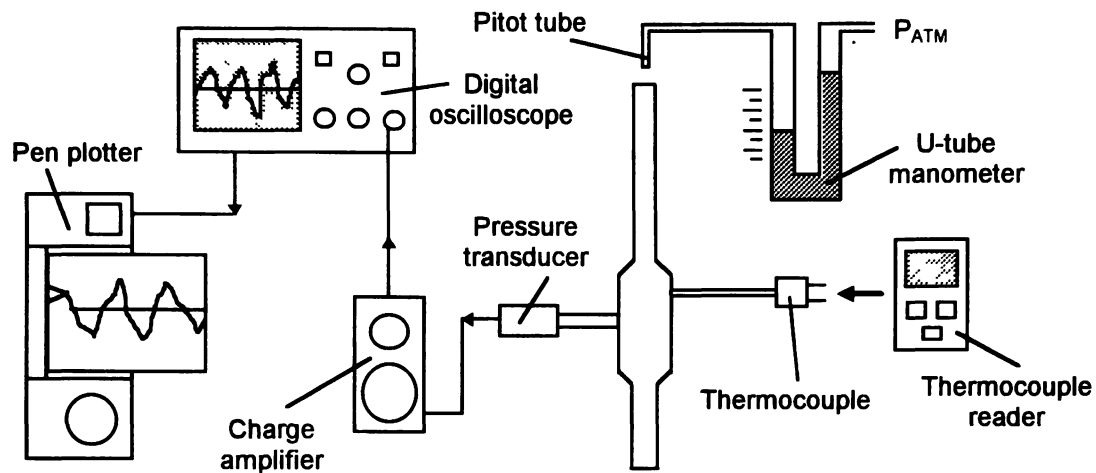


Figure 5-7. Data Acquisition Equipment Setup

### 5.3.2 Fuel and Air Inlet Pressures

These pressures were measured using typical aneroid-type pressure gauges. The gauges were calibrated as described in Appendix D.

### 5.3.3 Pressure Across the Engine

The total pressure across the engine was measured using a hand-held pitot tube attached to a U-tube, water-filled manometer (described earlier). Only the total pressure of the exhaust gases was measured since evaluating exhaust

velocity was not required. Readings in inches of water were taken at both the inlet and exhaust pipes while the engine was operating.

#### 5.3.4 Combustion Pressure Variation

This parameter was measured using the pressure transducer and equipment mentioned earlier in Run 22 of Section 5.2. The piezotron transducer was directly connected to the charge amplifier via coaxial cable. The amplifier was set to the piezotron mode, a short time constant, 1.247 mv/psi sensitivity and one volt/psi range. This range supposedly converted the 124.7 mv/psi signal for which the transducer is rated to one volt/psi, making interpretation of the oscilloscope data easier. The signal was then routed to the Hewlett-Packard digital oscilloscope which was set to five volts/division at 10 milliseconds timebase. The input channel was set to AC-coupled mode and employed a bandwidth limiter to reduce data scattering. The oscilloscope displayed both the maximum peak-to-peak voltage and average voltage of the signal. Whenever the screen would display a strong, uniform signal from the transducer, the screen was frozen and sent to the pen plotter via the oscilloscope's printing utility. Since the scope was set for five volts/division and the signal from the charge amplifier was one volt/psi, the pressure values could be interpreted directly from the signal trace.

The charge amplifier settings were found to be incorrect after all data had been acquired. Kistler Instruments had explained that since the transducer

sensitivity exceeded the range of the charge amplifier, the pressure was actually 100 times less than measured by the scope trace. This correction is accounted for in the discussion of the data in Section 5.5.

### 5.3.5 Temperature Measurements

The combustion chamber temperatures were measured using the thermocouple and digital reading instrument described in Run 21 of Section 5.2. The calibration of these instruments was conducted as described in Appendix D.

Temperature readings were taken every 15-percent along the combustor length on the axis of the engine. To establish consistency within the data, the engine was started and run for between 45 and 90 seconds before the temperature reading was taken, after which the engine was shut down and the thermocouple moved to the next location. The engine starting and stabilization process was repeated until all five readings were recorded.

## 5.4 Data Acquisition Procedure

The experimental procedure was carefully designed such that all data with the exception of temperatures could be collected at once. The procedure was adopted to conserve fuel. To expedite the data collection process, student volunteers assisted in setting up the equipment and reading instruments during the runs.

The first testing day with all instrumentation was September 29, 1995. Due to charge amplifier and cable problems, no pressure variation plots were made of the runs tested. The first run had the engine pulsing with axial fuel injection and 55-inch exhaust length. The fuel and air inlet pressures, manometer readings and the temperature at 15-percent combustor length were recorded. The engine was shut down and the thermocouple moved to 30-percent. The engine was then started and ran for 45 seconds at the same fuel/air ratio before the temperature reading was taken. This repeated until the temperatures at the five combustor lengths were measured.

The second run was conducted at the same fuel/air ratio as the first (conducive to pulsing) and an exhaust pipe length of 60 inches. The third run occurred at the same fuel/air ratio and an exhaust length of 50 inches. Since no correlation was ever found by other experimenters between exhaust pipe length and combustion temperature, the temperatures for these runs were not recorded.

For the fourth run, the exhaust pipe length was reset to 55 inches and the fuel/air ratio was increased to produce a steady operating condition. The steadiness of the condition was only observable by aural comparison with the previous runs that pulsed, since the pressure transducer could not be used to obtain a pressure trace. All data were recorded including the five combustor temperatures.

The fifth and last run was conducted at the same 55-inch exhaust length and fuel/air ratio as the first three runs, only the single, axial, fuel injector was

replaced with two open-hole-type injectors at 15-percent combustor length.

Since the fuel/air ratio and exhaust length were as in the first three runs, all data but the temperatures were recorded.

Once the problems had been solved with the charge amplifier and cabling, the *Astra* was tested again on October 3, 1995. The goal of this series of runs was to obtain the oscilloscope pressure traces for each of the conditions tested before and to repeat some runs for experimental comparison. The runs were structured identical to the first day of data recording. Temperature measurements were also repeated, except that the engine operated for 90 seconds between thermocouple readings instead of 45 seconds.

Two additional conditions were tested on this day. Now that the pressure transducer was working, the run which seemed to be operating in a steady condition on the first day was found to be pulsing (as will be discussed in the next section); Therefore, to achieve the steady condition, only fuel was injected into the engine and burned. The absence of the forced inlet air used to induce pulsing in all previous tests caused the flame to burn rich and steady. The data for this condition were recorded. The other condition tested was of just the inlet air and no fuel passing through the engine. The air pressure was the same as used in the pulsing runs. The pressure data from this condition is the basis on which the engine behavior is compared, as discussed in the next section.

## 5.5 Testing Results

The data measured during the two days of testing is summarized in Table 5-1. The conditions described at the top of the table indicate the type of operation (pulsing or steady), the fuel injection method (perpendicular or axial), and the exhaust pipe length ( $L_{EX}$ ). Each parameter will be discussed as well as any observations or significant facts about the data. Even though references to the combustion pressure traces obtained from the oscilloscope will be made, the plots will not be described in detail until later.

### 5.5.1 Fuel and Air Inlet Pressure

These values were recorded directly from the pressure gauges on the fuel and air systems. The engine pulsed well with the 5 psi fuel and 30 psi air combination as in the first four conditions of the table. The first run of the fifth condition (15 psi fuel and 30 psi air) was thought to be the steady operating state mentioned earlier. The second run of the fifth condition was the fuel-only state with no forced inlet air. The fuel pressure was held at 10 psi and the flame burned on its own.

The air-only condition was run at the same air pressure as the first four conditions to illustrate (by evaluation of the pressure traces) that the pressure changes caused by the pulse combustion cycle were independent of the forced inlet air.

Table 5-1. Astra Data at Various Operating Conditions

Run 1: 9/29/95 Run 2: 10/3/95

Condition Parameter	Pulse, Prp 15% L <sub>EX</sub> =55"		Pulse, Axial L <sub>EX</sub> =55"		Pulse, Axial L <sub>EX</sub> =60"		Pulse, Axial L <sub>EX</sub> =50"		Steady, Axial L <sub>EX</sub> =55"		Air only
	1	2	1	2	1	2	1	2	1	2	
Fuel/Air (psi)	5/30	5/30	5/30	5/30	5/30	5/30	5/30	5/30	15/30	10/1	0/30
$h_{T IN} / h_{T EX}$ (inH <sub>2</sub> O)	.35/.45	.3/.35	.6/.4	.35/.35	.3/.4	.4/.35	.25/.5	.25/.4	.45/.45	0/0	-.1/.2
T <sub>15</sub> (°R)	-	-	795	894	-	-	-	-	679	1640	-
T <sub>30</sub> (°R)	-	-	1035	1034	-	-	-	-	826	1307	-
T <sub>45</sub> (°R)	-	-	1351	1341	-	-	-	-	1114	1134	-
T <sub>60</sub> (°R)	-	-	1565	1714	-	-	-	-	1297	1050	-
T <sub>75</sub> (°R)	-	-	1760	1975	-	-	-	-	1539	1030	-
Pressure trace Figure No.	-	5-9(a)	-	5-9(b)	-	5-9(c)	-	5-9(d)	5-9(e)	-	5-9(f)
Frequency (Hz)	-	137.9	-	111.1	-	100.0	-	126.9	125.0	-	-
Max. pressure peak-peak (psi)	-	.2547	-	.3188	-	.2703	-	.2859	.3156	-	.0328
Avg. pressure (psi)	-	.00754	-	.01575	-	.00393	-	.00058	.00407	-	.00145

### 5.5.2 Total Pressure Measurement at Inlet ( $h_{T IN}$ ) and Exhaust ( $h_{T EX}$ )

If a pulsejet (valved or aerovalve) functions through self-aspirating pulse combustion, the exhaust pressure becomes a significant factor in determining the performance of the device. The exhaust pressure is directly related to the pressure rise within the combustor due to the pulse cycle. Since atmospheric pressure is the comparative condition for a self-aspirating engine, the greater the exhaust pressure above atmospheric, the better the performance. The *Astra*, however, never achieved self-aspiration and pulsed only when air was forced through the inlet. In this case, the exhaust pressure developed from forcing air through the engine without combustion became the comparative condition. Exhaust pressures above those of the air-only condition were indicative of the “pressure gain” due to the pulse combustion process.

The exhaust pressure in all pulsing cases is greater than the pressure measured from the air-only condition, indicating the inherent pressure gain resulting from pulse combustion. An examination of the exhaust pressure of the first run of the fifth condition, thought to be steady combustion by aural inspection, also indicates a pulsing behavior. Pulse combustion for that run is further supported by comparison of its pressure trace to others that were pulsing.

An important issue was considered when using the manometer to measure the exhaust pressure during pulsing operation. Since the exhaust gases were continuously reversing flow direction through both the inlet and exhaust pipes (as described in Chapter 2), the manometer readings represented



an average pressure between pulses. Since the average readings denoted a positive pressure, the exhaust pressure leaving the pipes was greater than the inlet pressure. This indicated that the mean combustor pressure was slightly greater than atmospheric, as it should be for a pulse combustion cycle.

The manometer heights measured for the air-only condition indicate a negative pressure at the inlet pipe. This negative value is not relevant in evaluating pulse combustion characteristics and was caused by the pitot tube measuring its own wake when the air was flowing around it. With the exception of the two runs (not including the air-only condition), the total pressure of the escaping exhaust gases at the exhaust pipe was either equal to or greater than at the inlet.

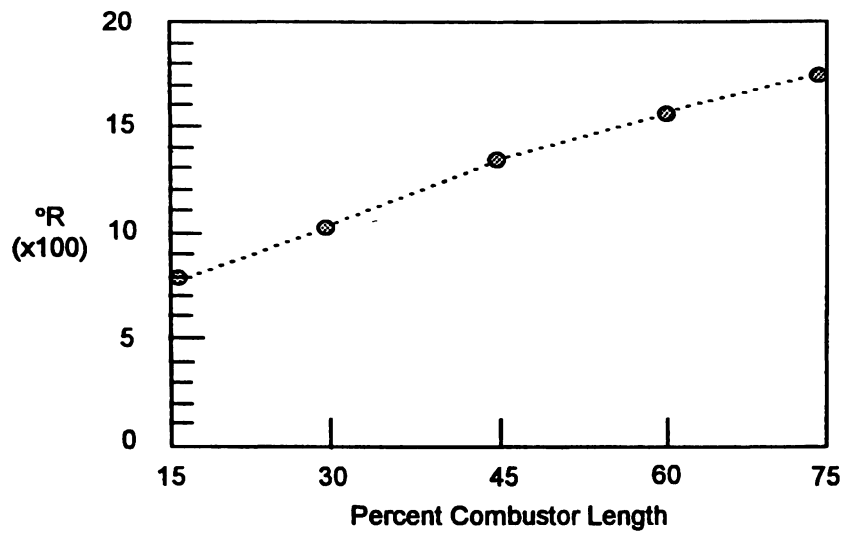
### 5.5.3 Combustion Temperatures

The temperature parameters are listed in Table 5-1 by their combustor location (*i.e.*,  $T_{45}$  indicates the reading at 45-percent combustor length). The Fahrenheit readings taken during the tests by the digital thermocouple reader were converted to Rankine for standardization.

Temperature readings were taken only for the second and fifth operating conditions. The readings from first runs of both conditions were recorded after the engine was operational for 45 seconds and the second run readings were taken after 90 seconds of operation. The stabilization times account for the temperature differences at some combustor locations between the first and

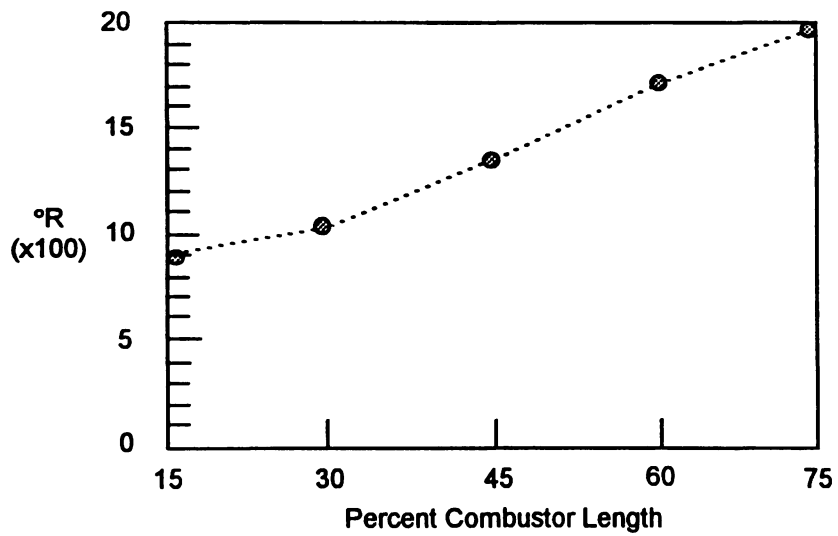
second runs of the second condition. With respect to the fifth condition, although the engine was set up identically for both runs, the fuel/air ratios were drastically different and so the two runs have no relation to one another. A graph of temperature versus combustor length is given for each of the four temperature runs in Figure 5-8. Figure 5-8(c) was originally thought to correspond to a steady operating condition and is labeled as such, even though evaluation of the data proved it was not.

The graphs indicate that for pulsing conditions, the hottest part of the combustion chamber is towards the rear and is independent of fuel injection location. This is not so for the steady condition, where the hottest part is towards the front of the chamber just after the fuel injection point. This trend indicates that the flow dynamics of the forced air retain the combustion at the back of the chamber. Although this contradicts the observations of both Ponizy and Wojcicki (4) and Keel and Shin (10), their pulse combustion devices are self-aspirating, whereas the *Astra* is not. In addition to the graphs, Table 5-1 shows broader range of temperatures over the combustor length associated with pulse combustion than with the steady condition. The temperature increases about 1000 degrees-R from the front to the rear of the combustor for the pulse condition compared to about 600 degrees-R for the steady case.



First Run - Pulsing, Axial-Injection,  $L_{EX}=55''$

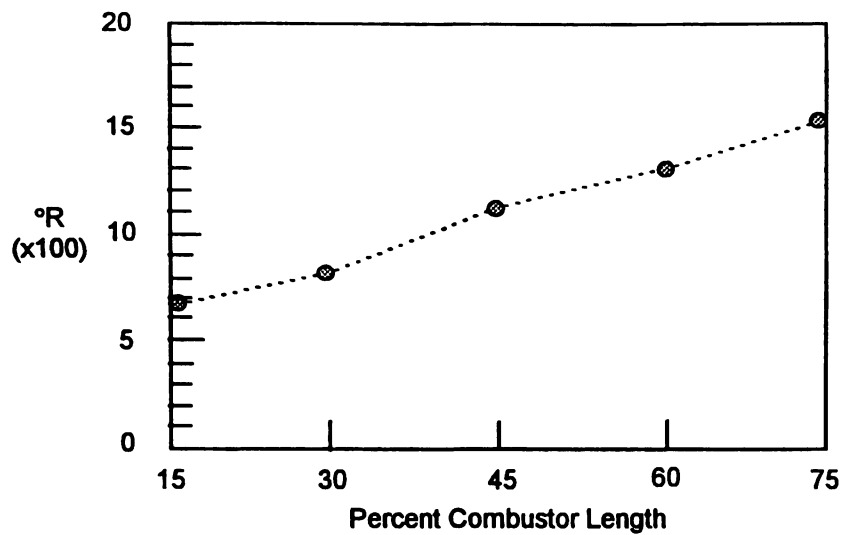
(a)



Second Run - Pulsing, Axial-Injection,  $L_{EX}=55''$

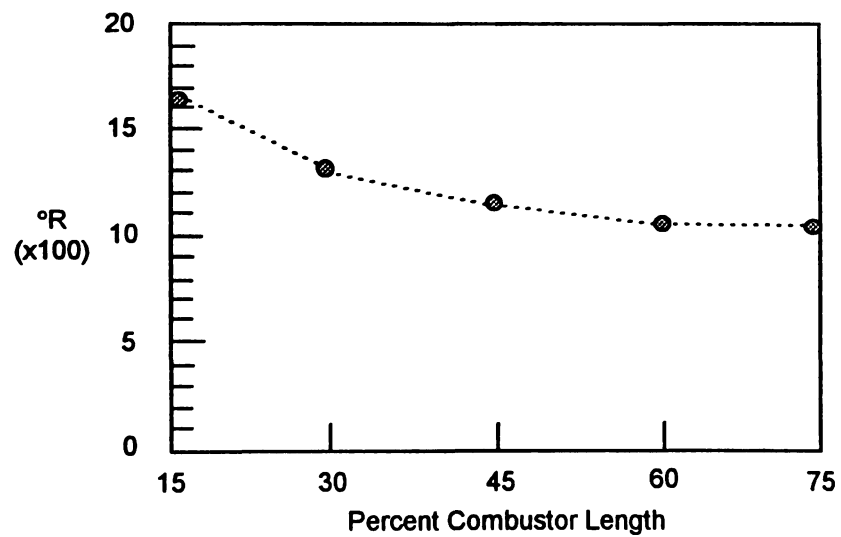
(b)

Figure 5-8 (continued). Combustion Temperature Versus Combustor Length



First Run - Steady, Axial-Injection,  $L_{EX}=55''$

(c)



Second Run - Steady, Axial-Injection,  $L_{EX}=55''$

(d)

Figure 5-8 (concluded).

## 5.5.4 Combustion Pressure Traces

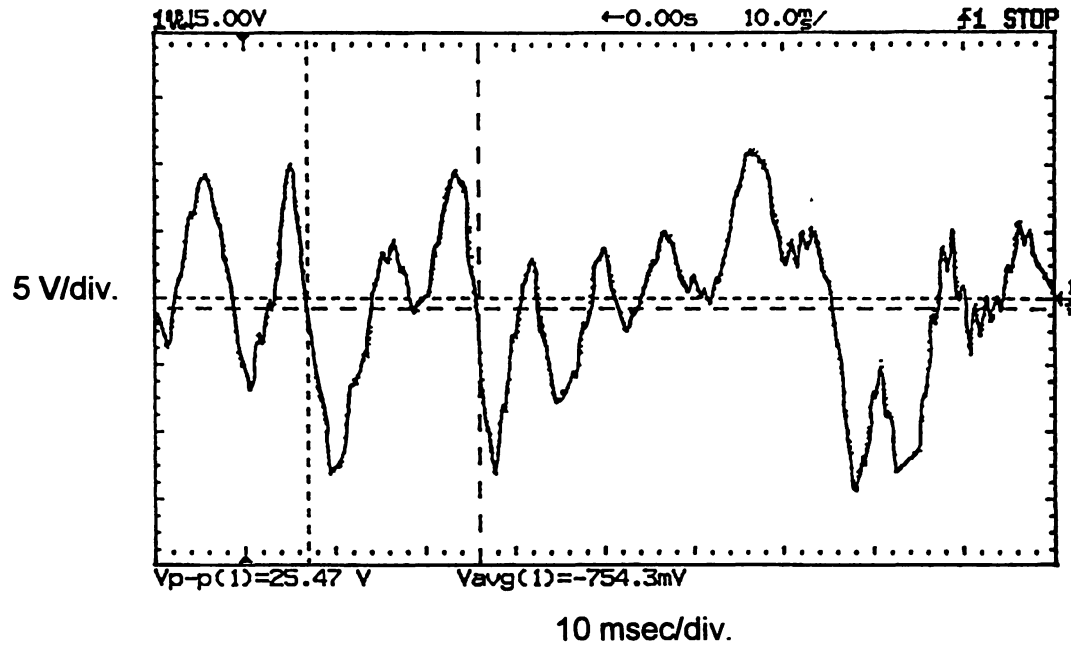
### 5.5.4.1 *Oscilloscope Plot Description*

Table 5-1 indicates the runs for which pressure traces were obtained from the oscilloscope. The figure number for each plot is given in the shaded row. As mentioned earlier in Section 5.3.4, the settings for the oscilloscope were five volts/division and 10 millisecond time base, which remained constant through all of the runs. The settings are listed at the top of each plot and on the axes of Figure 5-9(a). The scope also calculated the maximum peak-to-peak voltage and average voltage of the signal and displayed those values at the bottom of the screen. These values are also listed in Table 5-1.

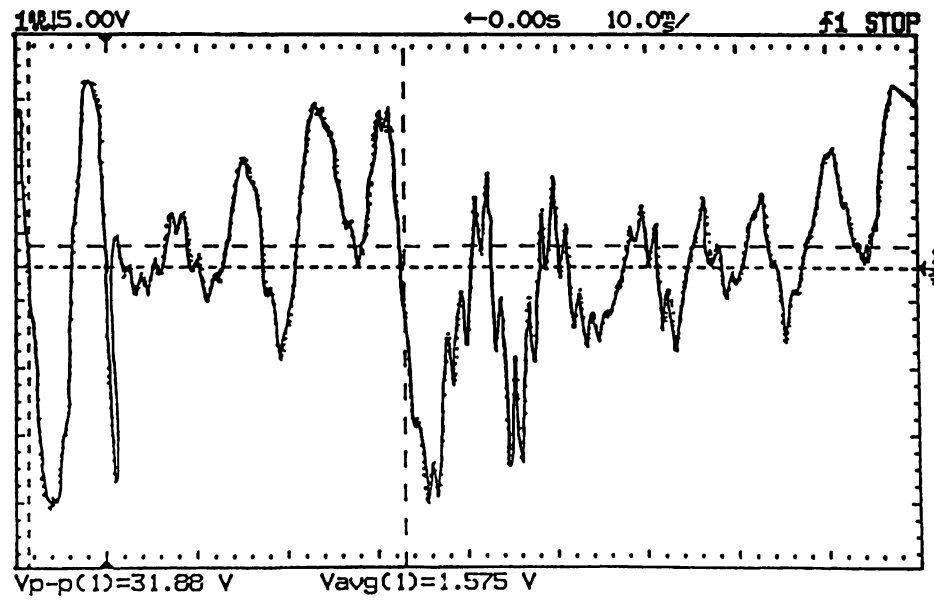
The small mark on the right-center of the traces indicates the zero-signal reference line, which is represented by a horizontal, small-dashed line. The horizontal, large-dashed line either above or below the reference line indicates the average voltage. The two vertical dashed lines present in of some traces are produced by the oscilloscope and are not important for this discussion. All additional text and symbols on the plots indicate other channel settings, also not relevant to this discussion. The display grid connecting the tick marks surrounding the trace was not plotted for clarity.

### 5.5.4.2 *Pressure Signal Trace*

There are many similarities in the signals from the oscilloscope that should be discussed before a comparison of Figures 5-9(a) through 5-9(f) can

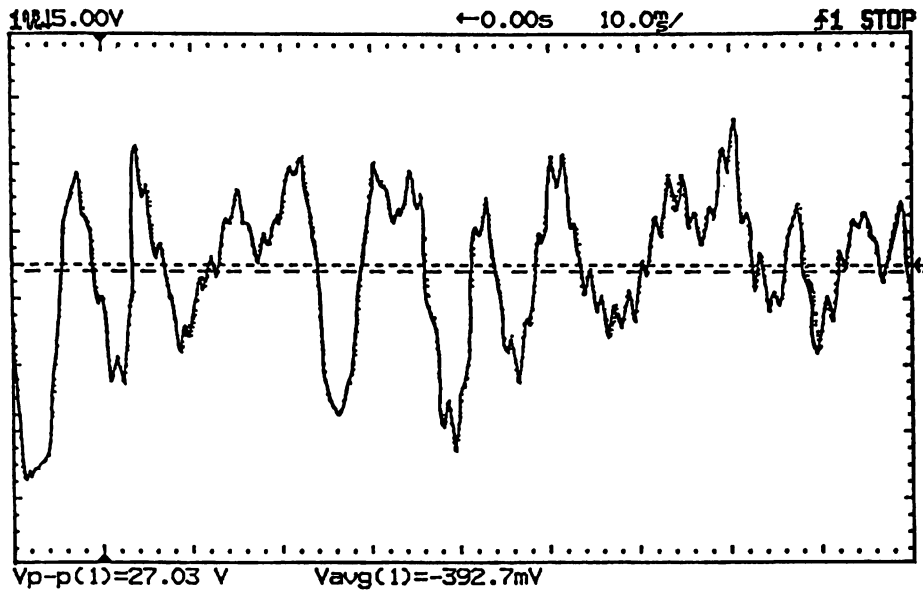


(a)

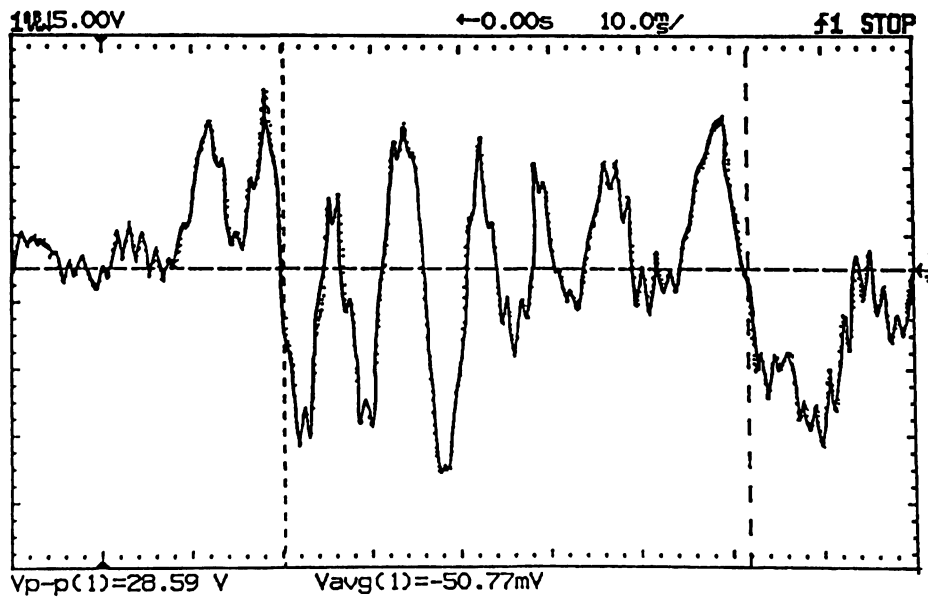


(b)

Figure 5-9 (continued). Oscilloscope Traces of Combustor Pressure Variation

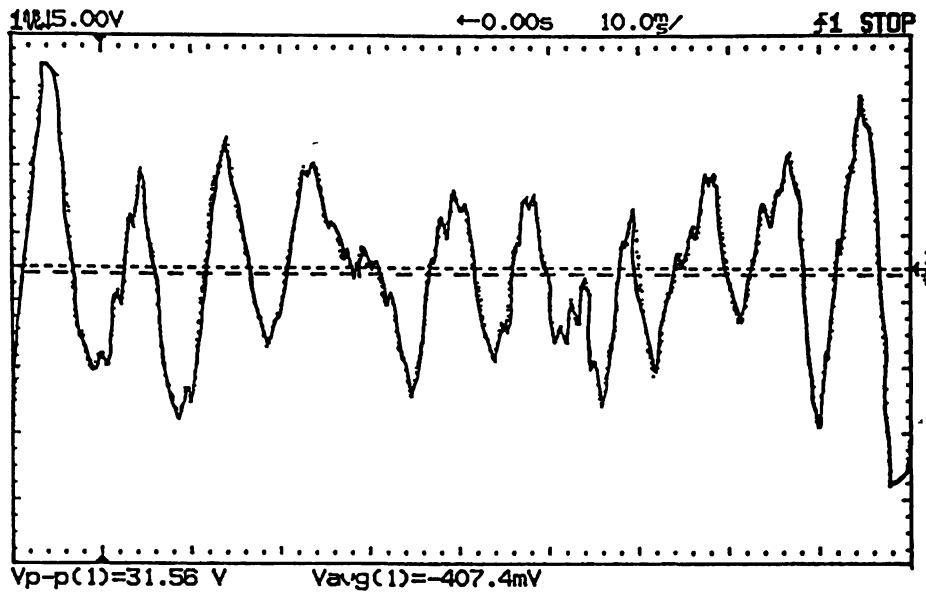


(c)

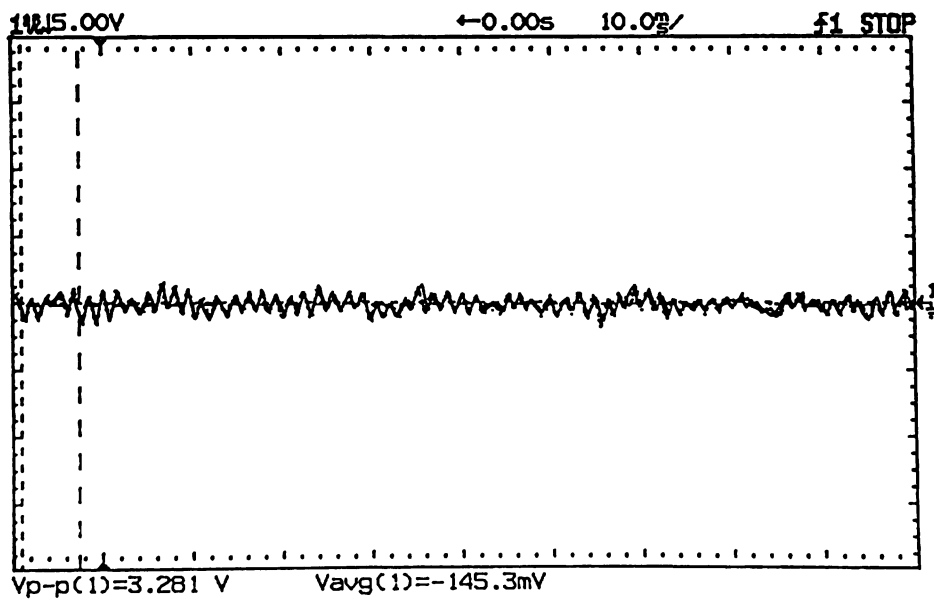


(d)

Figure 5-9 (continued).



(e)



(f)

Figure 5-9 (concluded).



be conducted. With exception of Figure 5-9(f), all of the pressure traces are very ragged and irregular in amplitude within certain limits. Examination of the pressure peaks and valleys reveals two or sometimes three smaller peaks at the top (or bottom) of each pressure wave that are generated from the dynamics of the combustion process. The non-uniform amplitude of the waves is produced by the unsteady flow dynamics between pulses. Nonetheless, the amplitudes in all of the traces are constrained within certain pressure limits as dictated by the pulse cycle of the engine.

#### 5.5.5 Pulse Combustion Verification

The pressure trace from the air-only condition is shown in Figure 5-9(f). As discussed in Section 5.5.3, this condition was the comparative baseline to determine whether the *Astra* was pulsing. When comparing the frequency and amplitude of Figures 5-9(a) through 5-9(e) to those of Figure 5-9(f), the significant differences in the waveform indicate strong pulsing conditions. In addition, the maximum peak-to-peak pressures for the Figures 5-9(a) through 5-9(e) are an order of magnitude higher than for the air-only condition, supporting the presence of pulse combustion. The maximum peak-to-peak pressures will be discussed later.

### 5.5.6 Engine Frequency

The operating frequency of the *Astra* was calculated from Figures 5-9(a) through (e). The frequency for each plot is listed in Table 5-1. The average of the five frequencies is 120.2 Hz, which is typical for a pulsejet of this configuration (as stated by Lockwood [7]). The operating frequency of the first condition in Table 5-1 is slightly higher than the rest, possibly due to the fuel injection method. Since the fuel was injected in two streams perpendicular to the engine axis at the 15-percent combustor length, the fuel was closer to the combustion region in the chamber and perhaps did not take as long to mix and ignite. As for the axial injection present during the other conditions, the fuel had to travel through the inlet bulkhead before reaching the combustor, resulting in a longer time between pulses and lower cycle frequency.

The frequency evaluation of first run of the fifth condition (Figure 5-9[e]) indicates that the engine was certainly not operating steady as was thought by aural inspection.

Variation of exhaust pipe length produced slight differences in the operating frequency, as theorized by the Helmholtz acoustic equations. With axial fuel injection, the 50-inch length produced a higher frequency (126.9 Hz) than did the 60-inch length (100.0 Hz). The frequencies produced by the 55-inch lengths were 111.1 Hz and 125.0 Hz. Since these frequencies were between the those of the 50 and 60-inch exhaust lengths, the variation of cycle operating frequency with exhaust length is supported.

### 5.5.7 Operating Pressures (Maximum Peak-to-Peak and Average Voltages)

Due to the charge amplifier settings discussed in Section 5.3.4, the voltages listed at the bottom of the figures are 100 times greater than their actual value. The corrected equipment settings were such that one volt represented one-hundredth (0.01) psi. The actual maximum peak-to-peak and average voltages (psi values) are listed in Table 5-1.

Averaging the maximum peak-to-peak pressures of the signals from Figures 5-9(a) through 5-9(e) shows that the *Astra* develops a combustion pressure rise of 0.29 psi. The average pressures in the last row of Table 5-1 were obtained by the oscilloscope by utilizing all of the data points and not just the peak pressures.

## CHAPTER 6

# CONCLUSIONS AND RECOMMENDATIONS

### 6.1 Conclusions

The experiments conducted in this project have revealed significant conclusions about pulsejets and their operation. This project has also verified some of the observations of previous experimenters. The information is organized into the categories of engine geometry and combustion conditions.

#### 6.1.1 Engine Geometry

In general, scaling a baseline aerovalve pulsejet design either larger or smaller is often successful, as demonstrated by Lockwood (7) and other researchers mentioned in Putnam *et al.* (1). Lockwood scaled up and scaled down an original SNECMA aerovalve design and the resulting engines functioned well. The *Astra* is a slightly scaled-down version of one of the Lockwood models yet does not self-aspirate as the baseline engine did. Since the *Astra's* geometry ratios (discussed in Chapter 2) are identical to those of a

Lockwood model, the absence of self-aspiration must be due to inadequate combustion characteristics.

The optimum characteristic lengths for an aerovalve pulse combustor defined by Narayanaswami and Richards (5) do not apply to all aerovalve pulse combustor or pulsejet designs. These parameters were duplicated on the *Astra* and produced no tendency to self-aspirate.

Definite trends regarding the geometric proportions of both aerovalve and mechanically-valved engines have been followed through the years of pulsejet development. These trends can be observed by comparing the ratios of component lengths and areas for different engines. The parameters used for such comparison have been defined in Chapter 2 and are applicable to all pulse combustor and pulsejet designs.

The exhaust pipe length of an aerovalve pulsejet defines the operating frequency, as theorized by the Helmholtz acoustic equations. The data from the *Astra* experiments support this by demonstrating that the longer the exhaust pipe length, the lower the pulse frequency. Experimentation with the *Astra* also shows that the pulsing conditions induced by a certain exhaust pipe length are unaffected by changing inlet geometry, but are affected by relocating the fuel injection point on the combustor. The central fuel injection locations will produce strong pulsing within a narrow range of exhaust pipe lengths, whereas a more rearward injection position broadens the range of exhaust lengths that produce pulsing.

### 6.1.2 Combustion Conditions

The temperature distribution inside the combustion chamber under self-aspirating pulse combustion conditions is significantly different than from non-self-aspirating conditions. Ponizy and Wojcicki (4) and Keel and Shin (10) have shown that the hottest combustion region is located near the front-central portion of the combustor for self-aspirating pulsejets. Temperatures inside the *Astra's* combustor show the hot regions to be near the exhaust nozzle. This effect is due to the forced inlet air required to sustain engine pulsing.

Even though an aerovalve pulsejet may be aurally and visually observed to function steady at high fuel and air inlet pressures, combustion pressure and temperature data may indicate that the engine is indeed pulsing. For this reason, instrumentation of a pulse combustion device is the most reliable method to verify operating condition.

Pulse combustion has a throttleable range, starting at a very lean, low-frequency condition and going up to the seemingly rich-burning, steady operation as mentioned above. The *Astra* experiments show that with the air pressure remaining constant at 30 psi, the fuel pressures corresponding to these conditions range from 2.5 to 9 psi, respectively. The most robust pulsing is established at about 5 psi.

## 6.2 Recommendations

The important recommendation for future experimentation with the *Astra* is to achieve self-aspiration. Since the engine geometry follows the design trends discussed in Chapter 2 and is similar to a functioning aerovalve model (Lockwood), the reason for no self-aspirating tendency is due to the combustion conditions. The fuel delivered into the combustor may not mix fast enough to allow self-aspiration. This can be investigated by testing new fuel nozzle injection patterns or modifying the engine to accept more than two injectors for a more uniform fuel delivery pattern. Tests should also be conducted to evaluate the fuel/air ratio of the engine by employing flow-measuring devices into the fuel and air systems.

The data collected from a self-aspirating engine will be different in all respects to that collected from the experiments conducted in this project. Once self-aspiration is achieved, all of the test runs described in the last half of Chapter 5 should be re-evaluated. The information and conclusions gathered from this project will provide a good foundation to compare the new data so that more in-depth studies of a self-aspirating aerovalve pulsejet can be accomplished.

## REFERENCES

1. Putnam, A. A., Belles, F. E., and Kentfield, A. C., "Pulse Combustion," *Progress in Energy and Combustion Science*, Vol. 12, 1986, pp. 43-79.
2. Winiarski, L., "A Logically Simple Method for Solving the Gas Dynamics of a Pulsating Combustor," *First International Symposium on Pulsating Combustion*, Sheffield, England, Sept. 20-23, 1971.
3. Merva, J., Lennox Industries, Allen, Texas - *Telephone Interview*, Jan. 12, 1994.
4. Ponizy, B. and Wojcicki, S., "On Modeling of Pulse Combustors," *Twentieth Symposium (Intern'tl) on Combustion*, The Combustion Institute, 1984, pp. 2019-2024.
5. Narayanaswami, L. L. and Richards, G. A., "Pressure-Gain Combustion Part I: Model Development," *Technical Report*, U. S. Department of Energy, Morgantown, West Virginia, 1993.
6. Kay, A. L., "Buzz Bomb," *Article of uncertain source or publication date*.
7. Lockwood, R. M. and Patterson, W. G., "Pulse Reactor Lift-Propulsion System Development Program," *Report No. ARD-301*, Hiller Aircraft Corporation, Palo Alto, California, Dec. 18, 1961.
8. Lockwood, R. M., "Pulse-Reactor Lift Propulsion Engines Permit Unlimited Terrain Freedom," *AIAA 64-369*, First AIAA Annual Meeting, Washington, D. C., Jun. 29 - Jul. 2, 1964.
9. Taylor, J. W. R. (Ed.), *Thermo-Jet Data*, *Janes' All the World's Aircraft*, p. 764, 1979-80.
10. Keel, S. I. and Shin, H. D., "A Study of the Operating Characteristics of a Helmholtz-Type Pulsating Combustor," *Journal of the Institute of Energy*, Vol. 64, June 1991, pp. 99-106.
11. Richards, G. A. and Gemmen, R. S., "Pressure-Gain Combustion Part II: Experimental and Model Results," *Technical Report*, U. S. Department of Energy, Morgantown, West Virginia, 1993.
12. van Wylan, G. J. and Sonntag, R. E., *Fundamentals of Classical Thermodynamics*, 3rd ed., John Wiley and Sons, New York, New York, 1992, p. 315.



13. Bland, W. F. and Davidson, R. L. (Ed.), Petroleum Processing Handbook, McGraw-Hill, New York, New York, 1967.
14. Nanmac Corporation, Digital Thermometer Instruction Manual, Nanmac Corporation, Framingham Center, Massachusetts, 1994.

**APPENDIX A**  
***ASTRA* CONSTRUCTION DRAWINGS**

## APPENDIX A

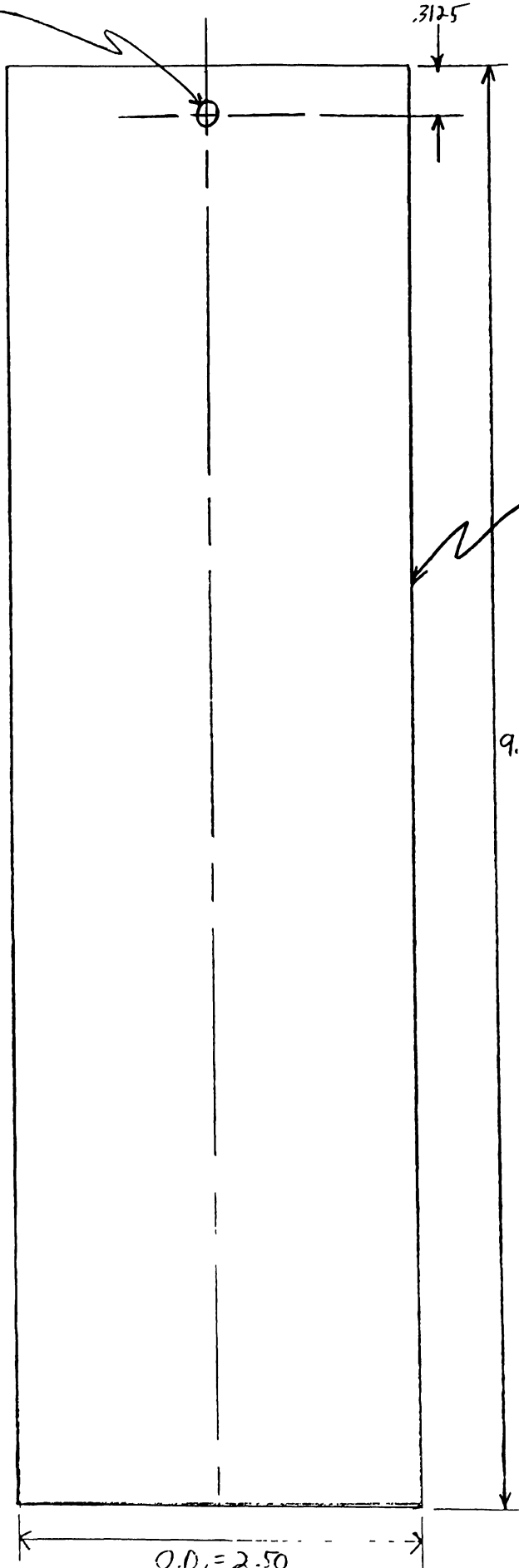
### ASTRA CONSTRUCTION DRAWINGS

#### Special Notes:

- The part numbers on the drawings are as listed in Figure 3-4
- All dimensions are in **inches** and angles in **degrees**
- Drawings may not be to scale due to reduction of the actual drawings to accommodate the required page format
- Only fabricated parts are given in this appendix, components assembled from off-the-shelf parts are not shown and are described in Section 3.4
- Sheet metal patterns are included as required

PART 2: INLET PIPE

#8 CLEARANCE  
OR 13/32"  $\phi$   
(3 HOLES - SEE PART 3)  
FOR LOCATION



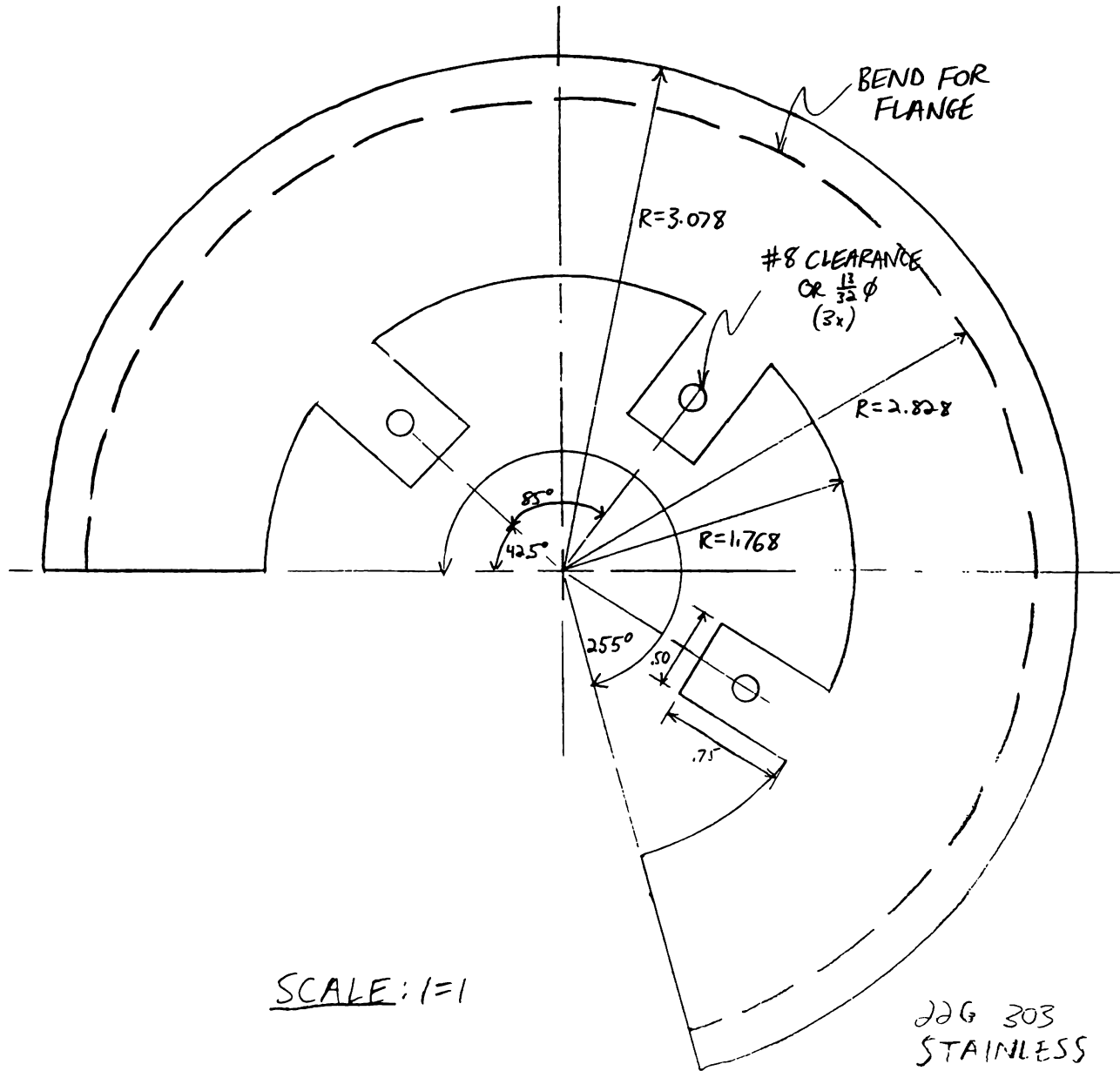
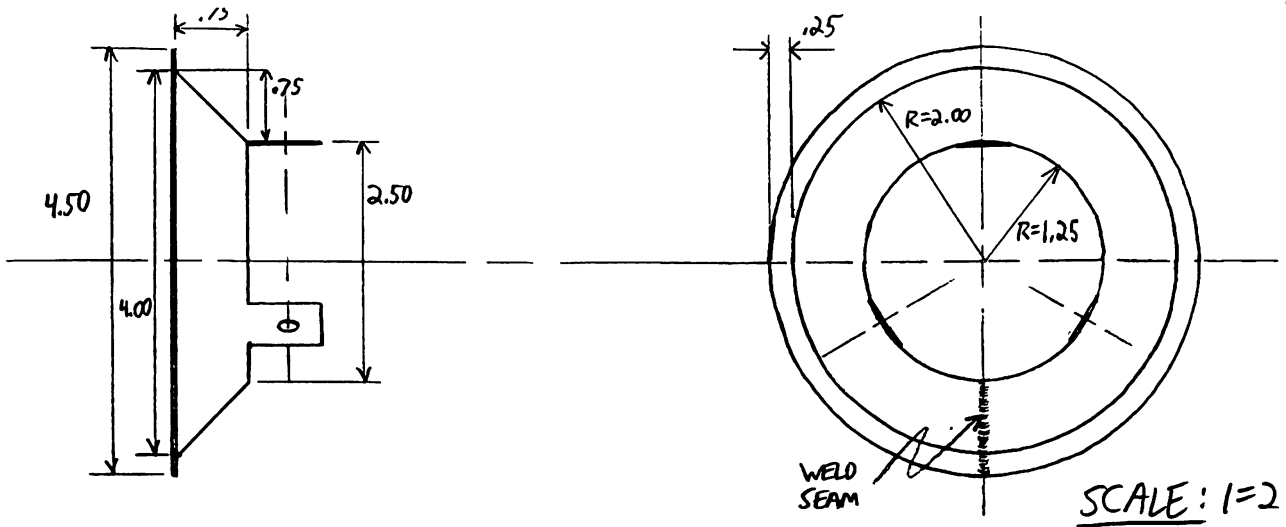
2.5"  $\phi$  GALVANIZED  
AUTOMOTIVE STOCK  
1/16" WALL THICK.

9.00

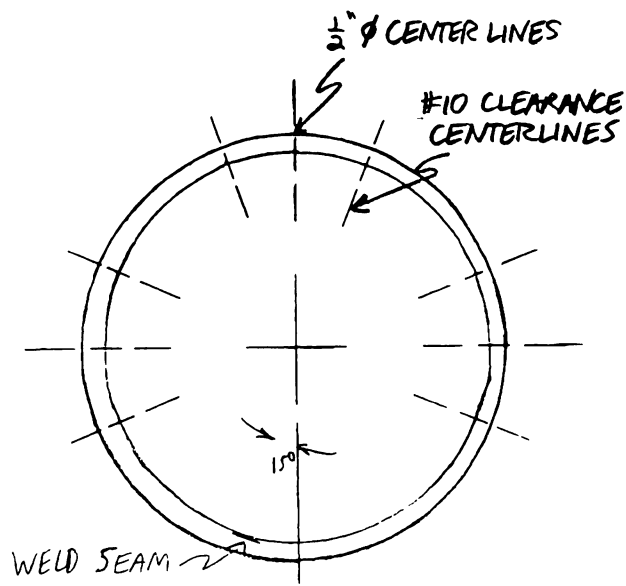
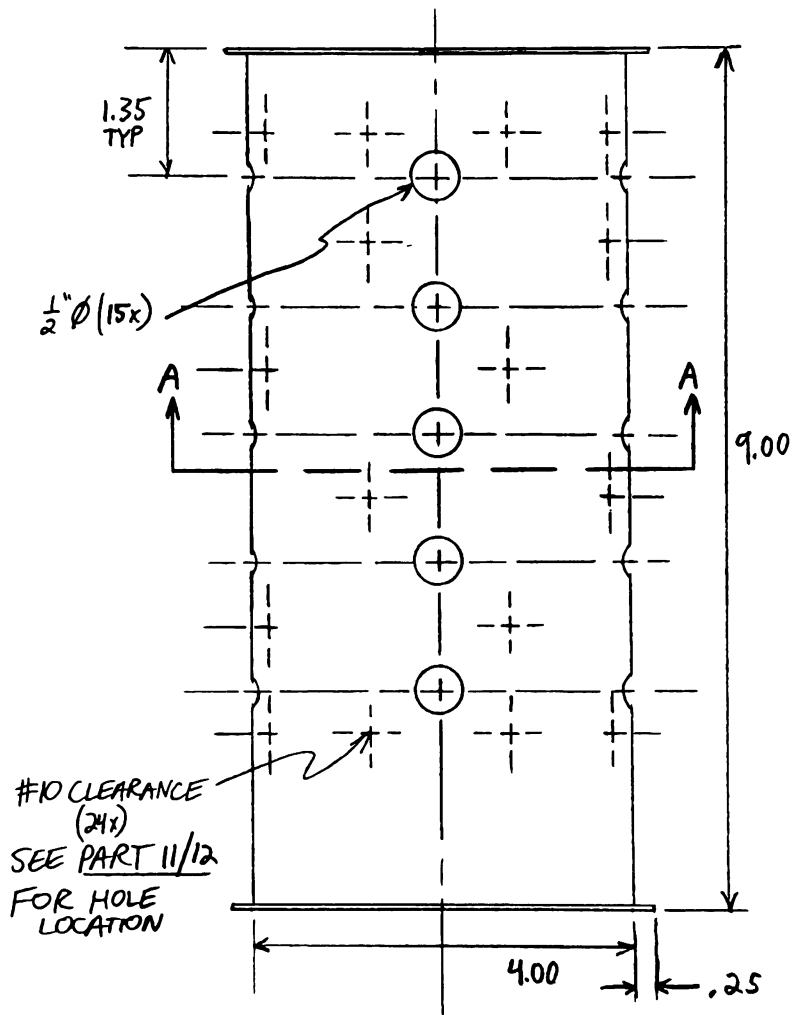
O.D. = 2.50

SCALE: 1=1

PART 3: INLET BULKHEAD

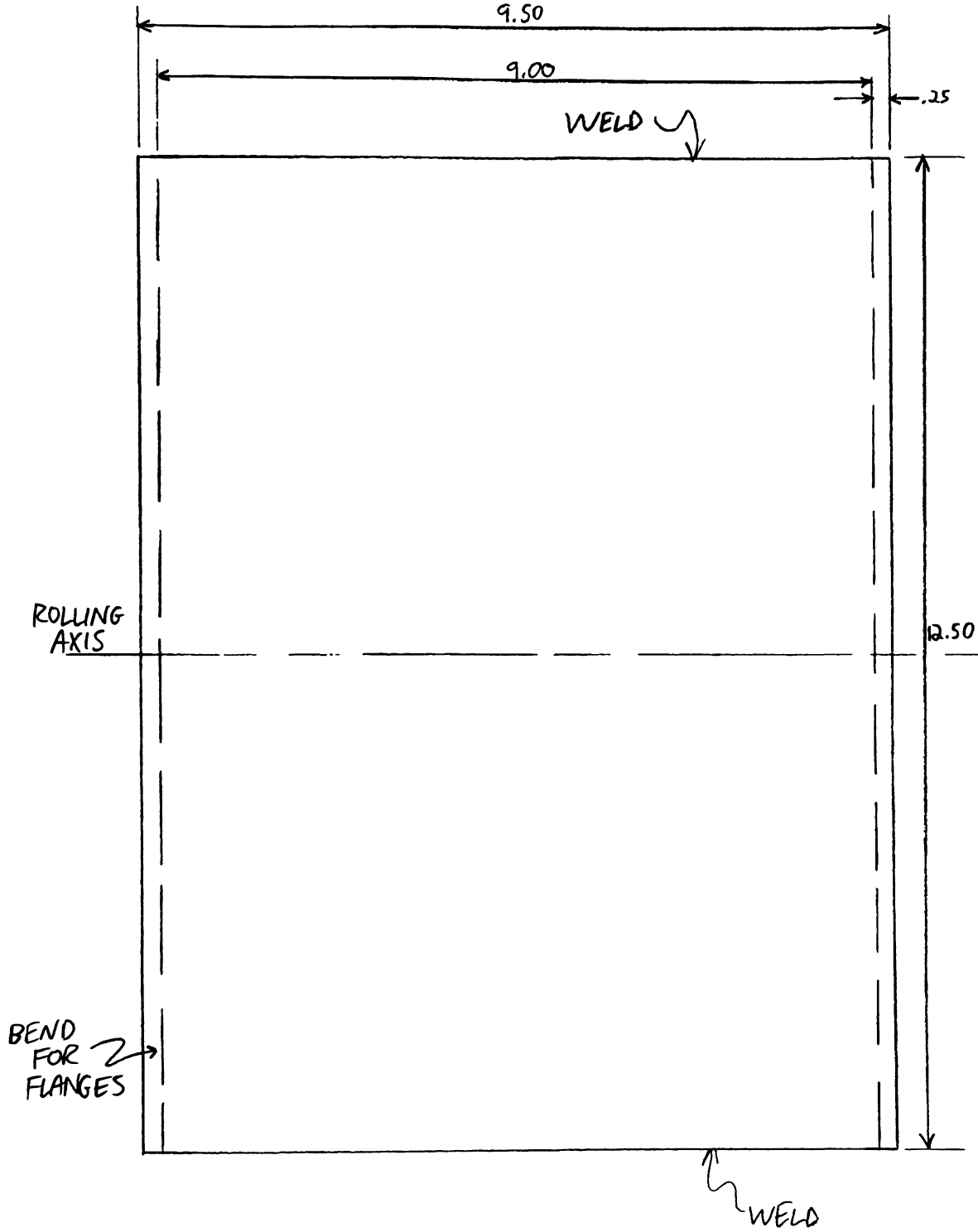


PART 4: COMB. CHAMBER



SECTION A-A

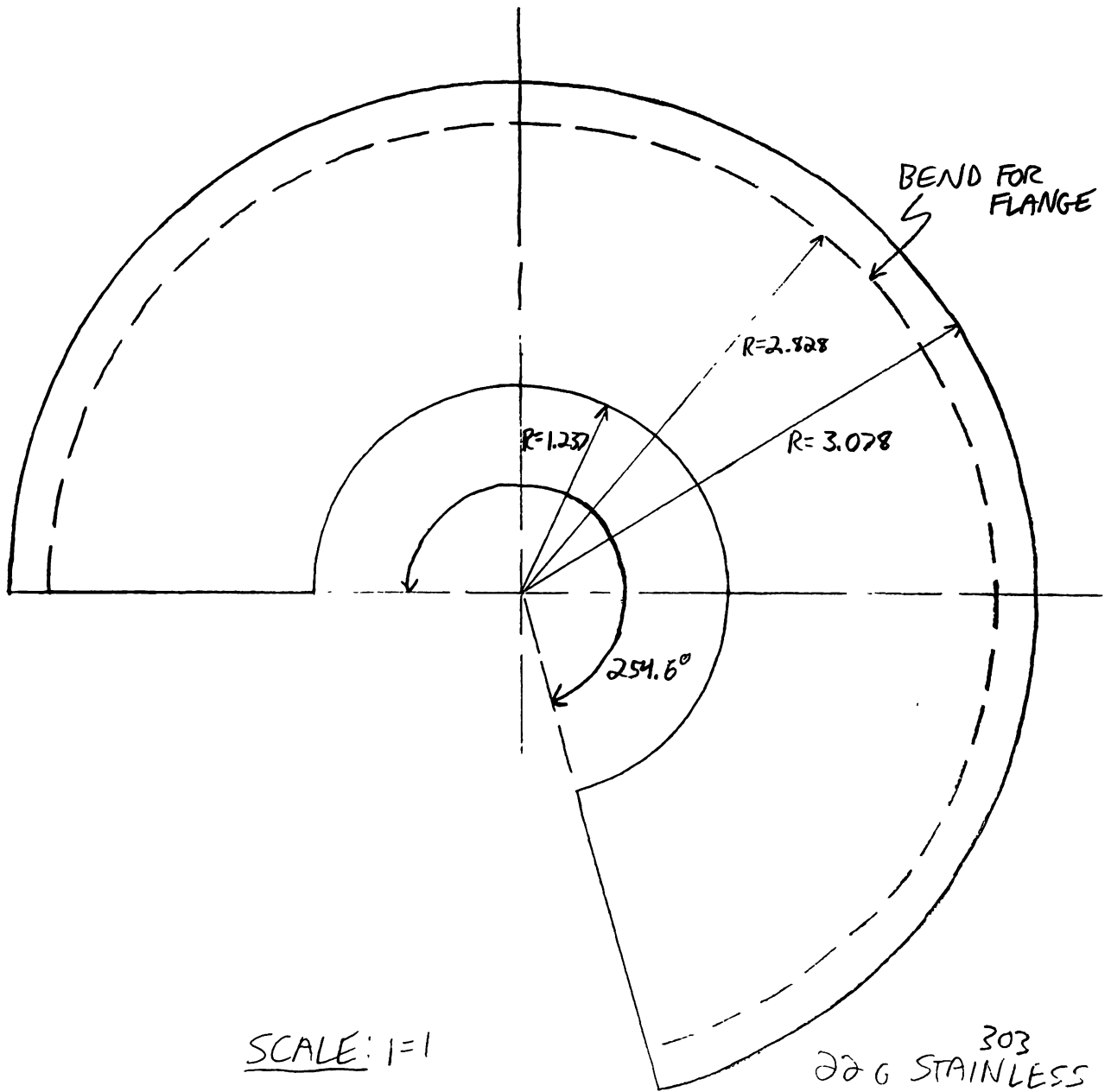
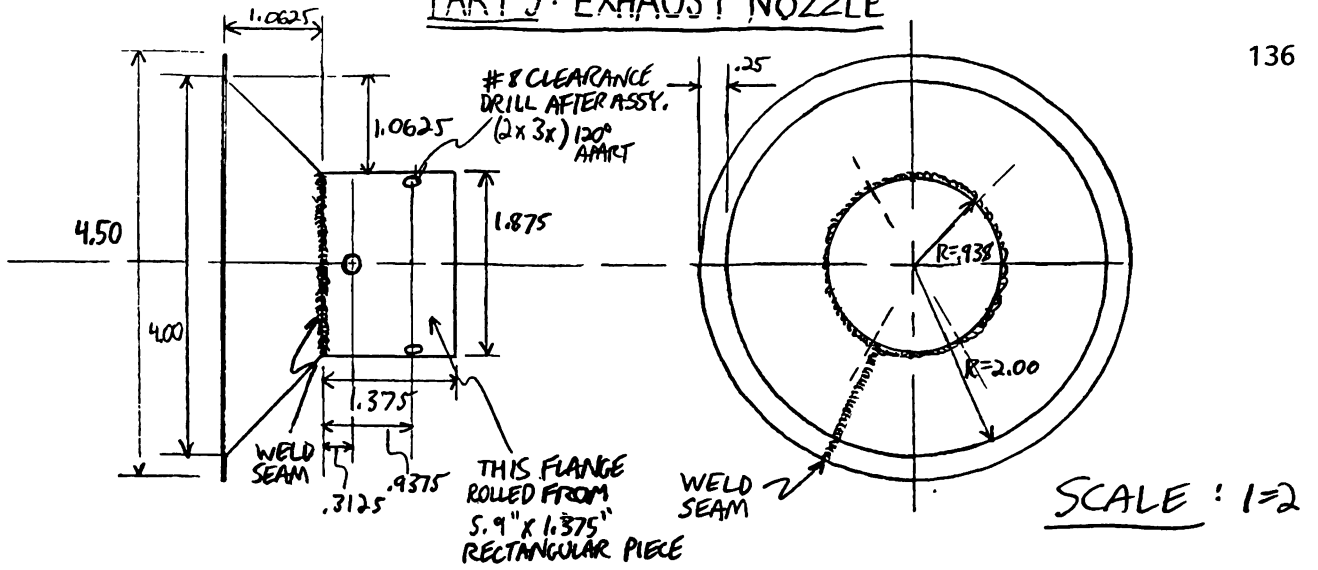
PART 4: TEMPLATE



22G 303 STAINLESS

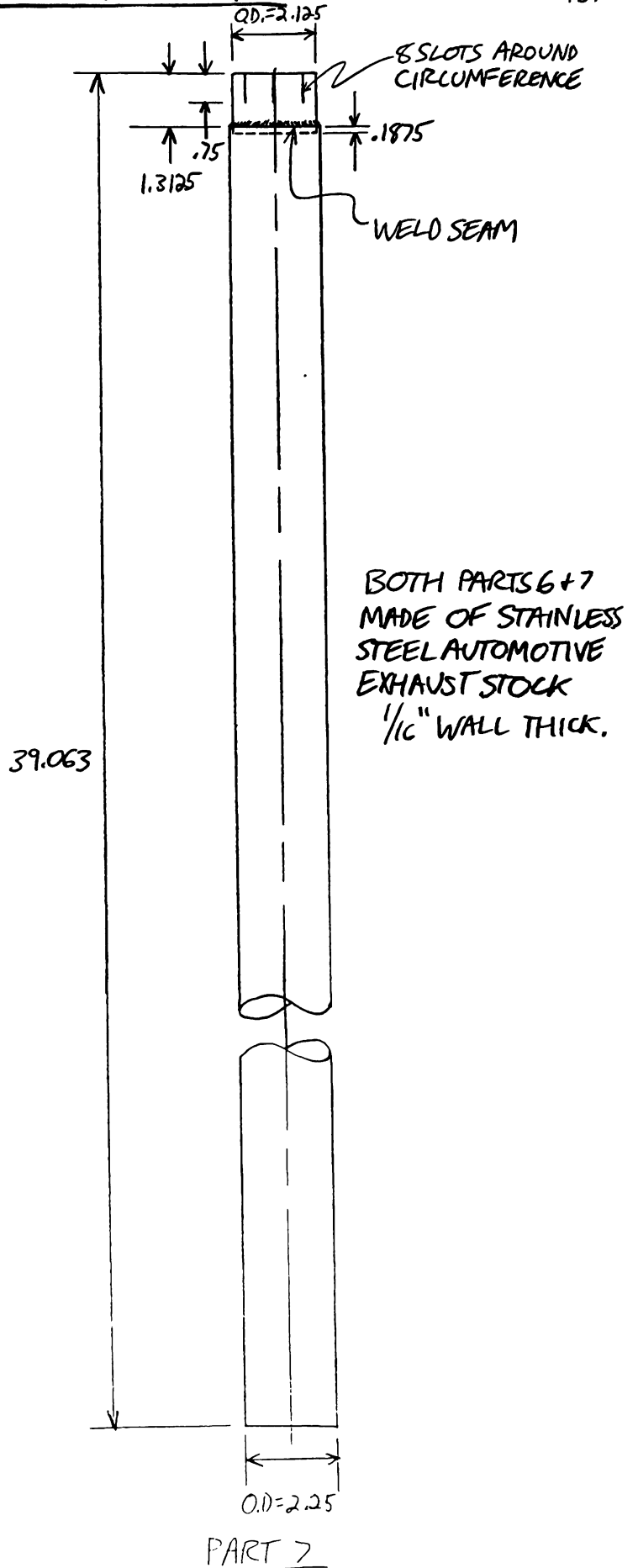
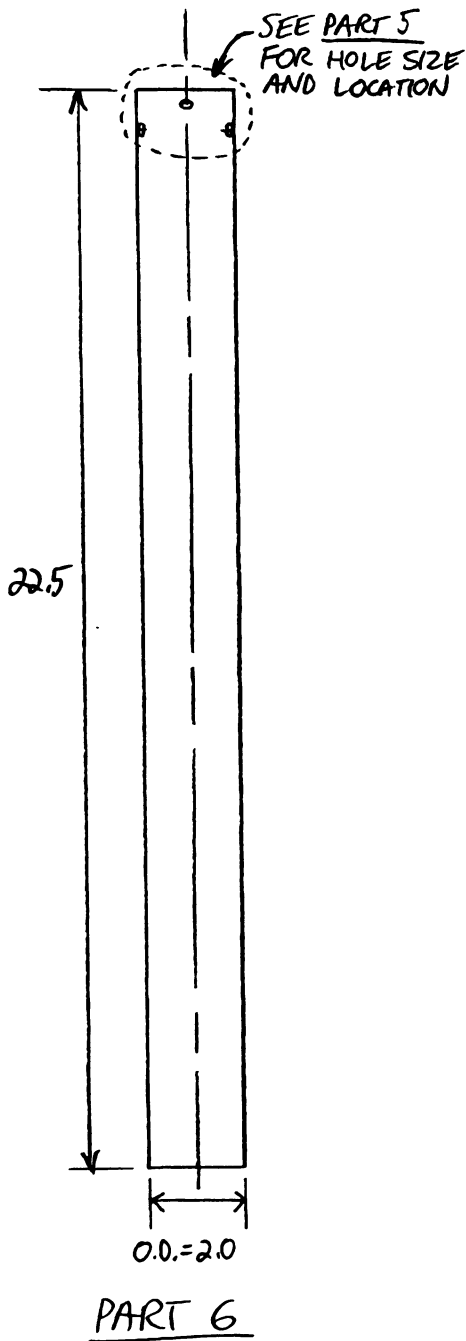
SCALE: 1=2

PART 5: EXHAUST NOZZLE



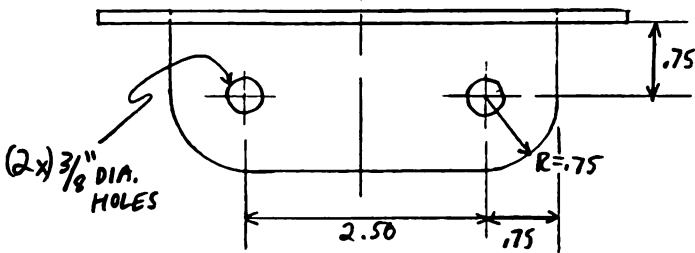
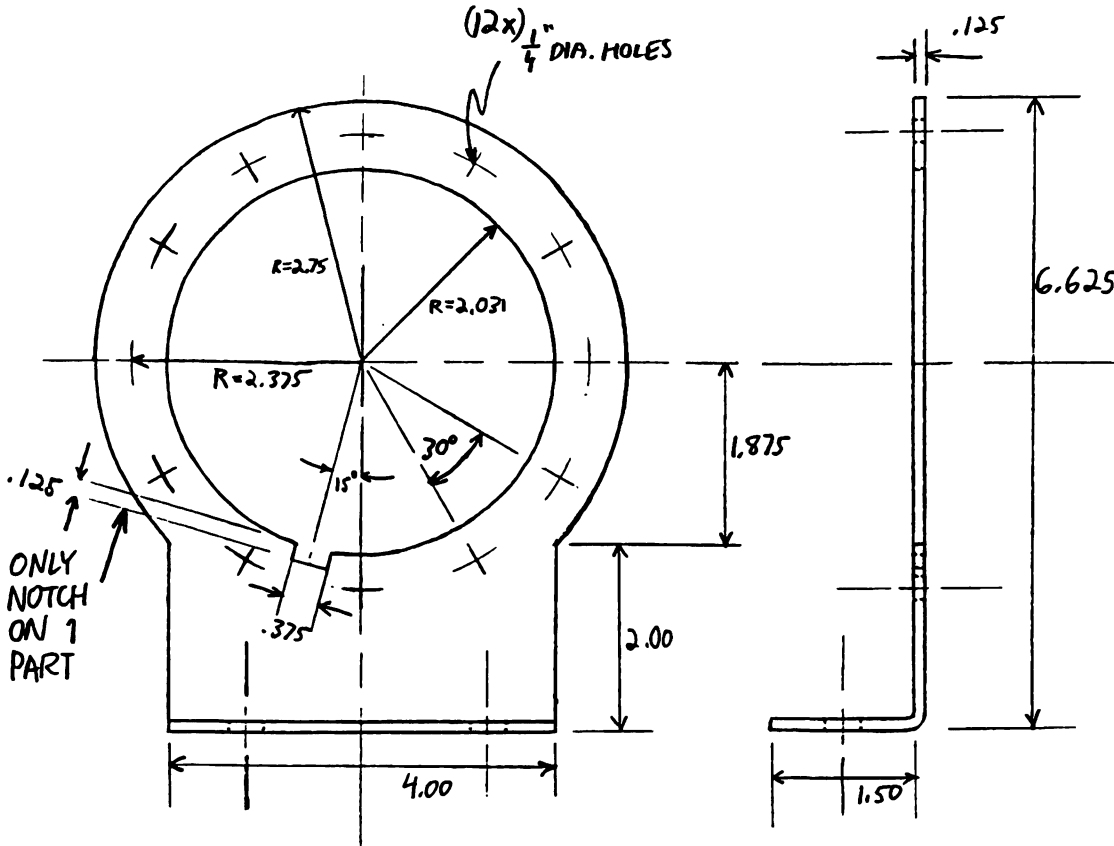


PARTS 6 + 7: VARIABLE-LENGTH EXHAUST PIPE

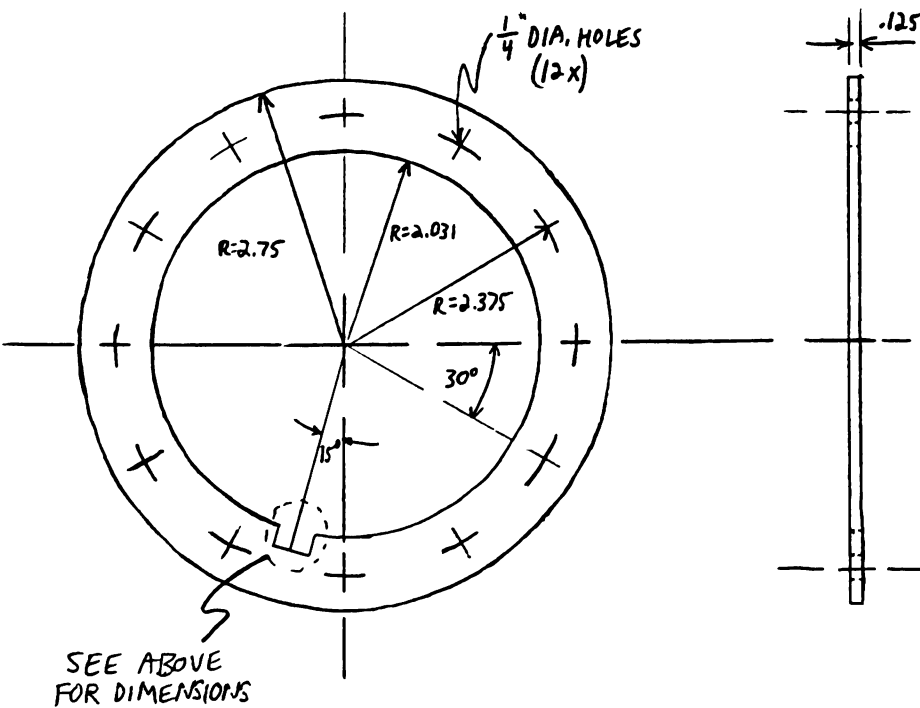


SCALE: 1=4

PARTS 8 + 9 ATTACHMENT RINGS



PART 8:  
MOUNTING RING (2x)

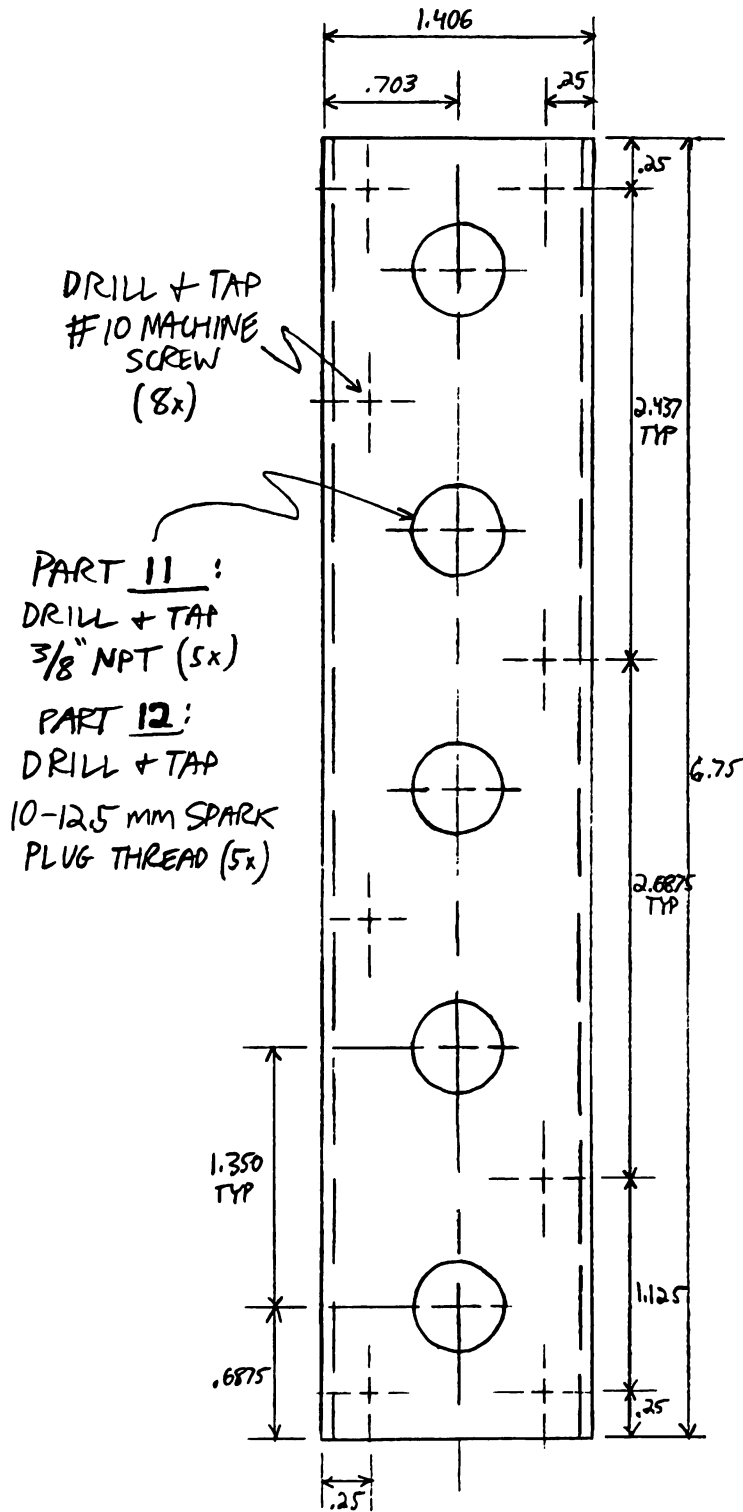


PART 9:  
ATTACHMENT RING

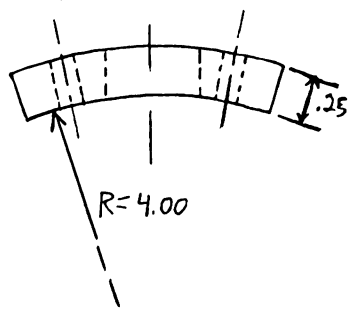
SEE ABOVE FOR DIMENSIONS

SCALE: 1=2

PARTS 11 + 12: FUEL NOZZLE/SPARK PLUG MOUNTING PLATES



SCALE: 1=1



## **APPENDIX B**

### **PROPERTIES OF LIQUEFIED PETROLEUM GAS (LPG OR PROPANE)**

TAKEN FROM:  
PETROLEUM PROCESSING HANDBOOK (REF 13.)

Average Properties of Commercial Propane  
and Commercial Butane\*

$\rho = .217 \frac{g}{cm^3} = .421 \frac{SLUG}{ft^3} = .0078 \frac{lb}{in^3} = 13.547 \frac{lb}{ft^3}$	Commercial propane	Commercial butane
Vapor pressure, psig:		
At 70°F.....	124	31
At 100°F.....	192	59
At 105°F.....	206	65
At 130°F.....	286	97
Specific gravity of liquid at 60/60°F.....	0.509	0.582
Initial boiling point at 14.7 psia, °F.....	-51	15
Weight per gal of liquid at 60°F, lb.....	4.24	4.84 *
Dew point at 14.7 psia, °F.....	-46	24
Specific heat of liquid at 60°F, Btu/(lb)(°F).....	0.588	0.549
Cu ft gas at 60°F, 30 in. Hg, per gal liq at 60°F.....	36.28	31.46
Specific volume of gas, at 60°F, 30 in. Hg, cu ft/lb.....	8.55	6.50
Specific heat of gas at 60°F (C <sub>p</sub> ), Btu/(lb)(°F).....	0.404	0.382
Specific gravity of gas (air = 1) at 60°F, 30 in. Hg.....	1.52	2.01
Ignition temperature in air, °F.....	920-1020	900-1000
Max flame temperature in air, °F.....	3595	3615
Per cent gas in air for max flame temperature .....	4.2-4.5	3.3-3.4
Max rate of flame propagation in 25-mm tube:		
Cm/sec.....	84.9	57.1
In./sec.....	33.4	34.3
Limits of flammability, % gas in air:		
At lower limit.....	2.4	1.9
At max rate of flame propagation .....	4.7-5.0	3.7-3.9
At upper limit.....	9.6	8.6
Required for complete combustion:		
Cu ft O <sub>2</sub> : cu ft gas .....	4.9	6.3
Cu ft air/cu ft gas .....	23.4	30.0
Lb O <sub>2</sub> : lb gas .....	3.60	3.54
Lb air, lb gas .....	15.58	15.3
Products of complete combustion:		
Cu ft CO <sub>2</sub> : cu ft gas .....	3.0	3.9
Cu ft H <sub>2</sub> O: cu ft gas .....	3.8	4.6
Cu ft N <sub>2</sub> : cu ft gas .....	18.5	23.7
Lb CO <sub>2</sub> : lb gas .....	3.0	3.1
Lb H <sub>2</sub> O: lb gas .....	1.6	1.5
Lb N <sub>2</sub> : lb gas .....	12.0	11.8
Ultimate CO <sub>2</sub> , % by volume .....	13.9	14.1
Latent heat of vaporization at boiling point		
Btu lb .....	185	167
Btu gal .....	785	808
Total heating values (after vaporization):		
Btu cu ft .....	2522	3261
Btu lb .....	21,560	21,180
Btu gal .....	91,500	102,600

\* Courtesy of Phillips Petroleum Co.

## **APPENDIX C**

### **RAW DATA FROM THREE-PHASE TESTING**

## APPENDIX C

### RAW DATA FROM THREE-PHASE TESTING

This data was taken during the testing of the *Astra* engine and helped to determine the best combination of the engine's four variable parameters conducive to pulsing operation. Additional detail is given in Section 5.2. The rating scale and abbreviations used on the data sheets are given below.

#### Rating Scale:

Each run was rated on a scale from 1 to 6. A rating of 1 indicated a muffled light-off and poor combustion stability (too rich or too lean). A rating of 4 or 5 indicated a robust light-off, strong combustion and a tendency to pulse. A rating of 6 indicated a robust light-off and either pulsing operation or very strong tendency to pulse after one cycle.

#### Abbreviations:

P T.	=	Pulse Tendency
B.B.	=	Big Bang
S	=	Spark Location in percent combustor length
L or R	=	Left and Right (respectively) Fuel Injector Location in percent combustor length
I	=	Inlet Length in inches
E or EXH	=	Exhaust Length in inches

Stars or Asterisks denote combinations selected to advance to the next testing phase

STATION FUEL PERFORMANCE LOG

(1)

DATE	INLET	EXH	SPARK	L FUEL	R	RATING			
4/6	8 3/4"	32"	.45	.15	.15	3 <small>BANG NO PULSE</small>			
			"	"	.15	.30	4 <small>BIG BANG</small>		
			"	"	"	.45	4 "		
			"	"	.60	.45	3 "		
			"	"	.45	.60	3 "		
			"	"	.60	.60	3 "		
			"	"	.45	.75	4 <small>BIG BANG PULSE TEND</small>		
			"	"	.45	.30	5 <small>B.B. SMALL P.T.</small>		
			①	*	.60	.30	.30	6 <small>B.B. ONE PULSE - IGN OFF</small>	
			"	"	.75	.30	.30	5 <small>B.B.</small>	
			"	"	.45	.30	.45	4 <small>B.B.</small>	
			"	"	.60	.30	.45	5 <small>B.B. SOME PULSE TEND</small>	
			"	"	.75	.30	.45	5 <small>GOOD LIFE OFF B.B.</small>	
			4/18			.30	.30	.60	4 <small>FLAME AT FRONT</small>
						.45	.30	.60	4 "
.60	.30	.60				5 <small>B.B.</small>			
.75	.30	.60				5 <small>B.B.</small>			
.45	.30	.75				4 "			
.60	.30	.75				5 "			
.75	.30	.75				6 <small>FLAME AT BACK B.B.</small>			
.45	.45	.45				3 <small>NOT TO EXCITING</small>			
②	*	.60				.45	.45	3 "	
"	"	.75				.45	.45	5 <small>GOOD LIFE OFF PULSE TEND</small>	
4/20	8 3/4"	32"	.60	.45	.60	5 "			
			.60	.45	.75	6 <small>BETTER PULSE TEND MORE ROBUST</small>			
			.60	.60	.75	5 <small>PULSE TEND</small>			
			③	*	.60	.60	.75	5 <small>FLAME LICKING AROUND INLET - P.T. DIMINISHED</small>	
			④	*	.60	.60	.75	5 <small>"(SAME)</small>	
			⑤	1"	.60	.60	.75	5 <small>P.T. BETTER</small>	
			"	1.5"	.60	.60	.75	5 <small>SAME</small>	
			"	2.0"	.60	.60	.75	5 <small>SAME</small>	
			"	2.5"	.60	.60	.75	5 <small>SAME</small>	
			"	3"	.60	.60	.75	5 <small>SAME</small>	
"	0	.60	.60	.75	4 <small>FLAME AROUND INLET</small>				
5/11	8 3/4"	32"	* .60	.60	.60	5 <small>PULSE TEND</small>			
			⑥						

IGNITION LOCATION INLET 0" PULSE CHART. MUST KEEP AIR FLOWING THRU INLET



PERFORMANCE LOG (BEST F/S. LOCATIONS)

(2)

DATE	EXH	S	L	R	INLET (")	COMMENTS/RATING	
4/20  ⑤	C O N S T A N T	.6	.6	.75	0	4 - FLAME AROUND INLET	
					1	5 - " LICKING AROUND INLET - PT DIMINISHED	
					1.5	5 - SAME	
					2	5 - P.T. BETTER	
					2.5 ★	5 - SAME	
					3	5 - SAME	
5/12  ⑥  ④  ③	A T  <u>32"</u>	.75	.6	.6	8 3/4	5 - PULSED, STILL FORCED AIR NEW P.O.L - TOO MUCH THROTTLE = REDUCED P.T.	
					3	5 - SAME	
					2.5	5 - "	
					2 ★	5 - A LITTLE BETTER	
					1.5	5 - "	
					1	5 - "	
					0	5 - A LITTLE BETTER	
					.60 .45 .75	0	5 - STRONG
					1	5 - SLIGHTLY WEAKER	
					1.5	5 - "	
					2	5 - "	
					2.5 ★	5 - A BIT STRONGER	
3 ★	5 - "						
5/18  ②  ①		.75	.45	.45	0	5 - STRONG P.T	
					1	5 - "	
					1.5	5 - " - MORE THROTLBL	
					2 ★	5 - STRONG P.T.	
					2.5	5 - A LITTLE LESS	
					3	5 - GOOD P.T - MORE THROTLBL	
5/18  ②  ①		.75	.45	.45	0	4 - PUSING ERATIC	
					1	5 - BETTER	
					1.5	5 - BETTER	
					2	5 - NOT AS GOOD	
					2.5 ★	5 - MUCH BETTER	
					3	5 - SAME	
5/18  ②  ①		.60	.30	.30	0	4 - WEAK PT	
					1	4 - RICH FLAME - DIMINISHED PT	
					1.5	4 - BETTER THAN ↓ - SEEMS MORE LIKE STEADY FLAME	
					2	4 - BETTER THAN ↓	
					2.5	4 - PUSING NOT AS APPARENT	
					?	4 - NOT VERY GOOD - FLAMED OUT	

①

②

③

④

★

⑥

⑦

⑤

★ FOR 8 3/4" SEE SHEET ①

FOR 8 3/4" SEE SHEET ①

FOR 8 3/4" SEE SHEET ①

FOR 8 3/4" SEE SHEET ①

# LENGTH PERFORMANCE LOG

(201)

DATE	S	L	R	I	EXH(")	COMMENTS / RATING
5/25	.6	.6	.75	2.5	22.5	5 - PULSING OK
<div style="border: 1px solid black; width: 30px; height: 30px; display: flex; align-items: center; justify-content: center; margin: 0 auto;">1</div>					23	5 - " ) TENDENCY TO GO STEADY
					24	5 - "
					25	5 - "
					26	5 - A LITTLE STRONGER
	26.5				27	5 - SAME
	27.5				28	5 - "
	28.5				29	5 - "
					30	5 - A LITTLE LESS
					31	5 - SAME
					32	SEE SHEET (2)
					33	5 - BETTER THAN 31"
	33.5				34	5 - SAME
					35	5 - A LITTLE LESS
					36	5 - SAME
					37	5 - A LITTLE BETTER
					38	5 - A LITTLE BETTER

<div style="border: 1px solid black; width: 30px; height: 30px; display: flex; align-items: center; justify-content: center; margin: 0 auto;">2</div>	.75	.6	.6	2	23	4 - NOT VERY GOOD
					24	5 - A LITTLE BETTER
					25	5 - SAME
					26	5 - "
	27.5				27	5 - A LITTLE BETTER
	28.5				28	5 - SAME
	29.5				29	5 - "
					30	5 - SAME
					31	5 - A LITTLE LESS
					32	SEE SHEET (2)
					33	4 - NOT AS GOOD AS 31"
					34	5 - BETTER (= 30")
	35.5				35	5 - EVEN BETTER
	36.5				36	5 - SAME
					37	5 - "
					38	5 - A LITTLE LESS

DATE	S L R I	EXH	COMMENTS/RATING
5/30	.6 .45 .75 2.5	23	4 - PULSING NOT THAT DOMINANT
		24	4 - SAME
		25	4 - " " " "
26.5	5 - SAME AS 26"	26	5 - A LITTLE BETTER
27.5	5 - BETTER THAN ↓	27	5 - SAME
28.5	5 - NOT AS GOOD AS 28"	28	5 - BETTER
↑		29	5 - SAME
		30	5 - "
		31	5 - SLIGHTLY LESS
<span style="border: 1px solid black; padding: 2px;">3</span>		32	SEE SHEET ②
		33	5 - SAME AS 31"
		34	5 - SAME
		35	5 - NOT AS GOOD
		36	5 - SAME
		37	5 - SAME
		38	4 - NOT GOOD AT ALL

6/1	.6 .45 .75 3	23	4 - P.T. NOT GOOD
		24	5 - A LITTLE BETTER
		25	5 - SAME
		26	5 - BETTER
26.5	LESS THAN ↓	27	5 - SAME
27.5	SLIGHTLY LESS THAN ↓	28	5 - "
28.5	SAME AS 34.5	29	5 - A LITTLE BETTER
		30	5 - A LITTLE LESS
↑		31	5 - SAME
		32	SEE SHEET ②
		33	5 - BETTER THAN 31"
34.5	BETTER THAN ↓	34	5 - A LITTLE BETTER
35.5	SAME AS 35"	35	5 - SAME
		36	5 - "
		37	5 - SLIGHTLY LESS
		38	5 - SAME

VBL EXH PERF LOG (CONT)

DATE	S L R I	EXH	COMMENTS/RATING
6/1	16.45.75 8 <sup>3</sup> / <sub>4</sub>	23	4 - PULSING, BUT FREER ABOUT $\frac{2}{3}$ OF OTHER INLE
		24	4 - SAME
		25	5 - A LITTLE BETTER
		26	5 - SAME
		27	5 - A LITTLE MORE ROBUST
		28	5 - SAME
		29	5 - SAME
		30	5 - PULSE OK. - NOT AS STRONG
		31	5 - SAME
		32	SEE SHEET ①
		33	5 - BETTER THAN 31"
		34	5 - SAME
		35	5 - "
		36	5 - SAME
		37	5 - SLIGHTLY LESS
		38	5 - SAME
	26.5 LESS THAN ↓		
	27.5 BETTER THAN ↓		
	28.5 SAME AS 34.5		
	34.5 BETTER THAN ↓		
	35.5 SAME AS 36"		

6/8	16.45.6 2	23	4 - NOT VERY GOOD - ALMOST NO P.T.
		24	5 - A LITTLE BETTER
		25	5 - "
		26	5 - SAME
		27	5 - SAME
		28	5 - SAME
		29	5 - A LITTLE BETTER
		30	5 - SAME
		31	5 - SAME
		32	SEE SHEET ②
		33	5 - SAME AS 31"
		34	5 - BETTER
		35	5 - SAME
		36	5 - STRONG P.T.
		37	5 - SAME
		38	5 - SAME
	35.5 SLIGHTLY LESS THAN 37"		
	36.5 SAME AS ↓		
	37.5 BETTER THAN 38 - STRONG P.T.		

## VBL EXH PERF LOG. (CONT)

(3.4)

DATE	S	L	R	I	EXH	COMMENTS/RATING
6/8	1.75	.45	.45	2.5	23	5 - P.T VERY GOOD
					24	5 - SAME
					25	5 - "
					26	5 - " - -
					27	5 - "
					28	5 - "
					29	5 - "
					30	5 - " -
					31	5 - "
					32	SEE SHEET ②
					33	5 - SLIGHTLY LESS THAN 31"
					34	5 - " -
					35	5 - SAME - FLAMED OUT
					36	5 - SAME ; BUT GOOD
					37	5 - "
					38	5 - NOT AS GOOD

**APPENDIX D**

**THERMOCOUPLE AND PRESSURE GAUGE  
CALIBRATION**

## **APPENDIX D**

# **THERMOCOUPLE AND PRESSURE GAUGE CALIBRATION**

### **Thermocouple Calibration:**

Actual calibration of the Nanmac Type K shielded thermocouple and the digital reading device was not possible according to the instruction manual (Ref. 14) since the procedure required electronic adjustment of the digital reading box. Therefore, the thermocouple accuracy was evaluated and compared to the manufacturer's specifications by measuring the temperature of boiling, distilled water.

A small pot of distilled water was brought to a furious boil on a residential electric range. After boiling for two minutes on high heat setting, the temperature reading was taken by immersing the thermocouple about two inches into the water while not touching the bottom or sides of the pot. The digital reading box was activated for about 15 seconds and the temperature displayed after that time was recorded. The burner setting was then reduced to medium heat and the water boiled again for two minutes. The temperature readings was collected in the same manner as above. The heat was then increased to medium-high and another reading was taken.

The data collected from the three readings are tabulated as follows:

Heat Setting	High	Medium	Medium-High
Temperature (°F)	214	213	213

\*Boiling, distilled water

\*Time after heat setting change to reading = 2 min. 15 sec.

The accuracy stated by the manufacturer for this type of thermocouple is:

Accuracy for Temp. Range of -50.0 → 1999 °F:  
0.3% of reading ± 2°F

When the readings in the table were corrected using the manufacturer's accuracy, they fell slightly above or below the 212 °F boiling point of distilled water. This indicated that the thermocouple was reading accurately and required no additional calibration.

#### Pressure Gauge Calibration:

Both the air and fuel pressure gauges were of the aneroid type and were calibrated using an oil-piston gauge. This device functions by applying a known weight to a piston suspended in oil. The pressure of the oil then moves another piston under the gauge to be calibrated, applying pressure to the gauge. As the weighted piston moves down, the piston under the gauge moves up, increasing the pressure. The known pressure developed by the weighted piston can then be compared to the gauge reading.



The oil-piston gauge used for this procedure applies pressure in units of bars. Since the gauges indicated units of psi, the conversion between bars and psi was used. This conversion factor is.

$$1.0133 \text{ bar} = 14.7 \text{ psi} (= 1 \text{ atm})$$

The readings from the pressure gauges during experimentation were used only to establish consistency during engine runs and were not used in any type of calculation. Nonetheless, the gauges were calibrated to test for accuracy and precision.

**The fuel pressure gauge** was calibrated first. There were no manufacturer specifications given on the gauge and no manual to accompany it. The table below tabulates the data collected during the calibration procedure.

Bar	psi	Gauge psi	Difference
0.2	2.9	3.125	0.225
0.25	3.62	3.75	0.13
0.3	4.35	4.68	0.33
0.4	5.8	6.25	0.45
0.45	6.53	7.0	0.47
0.55	7.98	8.25	0.27
0.65	9.43	10.0	0.57
0.75	10.88	11.2	0.32
0.65	9.43	10.0	0.57
0.55	7.98	8.25	0.27
0.45	6.53	7.0	0.47
0.4	5.8	6.25	0.45
0.3	4.35	4.68	0.33
0.25	3.62	3.75	0.13
0.2	2.9	3.125	0.225
<b>Average Difference</b>			<b>0.347</b>

The data indicates that the fuel pressure gauge is very precise (little hysteresis) and relatively accurate, indicating an average of 0.35 psi greater

than actual. Since the fuel pressure gauge only registers up to 15 psi, the applied pressures did not exceed 12 psi.

The air pressure gauge from the shop air line was the calibrated in the same manner. It also had no manual or manufacturer specifications. Since the air pressures used during experimentation were much greater than the fuel pressures, the calibration pressures were increased. The data for the air pressure gauge is tabulated below:

Bar	psi	Gauge psi	Difference
0.6	8.7	16.0	7.3
0.8	11.6	20.0	8.4
1.0	14.7	24.5	9.8
1.2	17.41	27.0	9.6
1.4	20.31	30.0	9.7
1.6	23.21	32.5	9.3
1.8	26.11	35.5	9.4
2.0	29.01	37.0	8.0
1.8	26.11	35.5	9.4
1.6	23.21	32.5	9.3
1.4	20.31	30.0	9.7
1.2	17.41	26.5	9.1
1.0	14.7	24.0	9.3
0.8	11.6	20.0	8.4
0.6	8.7	16.5	7.8
<b>Average Difference</b>			<b>9.0</b>

The data shows that although the air pressure gauge is precise (little hysteresis), there is significant error associated with the readings. The gauge indicates about 9 psi greater than actual pressure. This would be unacceptable if the gauge readings were used in any type of calculation, but for this project they were only used to establish consistent operating conditions of the pulsejet.